Wind energy prediction: a forecasting model based on ANNs and meteorological data on mesoscale

Antonella Rosalia Finamore

UNIVERSITY OF SALERNO

DEPARTMENT OF INDUSTRIAL ENGINEERING

Ph.D. Course in Industrial Engineering
Curriculum in Electronic Engineering - XXX Cycle

Wind energy prediction: a forecasting model based on ANNs and meteorological data on mesoscale

Supervisor
Prof. Vincenzo Galdi

Ph.D. student
Antonella Rosalia Finamore

Scientific Referees
Prof. Dr. Ray Biplob
Ten. Col. Francesco Zauli

Ph.D. Course Coordinator
Prof. Francesco Donsì

March 2021

“Prediction is very difficult, especially
if it is about the future.”

— *Niels Bohr* **—**

Acknowledgement

Although research may feel lonely at times, I consider myself lucky to have had the opportunity to develop my research topic in a youthful and stimulating environment. For that, I have to thank my supervisor, Professor Vincenzo Galdi, who welcomed me into his laboratory and, with all his contributions in terms of time, ideas and funding, made my PhD experience a productive and exciting one. His enthusiasm for research is contagious and has been motivational for me to pursue a PhD. I am also grateful to him for supporting me during difficult times (not only work-related) over the last few years.

I would like to thank the National Air Force Meteorological Service – C.O.Met. (*Operational Center for Meteorology*) and Dr. Salvatore Grasso, CEO of IVPC (*Italian Vento Power Corporation*), one of Europe's most important wind energy companies, for providing meteorological and wind production data. Furthermore, I would like to thank Engineer Gaspare Conio for sharing his expertise on wind power and for his continuous help with the best interpretation of raw wind power production data.

My sincere thanks goes to the Department of Industrial Engineering (DIIn) of the University of Salerno, especially to PhD course coordinator Professor Francesco Donsì, and the Academic Board of the PhD programme in Industrial Engineering for giving me the great opportunity to conduct my research, and for providing the resources to complete my PhD.

I am also grateful to my scientific referees, Prof. PhD. Ray Biplob and Lt. Col. Francesco Zauli, for taking time out from their busy schedule to examine this thesis and for helping to improve it with their valuable suggestions.

Research is much more fun if you do it in good company! I would like to thank the S.I.S.T.E.M.I laboratory. (University of Salerno) for supporting me during all these years. Thanks to Professor Calderaro, Engineer Barberio, Patty, Simo, Peppe, Felix and all the others for putting up with me and for all the good times we have shared. I would also like to thank my fellow doctoral candidates, Andrea and Catello, with whom I shared the PhD experience. We know how stimulating and exhausting it can be! Thank you also for all the thought-provoking conversations and debates. I hope you will be successful with your PhD studies. I am honoured to be your friend!

I would like to thank my closest friends, whom I did not get to see as much as I would have liked. In particular, I thank Francesca, Stefy, Stefania, Laura and Mary for always being there. You have had a great influence on my approach to life. Spending time together and laughing for no specific reason, as only we can do, helped me a lot to get through hard times. Thank you for teaching me that being friends does not mean seeing each other every day, but always being there for each other.

Last but not least, I would like to thank my family for their love and support, no matter when, no matter what. In particular, I thank my parents who continuously encourage me and support my choices and are always present in bad and good times; and my brother for his patience, affection and for his silent presence. I am so proud to be your sister! I must also thank Luca for his love and his support through the good and bad times in the last four years. I will never thank you all enough for putting up with me and supporting me. You are my rocks; I never could have made it without your help. This thesis is dedicated to you!

Antonella

List of publications

- A. R. Finamore, V. Calderaro, V. Galdi, A. Piccolo, G. Conio, S. Grasso, "A Day-Ahead Wind Speed Forecasting Using Data-Mining Model - A Feed-Forward NN Algorithm", *4th IEEE International Conference on Renewable Energy Research and Applications 2015*, November 2015, Palermo, Italy
- A. R. Finamore, V. Calderaro, V. Galdi, A. Piccolo, G. Conio, "A Wind Speed Forecasting Model Based on Artificial Neural Network and Meteorological Data", *16th IEEE International Conference on Environment and Electrical Engineering 2016*, June 2016, Florence, Italy
- A. R. Finamore, V. Calderaro, V. Galdi, A. Piccolo, G. Conio, S. Grasso, "Artificial Neural Network Application in Wind Forecasting: a One-Hour-Ahead Wind Speed Prediction", *5th IET International Renewable Power Generation Conference (RPG™)*, September 2016, London, UK
- A. R. Finamore, V. Calderaro, V. Galdi, A. Piccolo, G. Conio, "A Day-Ahead Wind Speed Prediction Based on Meteorological Data and the Seasonality of Weather Fronts", *IEEE PES GTD Grand International Conference and Exposition Asia (GTD Asia) 2019*, March 2019, Bangkok, Thailand
- A. R. Finamore, V. Calderaro, V. Galdi, A. Piccolo, G. Conio, "A one hour-ahead wind speed forecasting based on hybrid PSO-ANN approach and K-means clustering algorithm", *ELSEVIER Renewable Energy* (under review)
- A. R. Finamore, V. Calderaro, V. Galdi, A. Piccolo, G. Conio, "A comparison between three methods based on ANNs and data on mesoscale for short-term wind speed prediction", *Special Issue on Multidisciplinary Sciences and Engineering - Advances in Science, Technology and Engineering Systems Journal (ASTESJ)* (under review)
- A. R. Finamore, V. Calderaro, V. Galdi, A. Piccolo, G. Conio, S. Grasso "A two-stage wind forecasting approach based on data on mesoscale and wind production curves", *Special Section on: Advances in Renewable Energy Forecasting: Predictability, Business Models and Applications in the Power Industry IEEE Transactions on Sustainable Energy* (under review)

Table of contents

List of figures

List of tables

Abstract

Energy is essential to society for ensuring good quality of life by modern standards. Nowadays, fossil fuels are still the most used energy source, but, due to their depletion and contribution to climate change, the pursuit of a sustainable development has promoted an ever-growing trend to use new and pollution-free energy sources. Such a trend is impacting the energy scenario with massive transformations on a world scale.

From the Kyoto protocol in 1997 to the COP 21 Paris agreement in 2015, great challenges have been introduced in terms of both emissions' reduction and development of new energy sources, which are cleaner than the fossil ones. As a result, renewable energy sources (RESs) have seen a great development, favoured by a strong interest from governments, private companies, universities and public and private research centres. In fact, estimates suggest a RES penetration of over 55% in the next few years. Obviously, such a process is not likely to occur in the same fashion in all countries. As a matter of fact, RESs are not uniformly distributed, and incentive policies differ very much according to the single countries.

Among RESs, wind power is the most widespread in the world after hydropower: over the last few decades, the global wind installed capacity has grown rapidly, particularly in Europe, Asia, and North America. However, the unpredictable and intermittent nature of wind is the main obstacle to its integration on a large scale: grid operators have difficulties keeping the grid in a safe state when large volumes of this energy are injected into the power system. Hence, in order to manage wind capacity, accurate wind power forecasting is necessary. However, forecasting the wind power production is quite challenging as wind is extremely variable and depends on weather conditions, terrain factors, and height above ground level. Furthermore, wind power strongly depends on wind speed, thus for a successful integration of this type of energy into any power system, it is important to design a wind speed prediction model with a forecasting error which is as low as possible. Unfortunately, wind is the most difficult meteorological phenomenon to predict: wind forecasting thus represents a great challenge for researchers, meteorologist, and wind power producers.

In the literature, several forecasting models have been proposed, traditionally based on physical and statistical methods. In addition to those, a

number of more advanced methods based on artificial intelligence have been investigated in recent years, in the attempt to attain more reliable wind-power forecasts.

The aim of this thesis is to develop a forecasting model for estimating the generated power from the predicted wind speed on a given wind farm.

In this PhD dissertation, after introducing the problems connected to the integration of wind power on a large scale, a two-stage forecasting model is proposed. The wind power forecasting problem is divided into two sub-problems: wind speed forecasting and wind power forecasting. Unlike many models presented in the literature or by commercial tools, in the proposed approach weather information and wind production data are used separately. In order to solve the first sub-problem, two models for the daily and hourly wind speed prediction were developed.

The main difference between the models here proposed and those from the literature or commercial tools is the analysis of the weather fronts and their spatio-temporal evolution. In detail, in order to characterize the evolution of the meteorological fronts, a mesoscale study of a number of meteorological data was conducted. According to mesoscale theory, the weather phenomena occurring in a given area are connected to the evolution of the meteorological factors in the surrounding areas. Therefore, in the proposed approaches, instead of considering only the data relating to the site where the forecast is to be made, the prediction is carried out on the basis of the historical data of the area around the site, on a scale of a few hundred kilometres. To this regard, a simple nesting grid was built, similar to those used in the advanced global numerical weather prediction (NWP) models and adopted by the European Centre for Medium-Range Weather Forecast (ECMWF). However, unlike the mesoscale approaches, the nesting grid constructed in the proposed models is made up of a very limited number of points (16 + 1) instead of several hundred.

The first model, for the daily prediction, is based on a Multi-Layer Perceptron neural network (MLP) and dynamic clustering process. The model's inputs are the historical and current meteorological data, including pressure, temperature and wind intensity. These data, time-shifted by a proper delay related to spatial distance, are useful to describe the spatio-temporal evolution of the weather fronts at the point with respect to which the forecast is to be made. The forecasting results of a case study were compared with real-world data registered at the test site (located in southern Italy) and with the results obtained from the persistence model, the traditional benchmark for prediction models. The comparison and performance evaluation demonstrate the high effectiveness of the proposed strategy.

The second model proposed, for the hourly prediction, is based on an optimized artificial neural network (ANN), data correlation analysis, and clustering process. Again, the input data consist of pressure, temperature, and wind intensity (both historical and current values). As in the daily model, the

training set is constructed by a time-shifting τ of the meteorological data, which are then clustered into four groups, through the k-means algorithm. The model's effectiveness was verified by comparing the obtained forecasted values with the real-world registered values and with the results from the persistence model. Furthermore, the model's effectiveness was confirmed by performance evaluation, with respect to the main figures of merit proposed in the literature.

The last part of the work deals with the wind power forecasting problem, proposing a forecasting approach based on Betz's theory and historical wind production curves. The proposed forecasting model is fed by the outcome of the wind speed forecast from the previous stage, wind production curves and the structural characteristics of the particular wind farm to estimate the generated power. The method was tested with data from representative periods around the year: spring and fall equinoxes, summer and winter solstices, and the first week of spring. Once again, performance analysis and the comparison between the forecasted results, along with the recorded values and the persistence model, have all confirmed the effectiveness of the proposed approach.

In summary, performance analysis and comparisons have validated the proposed forecasting approaches, both for wind speed and wind power, showing a better performance when compared to well-known commercial tools and alternative models from the literature.

Throughout the entire work of the thesis, the real-world data of the case study were provided by the National Air Force Meteorological Service - C.O.Met. (Centro Operativo per la Meteorologia) and IVPC (Italian Vento Power Corporation) to which the author is grateful for the contribution offered.

Introduction

In the last few decades, due to environmental issues and the depletion of raw materials, RESs (renewable energy sources) have been growing rapidly, becoming an effective alternative to traditional energy sources. In fact, the growing energy demand and the importance of significantly reducing carbon dioxide emissions are likely to promote an even more massive spread of wind energy in the upcoming years.

The overall generation of energy from RESs on a world basis is expected to reach 55% in 2030.

Among renewable sources, wind energy is believed to become the first source of electricity generation by 2040. In fact, the GWEC (Global Wind Energy Council) estimates that the cumulative installed wind power capacity around the world rose from 432.9 GW at the end of 2015 to 591 GW in 2018, with new installations in Latin America, Asia and Africa contributing to the relentless growth of the installed capacity, along with the well-established giants of China, US, EU, India and Brazil. In Europe, thanks to the incentive policies implemented in the last twenty years, 18% of the electricity demand today is covered by wind power. In this scenario, Italy is the third European country, after Germany and Spain, for installed wind power, with wind power covering around 15.5% of the whole national electric energy production.

Although wind energy is pollution-free, it has some disadvantages, of both technical and economic relevance. The main disadvantage is intermittency, which makes wind energy difficult to integrate into any power systems and to be dispatched effectively. In fact, the growing penetration of wind energy has been increasingly causing significant problems to the ISOs (Independent System Operators), which are responsible for energy dispatching. Therefore, the necessity has been considered to activate sanctioning mechanisms for wind energy producers in case these do not comply with the estimated production plans in the short or very short term.

Since energy storage on a big scale is practically unfeasible, an accurate forecasting of wind power (with a depth of one or more days) has become important for all operators and stakeholders in the power system field. A precise and reliable estimate of energy production, in fact, allows ISOs (Terna in Italy) to better plan and manage the instantaneous balance between energy demand and energy production (necessary to ensure safe network efficiency)

in the planning and balancing phase, thus reducing the power reserves to be implemented, with direct and immediate benefits on the price of power.

Today, in addition to ISOs, wind producers also make use of wind forecasts to avoid incurring sanctions for not complying with the established production plans.

Therefore, in the scenario of renewables just described, the forecasting of the available wind power production becomes crucial as an indispensable solution for a sustainable development on our planet and an effective integration of wind energy.

In the literature, wind forecasting is classified into four categories, according to the temporal forecasting depth: very short-term (few seconds to 30 minutes), for network regulation actions; short-term (30 minutes to 6 hours), for making decisions to guarantee the correct network functioning; medium-term (6 to 24 hours), for operational security applications; long-term (2 to 7 days), used for ensuring optimal network efficiency.

Depending on the application, some researchers propose forecasting models based on statistical methods – like ARMA, ARIMA, etc. – for very short-term and short-term forecasts, while for medium- and long-term forecasts, they propose models based on machine learning approaches such as ANNs (Artificial Neural Networks). Recent works have proposed to address long-term forecasts by means of hybrid models, based on the combination of either different statistical methods, different machine learning methods or machine learning along with statistical methods.

Many of the aforementioned methods form the basis of commercial products developed by private companies or university spin-offs, such as Zephyr or Previento. All the solutions on the market use weather information and historical wind production data to predict the wind energy amount that a given wind farm can produce.

This PhD dissertation falls within this context, presenting an original two-stage hybrid wind power forecasting model for short-medium term wind power forecasting on WFs (wind farms).

Because wind power is strictly dependent on wind speed, the proposed model is made up of two stages: wind speed forecasting and wind power evaluation. Specifically, first the wind is predicted in the area where the wind farm is located, and then the prediction of the power produced follows, based on the expected wind.

In the first stage, in order to predict wind speed, a hybrid model based on weather front analysis, using an ANN is proposed. Then, in the second stage, based on Betz's law and historical wind power data, the wind power is estimated, taking into account the features of the wind farm considered.

The main difference between the new proposed procedure and the models in the literature as well as the commercial tools lies in the analysis of meteorological information, in particular the evolution of the weather fronts: according to mesoscale theory, in fact, the weather phenomena occurring in a

given area are connected to the evolution of meteorological factors in the surrounding areas. Therefore, in the proposed approach, instead of considering only the data relating to the site where the forecast is to be made, in accordance with the approach followed for weather prediction, the forecast is made on the basis of the historical data of the area around the site, on a scale of a few hundred kilometres. Moreover, unlike the mesoscale approach, which uses meshes with hundreds of points, the proposed model bases the prediction on a very limited number of points (16 + 1).

All the data used, both weather and wind power information, were provided, respectively, by the National Air Force Meteorological Service – C.O.Met. (*Centro Operativo per la Meteorologia*) and IVPC (*Italian Vento Power Corporation*), one of the main wind energy companies in Italy.

The structure of this PhD dissertation is as follows.

In Chapter I, the energy scenario, both in terms of energy demand and production, is introduced. The chapter begins with a brief overview of the environmental issues relating to the power system and the need of RESs for a sustainable development. The chapter then presents the situation of RESs worldwide, with a deeper look at the Italian landscape, focusing on wind energy. The second part of the chapter deals with the problem of the integration of wind energy into the electrical grid and the importance of the wind power forecasting problem, thus introducing the aims of this thesis.

In Chapter II, the wind power forecasting problem is discussed in detail. First, the intermittent nature of wind power and the different categories of the forecasting models based on time depth are presented. A number of methods existing in the literature and a number of commercial products implementing them are then illustrated. Particular attention is dedicated to models based on data mining techniques using ANNs, the methodology that will then be used in this thesis, thus defining the state of the art. The chapter ends with the presentation of the main figures of merit used in the literature to verify and to compare the performance of the proposed wind forecasting model.

After a study on the relationship between wind speed and wind power and on the physical phenomena and meteorological dynamics related to wind formation, in Chapter III the proposed method is presented. This is based on the mesoscale study of a limited set of physical data (wind speed, atmospheric pressure and temperature), useful for characterizing the presence of meteorological fronts and their space-time evolution, with the aim of predicting the wind at the site of interest.

In order to test the effectiveness of the proposed method, also in Chapter III, the model is applied to forecast the average daily wind in a particular site, a forecast useful for estimating the energy contribution that a given wind farm is able to ensure in the short and medium term. After the discussion on the model's design, a case study based on real data is presented. The model's effectiveness is examined through the evaluation of the performance and the

comparison between the proposed model and the persistence model, the most used benchmark in the literature for forecasting models.

In Chapter IV, a novel hybrid model for a one-hour-ahead wind speed prediction, also based on the physical model introduced in the previous chapter, is proposed. In the first part of the chapter, the methodology and structure of the model are described, focusing on the k-means clustering phase and the construction of the PSO-ANN model. To test the effectiveness of the proposed method, a case study is presented and discussed, also based on real data provided by the National Air Force Meteorological Service, in this case to generate hourly forecasts. In order to highlight the advantages introduced by the novel model, a forecasting error analysis and a comparison with the persistence model are carried out.

The thesis ends by presenting the development of a model for moving from site wind data to wind farm production data. Therefore, after the presentation of the proposed wind speed forecasting models, in Chapter V a wind power forecasting approach based on Betz's law and the WF wind production curves is presented and validated using data from a real wind farm located in Campania, southern Italy.

The PhD dissertation closes with conclusions that outline the contribution of the work described, resuming the main achievements of the study and proposing a direction for future research that might address yet unresolved issues.

Chapter I
Overview on energy scenario

I.1 The power system: general context and RESs penetration

All modern society is based on electricity, arguably the most valuable form of energy and one of the most significant indicators of the level of industrialization and well-being of a country. Although the use of electricity is linked to sustainability, efficiency and low environmental impact, the massive use of non-renewable sources becomes, over time, unsustainable as, due to their nature, non-renewables are subject to exhaustion and contribute to environmental pollution, the biggest problem associated with their use. While on the one hand electrification has been identified as the most credible solution to favour the social and economic development of the poorest areas of the world as well as for the reduction of polluting emissions in the final use of energy, on the other hand the search for production systems with a lower environmental impact has become a priority to solve the problem of atmospheric pollution. This is due to the release of harmful substances - including carbon dioxide (CO_2) – produced by combustion, the cause of the greenhouse effect, which produces an increase in the world average temperature. To reduce CO_2 emissions, an agreement between 176 countries – Paris COP21 – confirms the importance of CO_2 emission reduction (discussed and analysed in the Kyoto Protocol as early as 1990), and establishes the limit of temperature increase to 1.5 °C (EU Parliament, 2002) (COP21, 2016).

In the last few decades, there has been a growing attention to the development of energy policies to support the spreading of renewable energy sources (RESs). These are, by virtue of their eco-compatible nature, an effective alternative to fossil fuels, which reduces the impact on nature to almost zero, while also solving, at the same time, the problem of the exhaustion of raw materials.

The definition of renewable energy is not univocal: in fact, this term sometimes refers to sources considered clean for the environment, and sometimes to all sources alternative to the traditional ones (combustible fossils), which are capable of regenerating over time.

For the Italian legislation (Italian Parliament, 31 March, 1999), all following sources are considered renewable: "*... the sun, wind, water, geothermal resources, tides, the wave motion and the transformation of vegetable products or organic and inorganic waste into electricity*".

In general, RESs can be classified into the following (Towler, 2014):

• Biomass energy: biomasses are organic (plant or animal) materials, excluding fossil fuels and plastics deriving from purposely grown energy crops (e.g. miscanthus, switchgrass), or from wood or forest residues or, again, as waste from food crops or human, or from animal farming, etc. The technologies used to exploit this resource are based on two methodologies, i.e. biochemical and thermochemical conversion. In both cases, biofuels are obtained which, although burned, do not contribute with their use to the increase of carbon dioxide emissions, as the latter are comparable to the amount of CO_2 absorbed during the growth of biomass. The nearly zero impact on CO_2 emissions and their being widely available at low cost make biomasses a source of clean and renewable energy. This form of energy is more developed in Central and Northern European countries than in Italy, despite Italy's abundant resources in this respect;

• Hydraulic energy: the water flow is conveyed through special pipes to transform water force into pressure and kinetic energy. This energy subsequently powers a generator, which in turn converts said energy into electricity. Among RESs this is the oldest, and its contribution to the world's electricity production is currently 18% (IEA, 2018d). In Italy, according to the data provided by Terna – the Italian Transmission System Operator (TSO) – hydropower contributes to 14.3% of the total energy requirement (Terna, 2019);

• Geothermal energy: this is based on the thermal energy derived from within the Earth's sub-surface. When water comes into contact with magmatic layers, it heats up, until it becomes steam, carrying with it a large amount of energy that can be converted into electricity. The phenomenon generates, among other things, the spectacular "geysers". This major renewable source covers a significant share of electricity demand in countries located close to tectonically active regions. For this kind of electricity generation, high or medium temperature resources are needed, available in few countries in the world (Iceland, El Salvador, New Zealand), where geothermal energy provides core or ancillary services to the grid;

•Solar energy: this type of energy is produced by solar panels exposed to the sun so as to receive the maximum incident radiation. The ability to play with the shape of the panels allows optimal installation and good integration into buildings, thus helping the spreading of this particular form of energy. Based on the panels' technology, it is possible to generate two kinds of energy: thermal and electric. Photovoltaic panels convert light solar directly into electricity. In Europe, thanks to economic incentives, (*Conto Energia in Italy*), the installation of such plants has spread widely, thus causing a number of network management problems (Gazzetta Ufficiale della Repubblica Italiana, 2012).

• Wind energy: this form of energy is based on the transformation, through an electric generator, of wind kinetic energy. In detail, wind is the movement of air on the Earth's surface between high pressure and low-pressure areas (Landberg, 2015) due to the different warming of the surface, be it land, sea or lakes, generated by the non-uniformity of temperature on our planet. In fact, the Earth's surface is heated unevenly by the sun, depending on factors such as the angle of incidence of sunrays on the planet's surface - which differs according to the latitude and time of day -, on thermal conductivity and reflectivity of the surface, and the presence and thickness of clouds. The atmospheric pressure gradient originates the wind, which activates a rotor with a blade system connected to an electric generator. Wind farms (WFs), which group a set of wind generators, are divided into two categories (Manwell et al., 2010): onshore WFs, characterized by turbine capacities of about 2 MW, typically placed in open areas and on mountainous or hilly regions; offshore WFs, characterized by turbine capacities of about 3-5 MW, installed more than 10 km off the coast in order to take advantage of the absence of obstacles at open sea and the presence of stronger winds, thus ensuring a high energy yield (Figure I.1)

Figure I.1 *Examples of onshore and offshore plants*

I.1.1 Penetration of RESs

Until a few years ago, the consumption of electricity was concentrated in the member countries of the OECD (Organization for Cooperation and Economic Development), the assembly of the world's most industrialized countries open to the market, founded in 1961. However, in the last few decades, electricity generation and demand has increased in non-OECD countries more than in OECD countries, thus defining a new trend that currently appears irreversible (IEA, 2019). This is due to the increasing industrial development that is taking place in non-OECD countries such as China or India (Figure I.2).

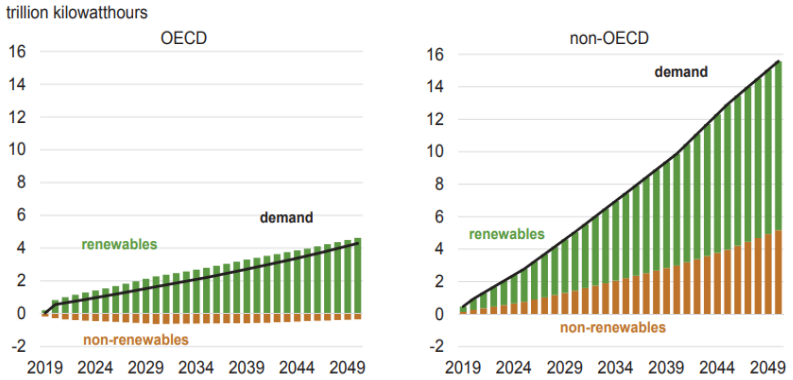

Figure I.2 *Electricity generation and demand in OECD countries and non-OECD countries*

Despite the increase in electricity demand in non-OECD countries, electricity generation from RESs is more widespread in OECD countries, in which RESs supplied 26.2% of global electricity at the end of 2018 (Figure I.3) (REN21, 2019).

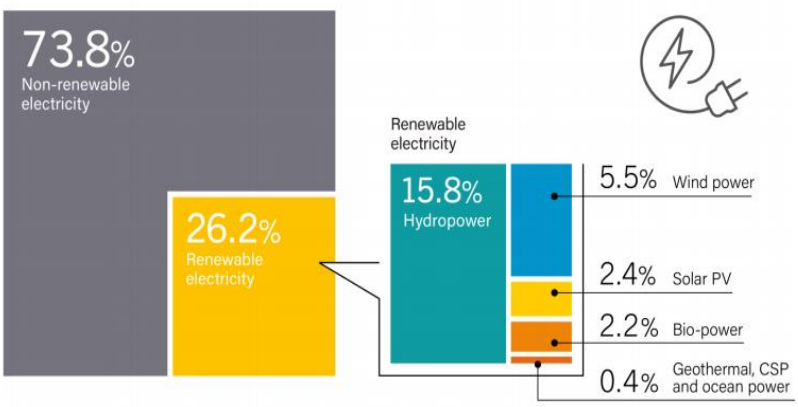

Figure I.3 *Renewable energy share of global electricity production, 2018*

Among RESs, the sources of most recent commercial and technological development are wind and photovoltaic solar, with a high reduction in the production from fossil fuels. In particular, according to IEA (International Energy Agency) forecasts (IEA, 2019), in OECD European countries, the expected electricity generation by 2050 will mainly derive from wind energy, which is likely to go through a constant growth in the next few years (Figure I.4).

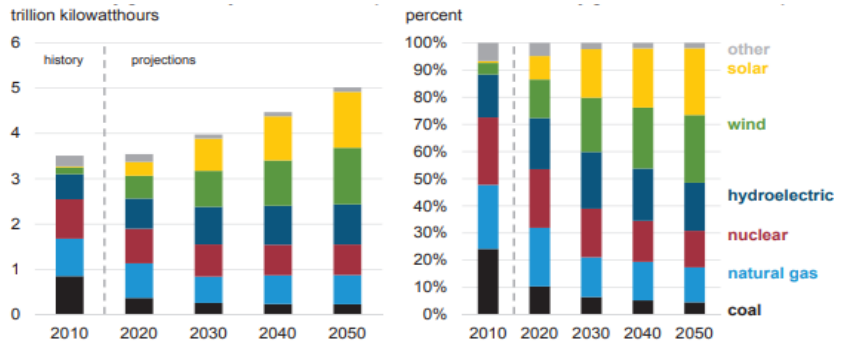

Figure I.4 *Net electricity generation from fuel and RESs – IEA source*

This trend is confirmed by surveys (BNEF, 2019), which report that the expected renewable production will reach, in 2050, 62% of global energy production, and such production is mainly due to wind and solar (around 48%), thus exceeding hydroelectric production (Figure I.5).

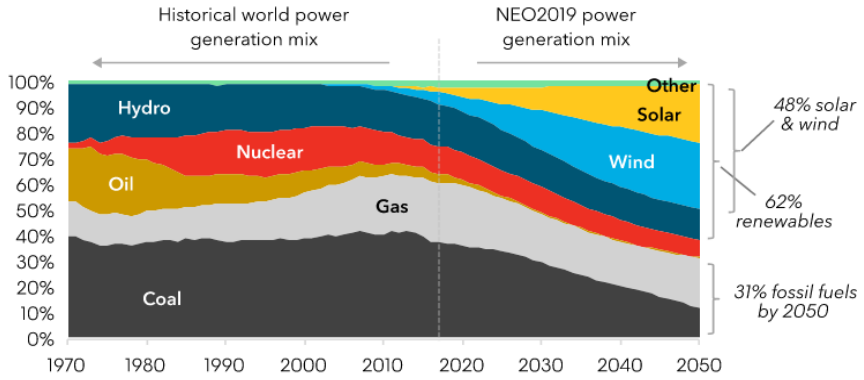

Figure I.5 *Global power generation mix expected in 2050 – (BNEF Report, 2019)*

In this scenario, due to the rapid growth of offshore wind, wind power is expected to become the first source of electricity generation by 2040, thus replacing traditional energy sources (Figure I.6) (IEA, 2018a) (IRENA, 2017) (IEA, 2018b).

Today, according to (IEA 2018c), two markets have the primacy in the production of wind energy: China and United States, where wind production reaches 40% of the total energy production. In particular, in 2018, China had the highest proportion of new installations, both offshore and onshore (around 45%) (GWEC, 2018). In addition, emerging countries such as Brazil, Mexico and even Chile are attractive markets for the wind sector, thanks to their national energy policies, developed to encourage economic growth while reducing high pollution contribution (BP, 2019a) (BP, 2019b). In fact, the Latin American (LATAM) wind market has significantly grown over the past ten years, reaching the total installed power of 25 GW, especially in Brazil, which continues to hold joint capacity auctions for onshore wind, thus aiming to reach 10% of the national energy production due to wind in 2021 (Aldana et al., 2019). Even in Europe, wind power is extremely widespread: in fact, it covers 14% of the EU's electricity demand, with leading countries such as Spain, Great Britain (Scotland), Denmark and Germany, where offshore wind power has spread widely. According to (Eurostat, 2019), in 2018, the installed wind power had more capacity than any other form of power generation in the EU, accounting for 48% of the total power capacity installations. In detail, Denmark is the country with the highest share of wind energy within its electricity demand (41%), whereas the UK registered the largest annual increase of wind energy within its electricity demand, rising from 13.5% to 18%.

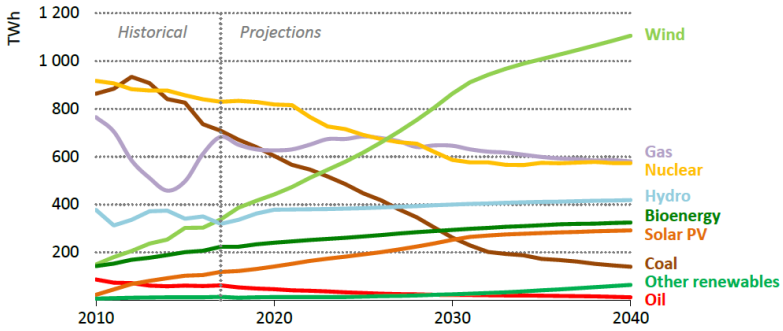

Figure I.6 *New electricity scenario in European Union (IRENA, 2019)*

The rest of Europe has also opened up to wind power, especially Eastern countries such as Romania, Poland and Bulgaria with their numerous installations, thus challenging the lower incentives imposed by the governments and performing exceptionally well (Eurostat, 2019).

I.1.2 Wind power in Italy

In Italy, electricity production has traditionally been linked to fossil fuels, in particular natural gas (around 60%). The sustainability policies launched in the late 1990s, supported by a significant incentive policy in the 2000s, led to

a significant increase in the penetration of RESs (GSE, 2019), to the point of covering, in 2018, 39.5% of the Italian electricity production (Figure I.7) (Terna, 2018).

In Italy, the electricity system's opening to the market and the disappearance of the vertically integrated state-controlled company fixed by Law 79, March, 31, 1999, has introduced a new organization and new rules for the production of electricity from RESs. A new agency was established, responsible for drafting the technical standards, the Authority for Electricity and Gas (AEEG), now ARERA (Autorità di Regolazione per Energia, Reti e Ambiente – Authority for Energy, Grids, and Environment).

New rules (Gazzetta Ufficiale della Repubblica Italiana, 29 Dicembre 2003) for building and operating a plant powered by RESs were issued, with a considerable simplification of the authorization procedures on a local basis, thus defining a favourable context for the development of renewable sources, especially for wind power plants. For instance, all plants powered by RESs were defined as systems "of public utility, not deferrable, and urgent". In particular, Legislative Decree 387/03 (Gazzetta Ufficiale della Repubblica Italiana, 29 Dicembre 2003) centralized the authorization procedures for power plants greater than 200 kW and simplified the bureaucratic process for small size plants with a nominal power of less than 20 kW, usually destined for self-consumption.

Besides simplifying and rationalizing authorizations, in order to support the spreading of RESs, Italy has implemented an incentive policy in 2002 introducing the so-called Green Certificates (GC). Since 2016, the mechanism of GCs has been replaced by a new kind of incentive, based on the remuneration by the GSE of the net production of energy, in addition to the revenues deriving from the energy sale (Ministry of Economic Development, 2016). The effects of these policies in the last 15 years are shown in Figure I.7: the contribution of RESs to the electric energy production in Italy has more than doubled, whereas that of coal has halved, with thermoelectric energy remaining stable.

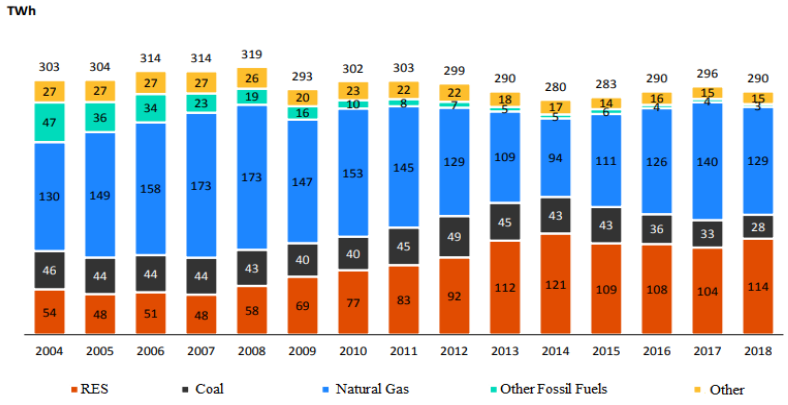

Figure I.7 *Electricity production in Italy – GSE source*

Today, Italy is the third European country, after Germany and Spain, for installed wind power, with wind covering around 15.5% of the whole national electric energy production (Terna, 2019).

Most installations are in the southern regions of Italy, due to the availability of the wind source. As of the end of 2018, Basilicata is the region with the highest percentage of plants on the national territory (25.0%), followed by Puglia (20.8%), Sicily and Campania (Figure I.8) (GSE, 2019).

As for the size of the wind power plants installed in Italy between 2017 and 2018, both in terms of numbers (+5.9%) and installed power (+499 MW, + 5.1%), 93% of them is greater than 1 MW, whereas plants smaller than 1 MW represent only 34 MW (about 7%) (GSE, 2019).

Figure I.8 *Distribution of wind farms at the end of 2018 in Italy*

However, the spreading of wind energy is hampered by a number of issues, including the noise of turbines, the visual impact, the acidification and eutrophication of soils, the emission of polluting substances, the impact on fauna, etc. (Bispo R. & al., 2019). Among the aforementioned problems, the visual impact is perhaps the most sensitive for the public, while the problem of noise is linked to the electric generators installed in wind turbines, which in the past were not specifically designed for the conditions of typical operativity of a wind turbine. The potential noise pollution caused by wind turbines is linked to two types of noise: mechanical, ascribable to the generator, and aerodynamic, ascribable to the rotor blades. New wind turbines have almost eliminated the problem of mechanical noise, and the sound levels are mainly related to the flows around the blades, partly controllable by reducing the rotation speed and by installing special aerodynamic appendages; however, this noise is normally less than 45 dB at 350 m distance (Hansen, 2015).

I.2 The wind power forecasting problem

As electricity cannot be stored, an instant-by-instant balance must be ensured between the energy produced by the generation systems scattered throughout a country and the energy required by the users. The ability to maintain a continuous balance between demand and generation is called dispatching. In Italy, maintaining this balance is the task of Terna, the Transmission System Operator (TSO) which manages the national electricity transmission network, monitors the electrical flows and applies the provisions necessary for the coordinated exercise of system elements, i.e. production plants, the transmission network and auxiliary services.

Although the wind is a clean and inexhaustible energy source, its intermittent nature makes its power very unpredictable. In fact, with the spreading of NP-RESs, Terna struggles to ensure the continuous balance between demand and generation, essential for the power system grid to work in safe operating conditions, thus avoiding blackouts or large overproductions.

The randomness of wind power causes the TSO dispatching problems in both technical and economic terms. In the next sections, these two kinds of problems are outlined.

I.2.1 Technical aspects

Due to the intermittent nature of their source, RESs, and in particular wind power production, are classified as non-programmable renewable energy sources (NP-RESs). The non-programmability of these sources makes it difficult to integrate their energy into the electricity grid. This is starting to become a significant problem in countries with a high percentage of renewable energy from NP-RES like Italy, where RESs such as wind and photovoltaic have dispatching priority.

The extreme variability and intermittency of wind energy might cause a number of stability problems to the transmission grid, which can override the dispatching priority constraint, as defined in legislative resolution 138/05 (AEEG, 7 July 2005) on the dispatching of production units from NP-RESs in critical conditions of the electrical system. The slower development of the transmission network compared to the growth of NP-RES has led to an increasingly frequent use of modulations of NP-RES plants, in particular wind turbines, to the point of making it necessary to introduce new regulations in Italy that can help a better integration of NP-RESs into the electricity system (AEEG, 20 December 2007) (AEEG, 25 July 2008).

To this regard, in order to overcome stability and safety problems, the TSO daily asks NP-RES power producers for a forecast production schedule (with a timeline of a few days). In detail, Terna daily runs a forecast of the national demand of electricity and, based on the forecasts provided by the NP-RESs power producers, it coordinates the generation plants so that the production is

adjusted to the actual demand for energy. Hence, in order to maintain the continuous balance between energy demand and production, and in order to integrate wind energy in the existent electric grid, an accurate wind power forecasting is necessary.

I.2.2 Economic aspects

In the market scenario, in order to make up the daily schedule of production, TSOs may purchase power generation from Independent Power Producers (IPPs) and utilities, or via bilateral contracts or electricity pools, or considering their own power production means, if they have any. In Italy, after the introduction of the "*Bersani*" decree (Italian Parliament, 31 March 1999), more players appear on the market, superseding the traditional structure based on a vertically integrated utility with local monopolies. In short, electricity markets in Italy basically consist of two mechanisms:

- the spot market: participants propose a given production cost for quantities of energy for the following day. The electricity spot price for the various periods is settled by an auction system, according to the different offers;
- the balancing of power generation, which is coordinated by the TSO. The TSO will determine the penalties that will be paid by IPPs who have failed in their obligations, depending on the energy lacks or surplus, such as power plant failures or the intermittence of wind power.

The unpredictability of wind energy also impacts the electric market, particularly the balancing market. The impact of NP-RESs, especially of wind energy, is even stronger in light of the dispatching priority, which is guaranteed for these types of RESs at a European level. In fact, according to the European directive 2009/28/EC (EU Parliament, 5 June 2009), "[...] *Member States ensure that, in the dispatching of electricity production, transmission system operators give priority to production plants that use renewable energy sources ensuring the safe operation of the national electricity system and on the basis of transparent and non-discriminatory criteria. The Member States ensure that appropriate market and network operational measures are taken, to ensure that there are fewer possible limitations of electricity produced from renewable sources*." Therefore, in the Italian electric system, it is expected that in the presence of several sales offers proposing the same price, the following order of priority applies:

- offers to sell essential units for electric system security;
- offers to sell production units powered by NP-RESs (i.e. production units that use solar energy, wind, sea-power, wave motion, landfill gas, gas residues from purification processes, biogas, geothermal energy or hydraulic energy, limited, in the last case, to water flowing units);

- offers to sell production units powered by different RESs;
- offers to sell cogeneration production units;
- sale offers of the CIP6/92 production units and of the production of Legislative Decree 387/03 (Gazzetta Ufficiale della Repubblica Italiana, 29 December 2003) or Law. 239/04 (Italian Parliament, 23 August 2004);
- offers to sell production units powered exclusively by national sources of primary fuel, for a maximum annual share not exceeding 15% percent of all primary energy necessary to generate the electricity consumed;
- offers relating to bilateral contracts;
- other offers to sell.

The points listed above indicate that RES production units – both programmable and non-programmable - have dispatching priority but only at the same offer price and compatibly with the safety of the electrical system. According the rules of dispatching priority and lower operating costs, when wind generation is present, the conventional generation is replaced. However, due to the huge variability of this primary energy, wind power producers are penalized by the market system and thus a great part of their production may be subjected to penalties. In fact, in Italy, according to legislative resolution 281/12 (Authority for Energy and Gas, 5 July 2012), RES producers have to pay the imbalance costs deriving from the failure or incorrect forecast of the energy introduced into the network. Before the approval of this resolution, the final consumer used to take full responsibility for any costs of unbalancing the national electricity network. Hence, it is obvious that an IPP cannot propose quantities of energy on the market and avoid the possible penalties without knowing what the output of wind farms will be (ARERA, 2016).

Therefore, in order to solve both technical and economic problems, an accurate wind power forecast is crucial.

I.3 Objective of thesis

The aim of this work is to develop a novel wind power forecasting model, combining local observations with wind trends on a medium scale to predict the generated wind power with a low forecasting error. More specifically, the purpose is to provide prediction models based on Artificial Neural Networks (ANNs), one of the most used machine learning approaches, and on meteorological data on mesoscale.

The proposed approach is composed of two phases: first, forecasting the primary energy source, i.e. the wind and its speed; second, calculating the electric power produced, once the wind forecast is known.

The work is organized as follows: after a brief review of the state of the art of all wind forecasting models proposed both in the literature and by

commercial products, a study is proposed on wind phenomena, necessary to understand which and how meteorological factors influence wind generation, thus highlighting the relationship between wind speed and other meteorological factors which form the basic idea of this thesis. In particular, through a meteorological front analysis, according to the main meteorological models (mesoscale), a point grid around the site chosen for forecasting was constructed which describes the spatial-temporal evolution of weather fronts. In order to describe the weather fronts' temporal evolution, the meteorological information of each grid point are shifted, according to how far a point is from the forecast site, by a time shift delay.

Based on this idea, two wind speed forecasting models, both for daily and hourly predictions, are defined and described. In order to analyse the performance of the implemented models, the wind speed forecasted values are compared with actual values measured by an actual meteorological station. Specifically, the validation of the model was carried out using the data made available by the meteorological service of the Italian Air Force (COMET) and is based on a series of data registered over several years on an hourly basis at COMET survey stations.

The models have been used to forecast wind values on a real wind farm located in southern Italy.

The results obtained were presented, compared with those obtainable from the literature models, and then discussed in the final part.
The thesis ends with brief conclusions that summarize the work.

Chapter II
State of art in wind power forecasting

This chapter presents a brief overview of the state of the art of the wind power forecasting problem.

In detail, once the different depths of prediction are explained, the related forecasting models are described, from statistical to machine learning. Furthermore, the fluid dynamic model on which the physical models are based is described. In addition to the traditional models, hybrid models and commercial tools are also mentioned.

The chapter ends with the description of the forecast evaluation metrics used in the literature to evaluate the models' effectiveness.

II.1 Principal aspects of the forecasting problem

In the power system, electric energy is not stored, if not in small quantities, and therefore it is necessary to guarantee an instantaneous balance between the power supplied and the power required. The spread of RESs has increased the difficulty for TSOs to ensure power balance for the safe functioning of the network (Jones, 2014). The unpredictability stemming from RES production generates uncertainty in the next-day production profile, so TSOs ask renewable energy producers to bear the higher costs associated with managing the imbalance caused. However, not all RESs have the same degree of unpredictability. For example, tidal or biomass energy are more easily predictable and programmable than wind or solar energy (Farret et al., 2017).

Among the RESs, the most difficult to predict is wind energy, due to the intermittency and unpredictability of its source, which changes very quickly during the day. In fact, grid operators usually see a wind farm's generation, due to its dependence on wind speed and meteorological conditions, as a 'negative load'.

In detail, wind power depends both on the plant and availability, on the characteristics of the wind turbine as well as the characteristics of the site, including its orography, wind speed, wind direction, changes in atmospheric pressure, etc. The producer, except for the weather factors linked to the wind, knows all these parameters. Hence, the integration of wind power is becoming a challenge that producers, grid operators etc. are facing due to wind variability, making wind forecasting important for optimally integrating wind energy generation (Chandra, 2017).

Wind speed constantly changes, and its non-stationary nature can be modelled using the Weibull distribution with two parameters, the scale factor A_w and the shape factor k_w. This function, widely used for product lifetime analysis and reliability engineering, best describes the probabilistic distribution of wind speed (Jain, 2016):

$$f(v) = \frac{k_w}{A_w}\left(\frac{v}{A_w}\right)^{k_w-1} \exp\left(-\left(\frac{v}{A_w}\right)^{k_w}\right) \quad \text{(II.1)}$$

where v is wind speed and the parameters A_w and k_w are estimated using a sufficiently long series of wind speed data. In general, the scale parameter A_w takes values between 2 and 8, and the shape factor k_w between 1.5 and 2.2 (Horst, 2008).

As previously mentioned, while the high variability of wind determines the uncertainty of the produced power, the relationship between wind and the produced power is much simpler and almost deterministic: wind turbines convert the kinetic energy of the wind into mechanical energy and therefore into electrical energy (Manwell et al., 2010). The energy conversion process of a wind turbine is described by its characteristic curve, known as the wind turbine power curve (Figure II.1).

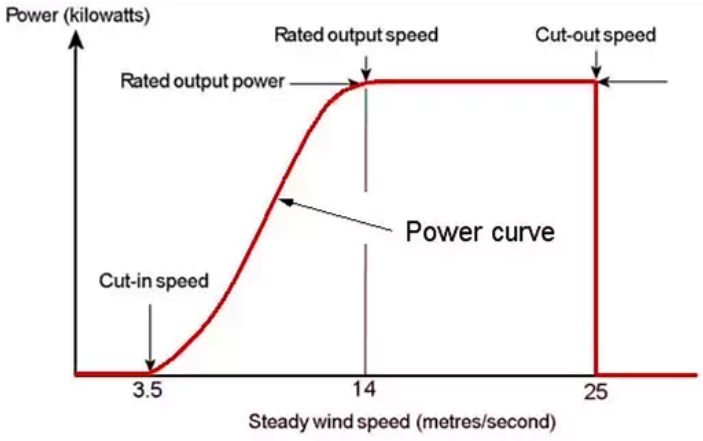

Figure II.1 *Typical wind turbine power curve*

As shown in Figure II.1, the power curve is divided into 4 regions: the power production is null below the cut-in wind speed (around 2 - 4 m/s), then sharply increases between the cut-in and the rated wind speed (12 - 15 m/s). In this region, a small variation in wind speed determines an even greater variation in power. The third region starts when the wind reaches the rated speed, which corresponds to the rated power P_n of the wind turbine, and ends at cut-off speed (around 25 m/s). This region is characterized by a nearly constant produced power. At the cut-off speed, the turbine stops for safety reasons: here starts the fourth region, characterized by zero power.

The sharp increase of the characteristic power curve in the second region is related to the cubic power law that describes the relationship between wind power and wind speed. In detail, wind power is proportional to air density, the area of the wind turbine rotor and the cube of wind speed (El-Sharkawi, 2015):

$$P = \frac{1}{2}\rho A v^3 \tag{II.2}$$

where ρ is the air density (kg/m^3), A is the area of wind turbine rotor and v is wind speed (m/s). Eq. (II.2) refers to ideal conditions, as it does not consider factors such as the Betz limit, the generator and gearbox efficiencies or other losses, which reduce by 20-30% the maximal theoretical power available. In real-life conditions, the wind power law becomes:

$$P = \frac{1}{2}\rho C_p \eta A v^3 \tag{II.3}$$

where η is the turbine efficiency ratio (up to 0.8) and C_p is the turbine performance coefficient (around 0.35), which is bounded by the Betz limit, the function of both the blade pitch angle and the ratio of the rotor blade tip speed to wind speed. In the same way, the power curve shown in Figure II.1 must be considered as theoretical, since it is obtained in wind tunnels characterized by well-defined conditions (a constant flow of wind with no turbulence), which do not consider the intermittent and complex behaviour of wind speed (Hau, 2013).

In this thesis, the theoretical expression of wind power is considered.

II.1.1 Intermittent nature of wind power

The extreme variability of wind speed leads to heavy fluctuations of wind power that greatly affect the power balance and network stability, especially when the amount of wind penetration is comparable to the available reserve margin. Hence, the main problem with the integration of wind power is the uncertainty of the primary source. Wind, from one instant to another, can unpredictably change its direction and intensity, as shown by the emblematic

case recorded in Texas in 2008 (Figure II.2) (NREL, 2009), thus generating a high variability in production that must be quickly compensated in some way.

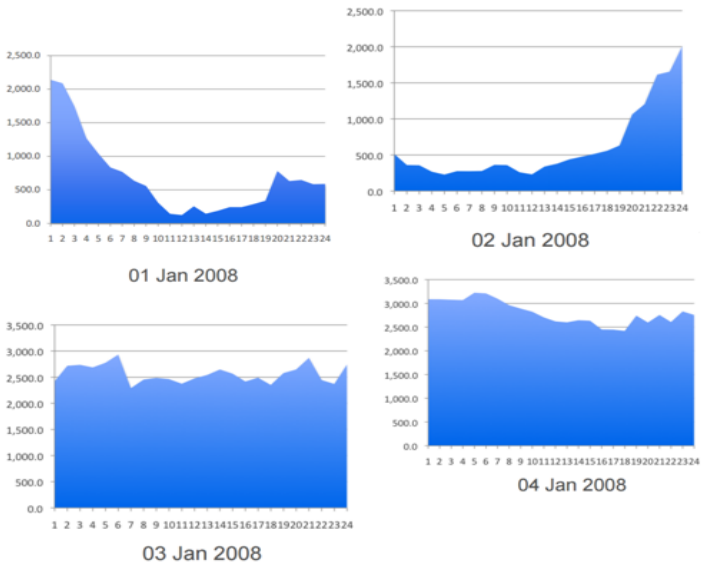

Figure II.2 *Hourly wind power variation in Texas, USA*

Therefore, even though wind power production is conditioned by multiple factors – weather conditions, local orography, seasonal variations, daily cycles which may be substantial or not, mainly due to thermal effects – wind fluctuations receive a great deal of attention, and the challenges to be faced, when wind generation is injected into electricity grids, are related to the managing of the wind's intermittence, which causes problems in balancing between the power generated and the power absorbed. The responsible for managing the electricity balance on the grid is the TSO, which guarantees at any given time that the electricity production meets the electricity demand. To manage this balance, taking into account the intrinsic uncertainty of the power demand, it is necessary to schedule the production over the area of interest in advance: load profiles are usually given by load forecasts (produced from experience or by prediction methods). The randomness of wind power generation, in the same way, requires in some way to be forecasted, so as to enable the TSO to schedule, with a defined degree of sustainable uncertainty, the production of programmable-power production plants (Shakir et al., 2020).

Therefore, being able to predict the produced wind energy by predicting the wind becomes crucial.

II.1.2 Types of wind forecast in the power system area

The causes that generate and attenuate the wind locally, due to its high variability on any time scale (hourly, daily or seasonal), and its non-linear dependence on weather factors – which influence the wind power generation associated to it – make its forecasting a complex challenge.

In the technical-scientific literature in the field of power systems and RESs, focus is typically given to the prediction of the power output and not to wind speed, hence the building of forecasting models with inputs based both on meteorological and production data. This approach is widely used by commercial tools for wind production forecast, often carried out on the basis of scientific works by researchers from university and public or private research centres. These tools are different from each other in terms of prediction horizon (a few minutes, hours or days), computational facilities (a small PC or a supercomputer), and desired accuracy.

Therefore, it is appropriate to understand what types of forecasts exist and what purposes they serve.

First of all, the forecasting of wind power generation may be considered according to different time scales, each characterized by a different forecasting model (Giebel et al., 2017). The table below summarizes the major prediction horizon groups and their main applications.

Table II.1 *Different prediction horizons and applications*

PREDICTION HORIZON	TIME RANGE	APPLICATION
VERY-SHORT TERM	Few seconds - 30 minutes	- Clearing of the electricity market - Network regulation actions
SHORT-TERM	30 minutes - 6 hours	- Economic dispatching plans - Decisions for the correct network functioning
MEDIUM-TERM	6 - 24 hours (1 day)	- Operational security in the next day energy market
LONG-TERM	2- 7 days	- Ensure optimal network operation by keeping scheduled plans

A second classification is made on the basis of the methodology used to construct the forecast. In this respect, wind forecasting methods can be grouped into four categories: statistics models, fluid dynamic and physical models, machine learning models and hybrid models. These models differ from each other as regards horizons, applications and inputs. For example, statistical approaches use, as inputs, only information about wind production

and consider as linear, for a few instants, the relationship between the wind power measured shortly before and the same power at a new instant. Instead, physical models are based on the physical laws that describe the physical phenomena related to the movements of air masses in the atmosphere, while data-mining approaches are used for describing the nonlinear relationship between wind power and wind speed. In recent years, in order to improve the forecasting performance and to combine the best characteristics of the different approaches, hybrid models have been developed. Below, table II.2 summarizes the different prediction models.

Table II.2 *Different forecasting approaches*

PREDICTION APPROACH	SUB-MODELS	EXAMPLES	CONSIDERATIONS
STATISTICAL METHODS	Persistence & Time series model	ARMA ARIMA Kalman filter, etc.	Mainly used for very short-term predictions The persistence model is a benchmark for prediction models
PHYSICAL METHODS	Numeric Weather Predictors (NWP)	Global Forecasting System Prediktor HIRLAM, etc.	These methods use the physical laws that describe the dynamic atmospheric behaviour
MACHINE LEARNING METHODS	-	ANNs GAs SVM, etc.	These methods describe the non-linearity of RESs and are mainly used for medium-long term forecasts
HYBRID METHODS	-	ANN + NWP ANN+ FL Time series + NWP etc.	These methods are used to obtain better forecasting performances than those obtained with traditional methods They are mainly used for long-term forecasts

In the next paragraphs, the different prediction models are described in detail.

II.2 Statistical approaches

Statistical forecasting methods, defined as quantitative techniques, are based on the Box-Jenkins methodology (Jenkins et al., 2008). They consist in an iterative procedure that allows to attain, starting from data observation, the construction of a model which provides a valid/effective description of the stochastic process that generates the historical series observed. Therefore, it can be defined as an approach to data in which the time series are oriented towards the model, and not vice versa.

In these models, wind speed is expressed by the autocorrelation of a non-Gaussian distribution, that is, using the autoregressive AR model as a linear predictor so as to predict the n^{th} sample from the previous samples, based on the relationship between the variable to forecast and the other past variables. Hence, wind speed is expressed in the following way:

$$v_t = \sum_{i=1}^{N} c_{t,i} v_{t-1} + \varepsilon_t t = N+T, N+2T, ..., N+mT \quad \text{(II.4)}$$

where $c_{t,i}$ are the AR coefficients estimated using the Yule-Walker equations, and ε_t is the prediction error (Paolella, 2018); if this term is omitted, the persistence method is obtained. These models are mainly used for decision-making or planning applications, such as network regulation actions, economic dispatching plans or to make decisions for the correct functioning of the network (Chatfield, 2000).

Below, the persistence model and other time series models are described in detail.

II.2.1 Persistence model

The persistence model is defined as a *naive predictor*, as it commonly refers to the principle of "what you see is what you get". It is one of the simplest wind power prediction models: the forecast values are calculated assuming that conditions remain unchanged between the current instant t and the instant ahead $t+T$. Hence, by definition, the error for zero-time steps ahead is zero (Chatfield, 2000). The persistence model, considering a stationary time series (mean and variance do not change over time), is implemented as follows:

$$y(t+T) = y(t) \quad \text{(II.5)}$$

In detail, this model considers wind at the next instant of time $t+T$ equal to wind at the current time t, implicitly assuming that the weather conditions are stationary. However, atmospheric phenomena are not stationary, and their

variation depend on seasonal, diurnal and inter-annual cycles as well as perturbations external to air observation. Hence, despite its apparent simplicity, this method might be used for first look-ahead times (a few minutes up to 1 hour), due to the scale of changes in the atmosphere, which are actually slow, in the order of days (in the case of Europe): a low pressure system, a driving force for the wind, takes about from one to three days to cross the whole continent (Barry et al., 2009).

A generalization of the persistence method is obtained by replacing the last measured value with the average of the last *n* measured values:

$$\hat{y}^n(t+T) = \frac{1}{n}\sum_{i=0}^{n-1} y(t-i) \tag{II.6}$$

In the literature, for short-term prediction horizons (e.g., a few minutes or hours), this model is considered the benchmark for all other prediction models to beat (Ssekulima et al., 2016)

II.2.2 Time–series models

The simplest and oldest models for short-term wind prediction are the time-series models, which are variants of the autoregressive model. Although designed for very short horizons – no more than 6 hours - this model is a typical reference point in wind energy, where the process is not fixed on any time scale. These models are not considered particularly well performing, as they are characterized by significant errors even over a time horizon of a few hours. To overcome this limitation, for short-term wind prediction both autoregressive with moving average (ARMA), or autoregressive integrated moving average (ARIMA), or Kalman filter approaches (Alencar et al., 2017) are used, thus introducing weighted over time averages.

The best-known time series model is ARMA, a mathematical model characterized by: **linearity** – multiplying all the inputs by a factor k, the output will also be multiplied by this value – and **time invariance** – a certain input sequence will give a certain output sequence regardless of the amount of instants elapsed since the instant zero. The concept of *instant zero* is purely conventional, since the system tends to "forget" the past, that is, to be influenced in an exponentially decreasing way over time (a feature known as "evanescence") (Jenkins et al., 2008).

This model describes weakly stationary stochastic time series in terms of two polynomial parts: the autoregressive component (AR) and the moving average component (MA). The AR provides a prediction using previous values of the dependent variable, while the MA part makes predictions using the series mean and previous errors.

Usually, the model is indicated with ARMA (*p, q*) where *p* is the order of the autoregressive part and *q* is the order of the moving average part. In detail, wind speed *v* can be expressed as follows (Paolella, 2018):

$$v_t - \mu = \sum_{i=1}^{p} c_{t,i} \cdot (v_{t-i} - \mu) + \varepsilon_t + \vartheta_1 \cdot \varepsilon_{t-1} + \vartheta_2 \cdot \varepsilon_{t-2} + ... + \vartheta_q \cdot \varepsilon_{t-q} \quad \text{(II.7)}$$

where μ is a constant, $c_{t,i}$ are the autoregressive model's parameters, ϑ_j are the moving average model's parameters and ε_t are the error terms (white noise).

Another widely used time-series model is ARIMA, a generalized random walk model which is fine-tuned to eliminate all residual autocorrelation. ARIMA is very similar to ARMA: in fact, the AR and MA components are identical to the ARMA model, whereas the additional "I" (*Integrated*) highlights that a difference of the order d has been applied to make the model stationary. In detail, if a model is not stationary, ARMA cannot be used, so the model becomes stationary by assuming a series of differences. Hence, the letter "I" in the ARIMA model is a measure of how many non-seasonal differences are needed to achieve the stationary status. If the differencing is not involved in the model, ARIMA becomes ARMA.

An ARIMA model is indicated with ARIMA (*p, d, q*) where *p* indicates the autoregressive terms and allows the effect of the past values in the model, *q* refers to lagged forecast errors considered as linear combinations of the error values observed at a previous instant, and the *d* takes into account the non-seasonal differences needed for stationarity (Montgomery et al., 2008). The forecasting of wind speed *v* can be expressed as follows:

$$\begin{aligned} v_t - \mu = &\sum_{i=1}^{p} c_{t,i} \cdot (v_{t-i} - \mu) + \varepsilon_t + \sum_{j=1}^{P} C_{t,j} \cdot (v_{t-j} - \mu) + \\ &+ \sum_{k=1}^{q} \vartheta_k \cdot \varepsilon_{t-k} + \sum_{\gamma=1}^{Q} \Theta_\gamma \cdot \varepsilon_{t-\gamma} \end{aligned} \quad \text{(II.8)}$$

where *P* and *Q* refer to integrated parts.

In the literature, these models are mostly used for both wind power and wind speed forecasting. In fact, in (Alencar et al., 2017) the authors present different wind power forecasting models based on ARMA and ARIMA approaches. In this paper, these models are used for very-short term and short-term wind power predictions. The data used for the implementation and tuning of models are provided by the national organization system of environmental data (SONDA), Petrolina station. In (Colak et al., 2015), the authors, by modelling the multi-time scale as very short-term, short-term, medium-term and long-term, analyse and implement the ARIMA and ARMA approaches for wind speed and wind power forecasting. The results obtained confirm that these models are more accurate for very-short term and short-term prediction.

In the literature, the ARMA approaches are sometimes mixed with the decomposition model, making the original data sequence stable. An example is in (Yu et al., 2017), where the authors propose a two-step model. In the first

part, the Empirical Mode Decomposition (EMD) decomposes the original wind speed sequence into a series of Intrinsic Mode Functions (IMFs), while the forecasting part is entrusted to the ARMA model. The authors demonstrate that the proposed method is more accurate, in terms of prediction error, than the traditional ARMA model.

Many researchers, in order to improve the performance of predictive models based on time-series models, suggest considering the non-linearity of wind. In this regard, in (Lydia et al., 2016), the authors investigate the effectiveness of linear and non-linear time-series models in terms of mean absolute error (MAE), root mean square error (RMSE) and mean absolute percentage error (MAPE). All types of models are ARMA but the difference between them is how the respective parameters are calculated: for linear ARMA models, they are obtained using the Gauss-Newton algorithm, while for non-linear ARMA models, data-mining algorithms are considered. The work highlights that non-linear ARMA models, known as ARMAX, perform better than linear ARMA models.

In the literature, another way to deal with the non-linearity of wind is the use of the aforementioned forecasting models based on ARIMA, as in (Yatiyana et al., 2017), where the authors present a forecasting model based on the ARIMA approach to predict the speed and direction of the wind flow in Australia using historical, real-world wind speed and direction data, collected on the test site over seven days. In (Eldali, 2016) ARIMA models are used for improving wind power forecasts in order to reduce dispatch uncertainty. In the paper, these models are tuned by using historical data of hourly wind power, provided by the Electric Reliability Council of Texas (ERCOT). Sometimes the ARIMA models are mixed with other auto-regression models. An example of this is the prediction model developed in (Tian, 2018). Here, the authors propose a hybrid model based on ARIMA approaches and a Logarithmic Generalized Autoregression Conditional Heteroscedasticity (LGARCH) model, thus achieving higher accuracy in wind power output short-term forecasting in the presence of strong uncertainty by analysing the non-stationary fluctuation characteristics of wind power. The effectiveness of this model is confirmed by performance comparison in terms of mean relative errors (MRE) between basic ARMA, ARIMA and the proposed approach.

In the literature on wind power forecasting, in addition to ARMA and ARIMA approaches, there also exist models based on the Kalman filter (Jiauzhou et al., 2016). The Kalman filter is used for wind forecasting on account of its ability to describe a dynamic system on the basis of its current state. This approach, also known as linear quadratic estimation (LQE), since the state of a system is notoriously only affected by uncertainty and at established time intervals, provides an “optimal” estimate of the state variables, and allows, starting from said estimate, to predict the system’s evolution. The algorithm is composed of two steps: in the forecasting phase,

the Kalman filter generates an estimate of the current state variables affected by uncertainty. Once the outcome of the next measurement has been observed (corrupted by a certain amount of error), the estimate is updated using a weighted average, with a greater weight if the estimate is certain, and vice versa. The algorithm is recursive and works in real-time, using only the current input measurements and the estimation of the previous state in combination with its uncertainty matrix, without needing further information on past values (Anderson et al., 2007). As previously mentioned, the Kalman filter approach has many applications in wind forecasting: in (Zuluaga et al., 2015) the Kalman filter is used for one-step-ahead forecasting of wind speed. In detail, three models are implemented in order to make the forecasting model based on the Kalman filter robust to outliers. The performances are analysed using two wind speed datasets. Another use of the Kalman filter is proposed in (Akcay et al., 2017), in which the proposed forecasting model is implemented for one-step-ahead and multi-step-ahead wind speed prediction, both based on the spectral analysis of long-term observations and the analysis of the missing values that can reduce the estimate's accuracy. Sometimes the Kalman filter approach is used to optimize the numerical prediction model, as in (Hua et al. , 2017), where the authors review, through the Kalman filter method, the weather research and forecast (WRF) model, in order to reduce the forecasting error and to increase the model's accuracy.

The literature on times-series models used in wind speed or wind power forecasting includes not only the models just described. In order to improve the performance of simple and typical ARMA models, there are other statistical approaches based, for example, on Wavelet Transform (Kiplangat et al., 2016), Gaussian Process regression (Zhang et al., 2016), Principal component analysis (Skittides et al., 2014) (Skittides, 2015), spatial and temporal correlation (Haiqiang et al., 2017), Bayesian approach (Xie et al., 2019) or space vector auto regression (Dowell et al., 2016).

II.3 Physical approaches

As time-series models reach forecast horizons of around 6 hours, in the last few decades the dedicated weather forecasts based on physical approaches have received particular attention in the wind energy sector. This approach is based on the use of the physics laws that describe the dynamic behaviour of the atmosphere to predict wind speed, temperature, pressure and humidity (Coiffier, 2012). These models are based on the following set of equations:

- *the first principle of thermodynamic*: the energy of an isolated thermodynamic system is not created or destroyed, but it is transformed, moving from one form to another;
- *the motion equation*;

- *the mass conservation equation*: during a chemical reaction, mass is conserved, i.e. the total mass of the reactants is equal to the mass of total products;
- *the energy conservation equation* (energy can be transformed and converted from one form to another, but the total amount of it in an isolated system does not vary over time) plus the set of equations of conservation of hydrometeors;
- *Navier-Stokes equations*: the system of three balance equations which describe a linear viscous fluid. These equations are able to describe any fluid, even turbulent;
- *the equation of water vapour*;
- *the continuity equation*: the speed at which mass enters a system depends on the speed at which mass leaves the system and the accumulation of mass within the system;
- *the gases equation of state*: the index of how a given set of physical conditions, such as pressure, volume, temperature, influences the state of matter;
- *the hydrostatic equation*: pressure variation is proportional to height variation, the average air density and the gravitational constant.

These equations do not have an exact solution and are solved by numerical approximate methods. The obtained models are thus known as numerical weather prediction (NWP) models. Here, the atmosphere has a discrete representation and it is divided into a number of finite dimensional volumes, creating a regular spatial grid. The size of the volumes characterizes the spatial resolution of the numerical model and the atmosphere is represented at different levels through grid points (Vasquez, 2015) (Figure II.3). In these meteorological models, the atmosphere and its evolution are described according to different weather scales, with respect to the horizontal size of the phenomena that occur in them.
These scales can be classified as follows (Kalnay, 2012):

- *global weather scale*: the longest-lived weather scale which describes phenomena spanning tens of thousands of kilometres in size, extending from one end of the globe to another;
- *synoptic weather scale*: describes the phenomena that extend from a few hundred to several thousand kilometres and have lifetimes of a few days to a week or more;
- *mesoscale weather scale*: includes weather events, such as weather fronts or local wind, that extend from a few kilometres to several hundred kilometres in size and whose evolution is of about a day or less. These events impact areas on a regional and local scale. The mesoscale

is classified into three categories: *meso-α* (2000-200 km), *meso-β* (200-20 km) and *meso-γ* (20-2 km) (Pielke, 2013);

- *microscale weather scale*: refers to weather events, such as turbulence, that are smaller than 1 kilometre in size and very short-lived and only last a few minutes.

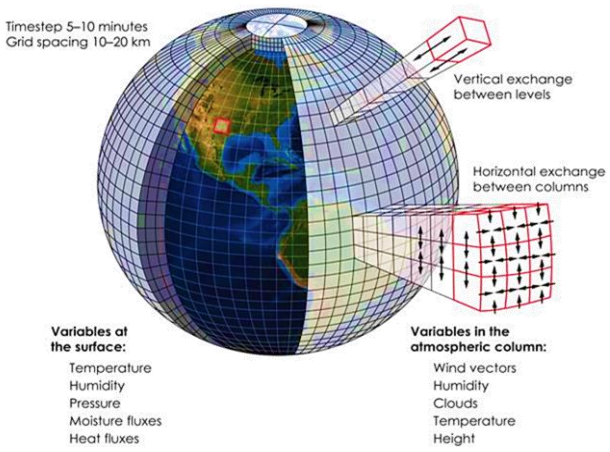

Figure II.3 *NWP weather forecasting modelling*

The NWP models provide, for a given time range, the average value of meteorological parameters characterizing the atmosphere at a grid point or, more specifically, for the spatial domain represented by the grid point. The NWP models are divided into two macro-categories: **global forecasting systems** (GFSs) and **local area models** (LAMs). These two categories differ according to the resolution of the model considered: GFS models reach horizontal resolutions of about 50 km, whereas LAMs use denser grids, with a horizontal resolution ranging from 20 km to a few km (Stensurd, 2009). In detail, global models integrate the physics equations of the atmosphere on the entire Earth (or on one hemisphere), producing long-term predictions. Conversely, in order to obtain more detailed forecasts on restricted areas, LAMs are used. These models, unlike GFSs, require very precise knowledge of both initial and boundary conditions: the result they produce is strongly affected by said conditions. Moreover, local models cannot work by themselves, nor are they suitable for developing large-scale predictions. Therefore, LAMs generally work symbiotically with GFSs. In this way, it is possible to obtain very good results, even on time scales exceeding 6 hours (Warner, 2010). This approach is the basis of the models used by two of the best-known NWP organizations: in USA, the National Centers for Environmental Prediction (NCEP) of NOAA (National Oceanic and Atmospheric Administration), which develops GSF and NAM-HIRES models; and the *European Centre for Medium-Range Weather Forecast* (ECMWF), which develops the Integrated Forecasting System (IFS) model (Coiffier, 2012).

The forecast can be summarized in four steps:

- collection of observations;
- determination of the initial state through data assimilation;
- forecast with the numerical model and post-processing;
- verification of forecasts.

As previously mentioned, for NWP models an accurate observation of the present - and the measurement of each factor connected to it- is important to obtain accurate wind forecasting. The data observed and collected in this phase are measured according to standard criteria, established by the World Meteorological Organisation (WMO) in this way, observations can be compared. The observed data are sent to the various meteorological centres via GTS, the Global Telecommunication System. The received data are pre-processed and transformed into the standard format BUFR (Binary Universal Form for the Representation of meteorological data), as the WMO established, by the SAPP software (Scalable Acquisition and Pre-Processing), developed by the ECMWF.

The system just described is used for several purposes: to continuously pre-process the observations necessary; to verify the numerical forecasts; for the operational needs related to the now-casting activity; to check the quality of the observational data received; to standardize the format of the various local observations available at a national level, and anything else not present on the international GTS circuit.

In Italy, the role of data collection centre lies with C.O.Met. (*Centro Operativo per la Meteorologia*, hereinafter referred to with the acronym COMET); the centre is also entrusted with receiving and processing meteorological remote-sensed satellite data, both through direct reception in L and X band, and through the European Organisation for the Exploitation of Meteorological Satellites (EUMETCAST) network, run by the European agency EUMETSAT.

After the collection phase, due to the diverse nature of the data, a checking procedure becomes necessary, as data coming from observation systems can be affected by uncertainty attributable to the measuring instruments, poor calibration or erroneous observation recording. This control is part of a data assimilation phase, in which the best possible initial state of the atmosphere for a certain time window is found: the data, irregularly distributed in space and time, are analysed by statistical-numerical algorithms to obtain the best estimate of the state of the atmosphere, represented on a regular three-dimensional grid at a fixed instant. It seems clear that an accurate definition of the initial conditions is essential to build a successful NWP model, as the uncertainty linked to initial conditions is predominant compared to other uncertainty sources.

One of the most advanced techniques is the stochastic Kalman filter. The version used by COMET is the Local Ensemble Transform Kalman Filter (LETKF) which in recent years has become an effective alternative to

traditional data assimilation systems based on variation schemes (Bonavita et al., 2005), (Bonavita et al., 2008). Furthermore, COMET is the first operational centre to use an ensemble analysis scheme to initialize an NWP model on a regional scale (Bonavita et al., 2010), (Meng et al., 2011). After the initial and boundary conditions are defined in the previous phase, the forecasting system proceeds with the prediction phase with LAM models. In recent years, high-resolution LAMs have reached an increasingly high level of reliability, becoming widely used in the very short and short-term forecasting activities of operational meteorological centres. The best known LAM is the **COSMO** (COnsortium for Small-scale MOdelling) model (http://www.cosmo-model.org/content/tasks/operational/leps/) which is a deterministic, non-hydrostatic limited-area atmospheric prediction model designed for working on the *meso-β* and *meso-γ* scale (Pielke, 2013) It is based on the primitive thermo-hydro dynamical equations describing a compressible flow in a moist atmosphere (Marsigli et al., 2005) and is the basis of the regional numerical weather prediction used at COMET. LAM models are not only deterministic, providing the "best" forecast of the future atmospheric state, but also probabilistic, especially the ensemble prediction. This means that the set of all possible predictions is evaluated. Assuming that the initial state is an approximation of the actual state of the atmosphere, a set of *N* initial states is generated within which the actual state of the atmosphere is also expected to fall. The physical equations are applied to each of the *N* elements of the initial set of states, thus obtaining *N* different evolutions within which the final actual state is supposed to fall (Kalnay, 2012). The ensemble prediction system (EPS) ends with the statistical analysis of all final states, and from it, the most probable meteorological evolution and its uncertainty will be obtained (Figure II.4).

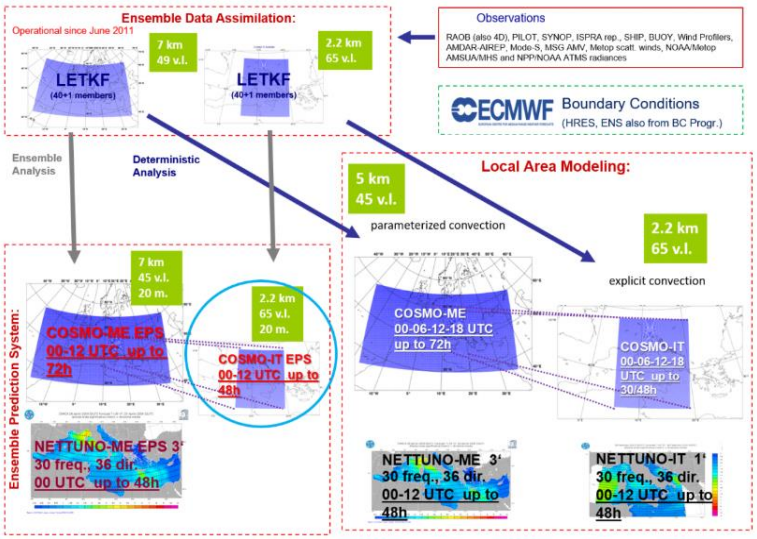

Figure II.4 *Operational LAM scheme of the AM Meteorological Service*

COMET utilizes the COSMO model in ensemble mode in two configurations:

- **COSMO-ME EPS**, consisting of 20 + 1 members integrated on a grid with a pitch of 7 km and 45 vertical levels, covering Central-Southern Europe and the Mediterranean basin, with two runs per day (00 and 12 UTC), for up to a 72-hour forecast. COSMO-ME EPS uses a selection of the initial conditions produced by the LETKF system and boundary conditions by the ECMWF EPS.
- **COSMO-IT EPS** (pre-operational), consisting of 20 + 1 members integrated on a 2.2 km pitch and 65 vertical levels, covering Italy, with two runs per day (00 and 12 UTC), for forecasts up to 48 hours. COSMO-IT EPS uses a selection of the initial conditions produced by the very high-resolution LETKF system and boundary conditions from COSMO-ME EPS.

In addition to the COSMO model, the other main European LAM consortia are the **ALADIN** (http://www.cnrm.meteo.fr/aladin), **HIRLAM** (http://www.hirlam.org) and **LACE** (http://www.rclace.eu) projects and **U.K. MetOffice** (http://www.metoffice.com/research/nwp/index.html), which run on European areas at grid resolutions of 7-12 km.

In the last phase of the NWP processes, the predictions of a numerical model for a given instant are compared with the corresponding observations or analyses for the objective determination of a number of statistical quantities (average error, mean square deviation, etc.). The values of these quantities, calculated over a sufficiently long period from a statistical point of view, provide information on the quality of the numerical forecast (Vasquez, 2002).

In the literature, there are a number of applications for the LAMs to predict wind power and speed on a wind farm, such as (Xu et al., 2015), (Stathopoulos et al., 2013) or (Alessandrini et al., 2013). In particular, these NWP models are implemented by combining them with data-mining models in order to adjust the LAM inputs. Otherwise, like in (Li et al., 2015; Li et al., 2017), the prediction model is optimized by a PSO algorithm in order to forecast wind power with low prediction error. In (Sanz et al., 2008), the authors propose a short-term wind speed prediction model based on hybridizing a global and mesoscale combined with artificial neural networks in order to improve the effectiveness of the NWP model. Furthermore, wind prediction models have been developed in the literature in the last few decades, based on Computational Fluid Dynamics (CFD), which are able to capture the details of smaller scales in the flow when factors such as buildings or fine-scale topography are considered obstacles to the normal flow of wind speed (Zajaczkowski et al., 2011).

II.4 Machine Learning approaches

Machine learning is a method of data analysis that automatizes the construction of analytical models. It is a branch of Artificial Intelligence and is based on the idea that systems, learning from data, can identify models independently and automatically, thus making decisions - once the model has been identified (learning) – with minimal human intervention.

Specifically, machine learning uses algorithms that learn from real-world data, iteratively. The most important aspect of machine learning is repetitiveness, because the more the models are exposed to the data, the more they will be able to adapt independently. Therefore, systems based on machine learning approaches learn from previous processing to produce results and make decisions that are reliable and replicable (Mohssen, 2016).

A prediction model based on machine learning approaches consists of two phases:

- network learning/training;
- forecast.

The training of an artificial neural network can be both supervised and unsupervised. In the first case, the network learns the relationships that exist between the data, using a set of examples that make up the training set. The goal of supervised learning is a prediction that is as truthful as possible, based on a limited number of examples. An example of supervised training is the back-propagation algorithm. Conversely, unsupervised learning uses only the input data without knowing the desired output, and therefore without knowing the relationships between input and output. In fact, it is the network that must find and then learn the aforementioned relationships, based on the characteristics of the input data. Furthermore, learning can occur by reinforcement, which is based on creating algorithms capable of learning and adapting to changes in the environment (Colins, 2017).

In the power system, machine learning methods are able to observe the nonlinear part of wind. For this reason, such approaches are among the most used for wind forecasting (Kariniotakis, 2017). Within these methods, the most developed are artificial neural networks (ANNs), support vector machines (SVMs) and genetic algorithms (GAs), which are described in detail in the next paragraphs.

II.4.1 Overview of machine learning methods

Machine learning methods can be used for solving a wide range of problems such as regression, classification and prediction, in many application fields. For instance, methods based on the Support Vector Machines approach are used for regression and classification analysis (Cortes et al., 1995). SVMs fall within statistical theory. They are based on supervised learning through which it is possible to generalize and to classify new data on the basis of those

learned previously. Hence, given a set of input vectors and a collection of distinct classes, a model is built which assigns a new element to one class or another. A classic example of classification consists in assigning each of the vectors of the input set a unique class value. The data used as examples in the SVM model are represented as points in space, mapped in such a way that the different categories are divided by the widest possible gap; in this way, the new elements will belong to a category according to the side of the gap within which they fall. More formally, an SVM model builds a hyperplane or a set of hyperplanes to classify all data inputs in high dimensional space, according to distance between it and the nearest training data point of any class (Figure II.5). The hyperplane is called a functional margin, whereas the closest values to the margin are called support vectors. In general, the larger the margin between the hyperplane and the support vectors, the lower the classifier generalization error (Abe et al., 2010).

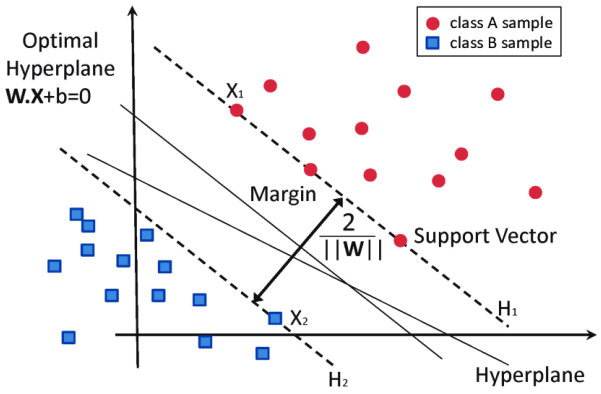

Figure II.5 *Hyperplane classifier*

In the literature, there are a number of applications of SVMs in wind forecasting, as in (Bonfil et al., 2016), where the authors propose a forecasting model based on SVMs for short-term wind speed forecasting. The implemented model, in comparison with the persistence and autoregressive models, presents good performance in terms of MAE, mean bias error (MBE), root mean square error (RMSE), mean absolute scaled error (MASE), and directional accuracy (DA).

Some researchers implement and utilize other versions of SVMs, such as in (Yuan et al., 2015), where the authors present a forecasting model based on least square SVM and a gravitational search algorithm to predict wind power. Sometimes, SVM models are combined with an optimization algorithm, as in (Kong et al., 2015), in which a prediction model is proposed, based on a reduced SVM with the parameters optimized by a particle swarm optimization (PSO) algorithm. In other works, SVM models are combined with statistical analysis, as in (Liu et al., 2017), in which the orthogonal test (OT) is used to describe the various factors related to the different irregular characteristics of the location, which bring difficulty in forecasting. Sometimes, SVM models

are integrated with other machine learning and soft computing approaches such as Fuzzy Logic (FL), a multipurpose logic and an extension of Boolean algebra, suitable for creating very powerful and flexible regulators, reasoners and classifiers. Based on a set of linguistic rules for modelling the real world, just like for human reasoning, FL is mostly used when the system is described qualitatively and there is no suitable model for the purpose considered, or when the multiplicity of objectives to be achieved poses decision difficulty. A FL process starts with a fuzzification of the data (Ross, 2016), then the aggregation procedure is used to combine all forecasted values, as, for instance, in (Zhang et al., 2012), (Kavousi et al., 2016) or (Shiarifian et al., 2018); finally, the FL process, through the defuzzification procedure, returns the result expressed in terms of Fuzzy variables, which is reported into the final forecast, thus improving the accuracy and consistency performance of the predictor model.

Another machine learning method used in the literature is the Genetic Algorithm (GA), a metaheuristic method inspired by Charles Darwin's theory of natural evolution, introduced by John Holland in the 1960s and developed by his student David E. Goldberg in the late 1980s. GAs can be used effectively to solve both constrained and unconstrained optimization problems, where the objective function is discontinuous, non-differentiable, stochastic, or highly nonlinear or not convincingly solved by standard optimization algorithms. The GA uses three main procedure/actions – selection, crossover and mutation – to seek the optimal solution of an optimization function represented by fitness. The GA procedure is implemented as a repetitive evolutionary process: it repeatedly modifies a set of individual solutions; at each step, it selects random solutions, and from these, it constructs a new set of solutions. The algorithm ends when, over successive iterations, the set evolves toward an optimal solution (Mitchell, 1996). Sometimes in the literature (Yin et al., 2017) (Kassa et al., 2016) ,this method is used for optimizing the parameters of Artificial Neural Networks (ANNs), one of the most used machine learning approaches in wind forecasting. These will be described in detail in the next paragraph.

II.4.2 Artificial Neural Networks

ANNs represent the main machine learning methods used in the power system to solve classification, regression and forecasting problems. ANNs, like the FL and GA models described above, are models of information processing belonging to a branch of computational intelligence (or soft computing), inspired by biology. In particular, this method reproduces, to a more limited extent, the functioning of human brain and its computational processes during the phases of learning and recognition.

The main characteristic of an ANN is its being able to learn mathematical-statistical models through experience by reading experimental data, without

having to explicitly determine the mathematical relationships between the input unknowns and the output solutions of a specific problem. Therefore, the parameters characterizing the function of an ANN are not assigned, but trained through a learning process based on historical data known as *examples*.

Like biological neural networks, ANNs are composed of processing units (known as *neurons*) operating in parallel, which can be divided into subsets called *network layers*. Neurons communicate from one layer to another through connections, similarly to biological synapses (Figure II.6) (Fausett, 1994).

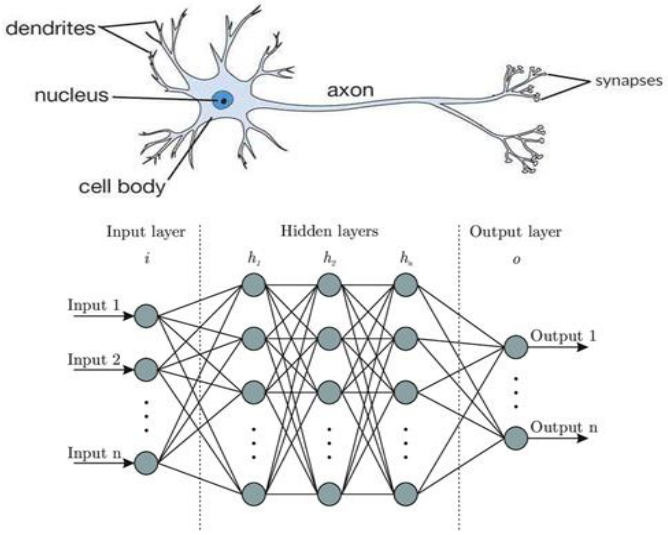

Figure II.6 *Biological neural network and ANN*

According to the organization of the connections between neurons, ANNs can be grouped in two main families (Figure II.7):

- *recurrent networks or feedback*: the connections carry the signal both forward and backward. The Elman and Hopfield networks are the most known recurrent ANNs. The Elman network has three layers and an intermediate layer with a set of context units with a weight of one. In this ANN, the input is passed forward and fixed back connections save a copy of the previous values of hidden units in context units. In this way, the network can maintain a memory of state. Conversely, the Hopfield network features symmetric connections, and if the connections are trained using the Hebbian learning algorithm, the ANN can be considered as a solid content-addressable memory that is independent of connection alteration (Shanmuganathan et al., 2016);
- *non-recurring or feedforward networks*: the connections carry the signal only forward. The simple perceptron and the Multi-Layer Perceptron (MLP) belong to this category. The perceptron is the

first feed-forward ANN implemented, and the MLP network derives from the former (Shanmuganathan et al., 2016).

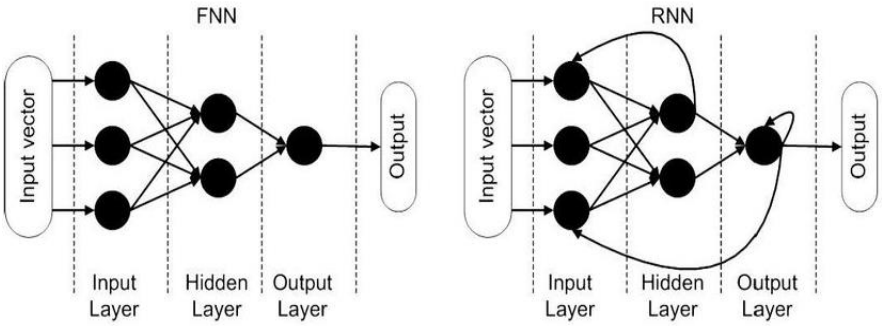

Figure II.7 *Feedforward and feedback ANN*

However, the training procedures can be divided as follows (Shanmuganathan et al., 2016):

- supervised learning: this is a type of learning in which the aim is to minimize the error of network prediction on a finite set of typical examples divided into input-output pairs (training sets). Training can be online, if the correction of the synaptic weights (w) occurs incrementally using one example at a time, or batch type, if the correction is made on the whole error calculated at the end of the training. If the training has been successful, the network learns to recognize the implicit relationship between input and output variables;
- unsupervised learning: information on the environment is received externally without giving any indication of the output values. It is used when the data are not sufficient or incomplete;
- reinforcement learning: this is a machine learning technique. The network interacts directly with the external environment, adapting itself directly to the mutations of it, through the distribution of *rewards* or *punishments*, which guide the algorithm in the learning phase; the network is then trained to increase the probabilities of getting *rewards* and to decrease those of receiving *punishments*.

Perceptron and MLP network

The perceptron network is composed of only two layers, input and output, and one single neuron.

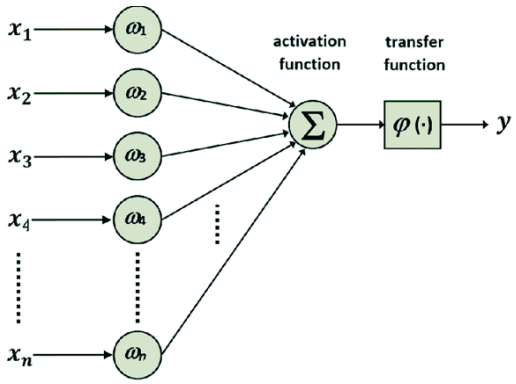

Figure II.8 *Perceptron network scheme*

As shown in Figure II.8, the perceptron network has an activation function and a transfer function: the former calculates the activation potential of the neuron, equal to the sum of all the inputs multiplied by the respective synaptic weights; with the latter, instead, the value of the output signal is calculated on the basis of the activation potential.

The expression of the output of a simple neural network is the following:

$$y = \varphi \sum_{i=1}^{n} w_i x_i \tag{II.9}$$

where $x = [x_1, \ldots, x_n]$ is the input vector and $w = [w_1, \ldots, w_n]$ is the weight vector, while φ is the transfer function which can be the same for all layers or different. The most common transfer functions are:

- **linear function without saturation**: $\varphi = f(P) = kP$, where k is the angular coefficient of the straight line;
- **linear function with saturation**: $\varphi = f(P) = \min(S_{\max}, \max(0, kP))$, where k is the angular coefficient of the straight line and $S_{\max}$ is the function amplitude;
- **Heavyside function**: $\varphi = f(P) = signum(P)$ which can assume binary (0,1) and bipolar values (-1,1), according to the sign of P;
- **Sigmoid function**: $\varphi = f(P) = \frac{1}{1+e^{-kP}}$, which can assume continuous values between 0 and 1, derivability and asymptotic saturation for $P \to \infty$;

- **hyperbolic tangent function**: $\varphi = f(P) = \frac{e^{kP} - e^{-kP}}{e^{kP} + e^{-kP}}$, with values between -1 and 1 and derivable.

Since the Perceptron is particularly simple, it is not suitable for solving problems of non-linear separation. For this reason, it was necessary to create a new network, the MLP (multi-layer perceptron) (Shanmuganathan et al., 2016), the most widely used type of ANN today. This network consists of an input layer, one or more intermediate layers (hidden layers) and an output layer (Figure II.9).

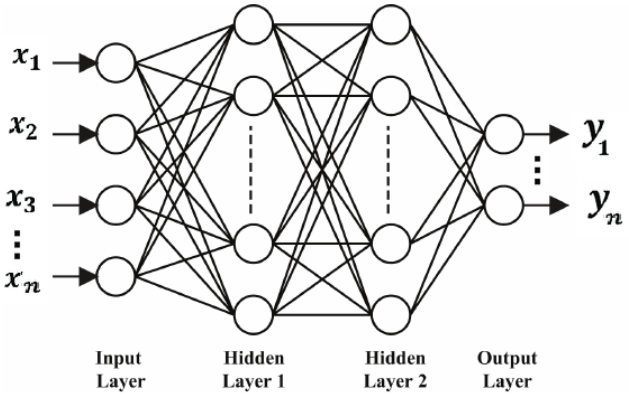

Figure II.9 *MLP network architecture*

In this new architecture, the outputs of a layer become the inputs of the next layer (feed-forward network), except for the last one, where the outputs correspond to the actual network outputs. The transfer function used for the intermediate layers and for the output layer must be non-linear – typically, sigmoid – while the input layer acts as a "buffer" for network inputs and uses a ramp with the saturation transfer function, to limit the range of values that the network inputs can assume. As mentioned above, since the MLP is a feed-forward network, the actual outputs of the network will be calculated last, that is, we will first proceed to calculate the outputs of the first layer, then those of the intermediate layers, and finally those of the output layer, which correspond to those effects. Typically, when the problem to be dealt with becomes more complex, it is possible to increase the number of intermediate layers up to a maximum of hidden layers equal to 2, thus extending the network resolution capacity to concave-convex problems also.

Usually, a back propagation learning algorithm is used to train an MLP network. The aim of this training algorithm is to minimize the cost function of the network, that is, the root mean-square error between all network outputs and the values desired, contained in the training set. Given a network with n input x_i (with i = 1,2, ..., n), a hidden layer of q neurons Z_k (with k=1, 2, ..., q) and an output layer of m neurons y_j (with j = 1, 2, ..., m) the training set

consisting of p examples, and all neurons having the same transfer function, the error function of the output layer is expressed as follows:

$$E = \frac{1}{2}\sum_{r=1}^{p}\sum_{j=1}^{m}\left(y_{rj} - d_{rj}\right)^2 \qquad \text{(II.10)}$$

where y_{rj} is the output y_i relative to example r, and d_{rj} is the corresponding output desired. At this point, by applying the gradient rule, the expression used for updating the synaptic weights of the connections between the hidden layer and output layer (ΔW_{jk}) and input layer and hidden layer (ΔW_{ki}) is obtained:

$$W_{jk}(t+1) = W_{jk}(t) + \Delta W_{jk} \quad \text{with } \Delta W_{jk} = -\eta \frac{\partial E}{\partial W_{jk}} \qquad \text{(II.11)}$$

$$W_{ki}(t+1) = W_{ik}(t) + \Delta W_{ki} \quad \text{with } \Delta W_{ki} = -\eta \frac{\partial E}{\partial W_{ki}} \qquad \text{(II.12)}$$

The updating procedure is iterated for all the examples of an *era* (in the online mode) and for all the periods available. It stops when a predetermined error value is reached.

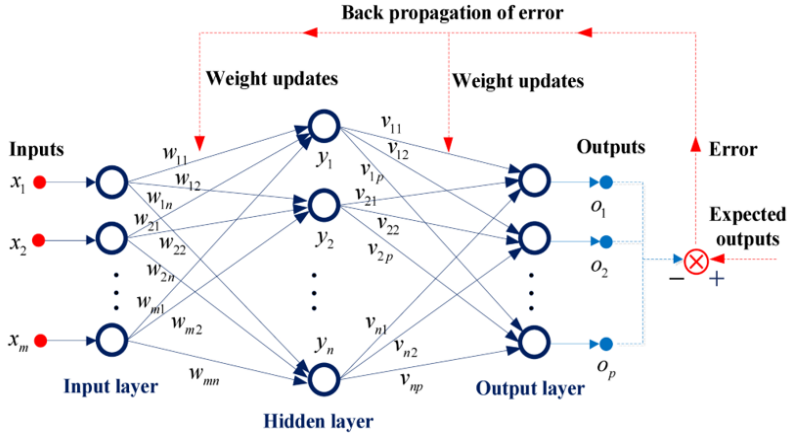

Figure II.10 *Back propagation algorithm for an MLP*

In the literature, the ANN is the most used approach in wind forecasting (Giebel et al., 2017), (Kaur et al., 2016). In fact, in (Moustris et al., 2016), a 24-*h* wind speed prediction model based on the ANNs and the hourly based wind speed is proposed. Sometimes, in order to obtain an accurate wind speed forecasting model, the ANN is combined with a Weibull distribution (Kadhem et al., 2017). More in detail, the implemented method produces wind speed data predictions according to the dependence on seasonal wind variations over a particular time frame, usually a year, in the form of a Weibull distribution. ANNs also are used in short-term wind forecasting, both for wind speed and wind power. In detail, according to (Marugàn et al., 2018), ANNs

can be used for several applications, including forecasting and predictions, design optimization, fault detection and diagnosis, optimal control. In (Chang et al., 2017) and in (Kurdikeri et al., 2018), ANNs are used for wind speed and wind power predictions. In detail, in the former work, the authors propose a particular radial basis function neural network-based model with an error feedback scheme for forecasting wind speed and wind power, In the latter paper, instead, the authors make a comparative study of feed-forward network models and recurrent neural network models.

II.5 Hybrid approaches

In addition to the aforementioned approaches, as seen in the literature, hybrid models have been implemented to forecast wind energy or wind speed. These models are a combination of statistical and machine learning approaches or of two different machine learning approaches, and they are mainly used for medium- and long-term forecasts (Chang et al., 2016), (Makhloufi et al., 2017). For example, in the medium-term prediction model, an ANN combined with an FL can improve predictions: the FL approach can be used for the training phase and the ANN for the prediction phase. In this way, the first part of the model is faster and therefore the methods tend to converge more quickly (Singh et al., 2018).

Another example is to construct a forecasting model based on merging a statistical process, such as a moving average process, and a machine learning approach such as an SVM. To this regard, in (Chen et al., 2018), the authors propose a forecasting model based on a nonlinear-learning ensemble of a deep learning time series prediction. In detail, LSTMs (Long Short-Term Memory neural networks) are used to explore and exploit the implicit information of wind speed time series, when diversiform data can generate a weak generalization capability, whereas SVM and EO (Extremal Optimization) algorithms are used for the prediction phase. Some researchers propose novel methods based on merging neural networks and optimization algorithms in order to forecast wind speed with a low prediction error. In these works, the optimization phase is important to obtain the best parameters of data mining models, which are then employed in the forecasting phase (Meng et al., 2016), (Wang et al., 2016a), (Wang et al., 2016b).

Moreover, in a number of works, hybrid models are employed in short term wind forecasting, thus obtaining good performances in terms of prediction error, as in (Jiang et al., 2017), (Liu et al., 2014), (Zhang et al., 2015), or (Eseye et al., 2017). Conversely, we propose models based on a combination of Wavelet Transform and SVM, or GA and FL, or SVM and Empirical Decomposition. In these models, the forecasts are obtained through two steps: the first, in which the model's parameters are searched and initialized through statistical methods or data mining approaches; and the second, in which machine learning methods are used for wind forecasting.

II.6 Commercial tools

The importance of having tools for the prediction of the electricity produced by wind power has created an actual market sector. The commercial wind power prediction tools (WPPTs) available on the market are based on the methods just described. WPPTs are implemented, in almost all cases, by universities or research centres (Ackerman, 2012). Some examples of commercial tools are described below.

Wind Power Prediction Tool

This tool is an applicative example of how to make use of the aforementioned statistical methods to predict the power produced by wind turbines in larger areas. It was developed through the collaboration between Eltra, Elsa and the IT Department and Mathematics of the University of Denmark. The tool uses online data from only a portion of the entire set of wind turbines in the area; in fact, the area of interest is divided into sub-areas and each of them represents a particular wind farm. The weather forecast of wind speed and direction is used to predict the power produced by the wind for periods ranging from half an hour to 36 hours. Once the forecasts for each sub-area are attained, they are reprocessed to obtain the forecast of the whole area of interest. The inputs of this tool are wind speed and direction, the temperature and the output power of the reference wind farm, and they are sampled every 5 minutes; furthermore, forecasts must be added to these weather inputs. These are charged every six hours and cover a 48-hour period. In WPPTs, one of the statistical methods described is used to determine the optimal weights between local measures and variables of weather forecasts (Giebiel, 2003).

Zephyr

This tool is the result of the merging of the statistical and persistence methods. In this way, it is possible to make predictions for a period of time greater than with WPPTs; in fact, forecasts can be made both in the short term (0-9 hours) and the long term (36-48 hours). The tool was developed by the Department of Computer Science and Mathematics and by the National Risø Laboratory[1] in Denmark (Giebiel et al., 2002).

Previento

Previento[2] is able to make power forecasts in a large area both for now-casting and a long-term forecasts. It uses a predicting method based on human observation, using persistence (the next event is expected considering only the

[1] http://www.risoe.dk.
[2] http://www.previento.de.

previous event). This tool was developed by the University of Oldenburg, Germany (Focken et al., 2001).

eWind

Developed by True Wind Solutions, USA, eWind is made up of four main components:

- a set of three-dimensional atmospheric numerical models based on physics;
- adaptive statistical models;
- models for building the plant;
- system for receiving the forecast.

The first of the points listed above is similar to the one used for weather forecasting. Adaptive statistical models are a set of empirical relationships between the output of atmospheric models based on physics and the specific parameters to predict for a certain area. These parameters are wind speed and direction of the wind turbines that send power to the substations. The third component connects the atmospheric variables with the output of the wind turbines. The output of a wind turbine is a combination of the latest atmospheric data and of the output data of the wind turbine. The last part of the system refers to the user's choice of how to obtain the information relating to the forecast (Giebiel, 2003).

SIPREOLICO

This is a prediction tool based on statistics, developed by the Carlos University of Madrid, Spain. For a single turbine, this tool uses four types of inputs: the wind farm's characteristics, the historical data of the wind and the power produced by the turbines, and weather predictions. The predictions depend on what type of input is available. The input data can be partial or complete. Partial data are those available for each wind farm, i.e. weather forecast and standard curves of power, plus real power curves, while complete data are those just listed plus real-time data of generated energy (Sánchez et al., 2002).

II.7 Forecasting evaluation metrics

The efficiency and effectiveness of a forecasting model are usually evaluated through four figures of merit: mean absolute error (MAE), mean absolute percentage error (MAPE), mean square error (MSE) and root mean square error (RMSE) (Kariniotakis, 2017). All evaluation metrics are described in detail below.

In statistics, MAE is a measure of difference between two continuous values, which, in a forecasting model, are the predicted and desired values. This metric is a common measure of forecast error and is defined as follows:

$$MAE = \frac{\sum_{i=1}^{n} |e_i|}{n} \text{ with } |e_i| = |y_i - d_i| \tag{II.13}$$

where y_i is the i^{th} forecast value and d_i is the i^{th} desired value.

MAPE is the index of how accurate a forecasting model is. The forecasting accuracy is measured in percentage and it is calculated as mean of absolute percentage error for each time period. The expression of MAPE is given by:

$$MAPE = \frac{1}{n} \sum_{i=1}^{n} \left| \frac{y_i - d_i}{d_i} \right| \times 100\% \tag{II.14}$$

MSE evaluates the quality of a predictor, according to the average of the squares of the errors, that is, the average squared difference between the forecasting values and the desired values. Given a vector of n predictions, D is the vector of the desired values of the variable being predicted, and the Y is the vector of the forecasted values. The MSE of the predictor is calculated as follows:

$$MSE = \frac{1}{n} \sum_{i=1}^{n} (D_i - Y_i)^2 \tag{II.15}$$

Finally, the last figure of merit, RMSE, represents the standard deviation of the prediction errors, known as residuals. These measure how far from the regression line the data points are; RMSE is also a measure of how the data is concentrated around the line of best fit. Root mean square error is commonly used in forecasting and regression analysis to verify experimental results. RMSE is expressed as:

$$RMSE = \sqrt{\frac{1}{n} \sum_{i=1}^{n} (D_i - Y_i)^2} \tag{II.16}$$

where, as before, D and Y are respectively the desired vector and the predicted vector.

Chapter III
Day-ahead wind prediction

In the following chapter, the proposed model for daily wind speed forecasting is described. The chapter begins with a description of the methodology underlying the proposed model, based on the space-time relationships between weather variables and on the evolution of the weather fronts; the model's flowchart is then presented and described in each of its parts. Afterward, the proposed model is validated through the analysis of a case study focusing on real-world data.

The chapter ends with a discussion of the forecasting results obtained and an analysis of the neural predictor's implemented performances, with respect to the main figures of merit used in the literature.

III.1 Methodology

Due to the nature of wind and its dependence on the evolution of weather phenomena, the wind speed forecasting problem is considered a site-dependent problem.

In general, many of the wind forecasting models proposed in the literature (both for wind speed and wind direction) are based on the relationship between one-day-ahead and historical data, both referring exclusively to the site chosen for the forecast (Wang et al., 2016) (Karakuş et al., 2017). Even in most of the forecasting models and commercial tools used in the field of wind generation, wind speed prediction models are based on the relationship between wind speed and other meteorological factors influencing wind production fed by data referring exclusively to the site chosen for prediction (Dong et al., 2016) (Zheng et al., 2017) (Ackerman, 2012).

Unlike the aforementioned approaches, the proposed day-ahead forecasting model is based on the relationship between the wind information of the site chosen for the prediction and the evolution of some weather parameters in the larger area around the site itself. More in detail, the proposed approach analyses both the influence of the weather front evolution on wind

generation and the relationship between wind speed and the main meteorological factors (specifically barometric pressure and temperature) which influence wind generation at the point where the forecast is to be made, and on a larger area around the site itself. In fact, according to meteorology, wind is the phenomenon of air displacement from high to low pressure on large areas, from synoptic to mesoscale (Landberg, 2015). Precisely because of the vastness of the area that affects the wind phenomenon, air does not simply move from high to low pressure, but rather deflects to the right in the Northern Hemisphere, circulating clockwise around high-pressure centres and counter-clockwise around low-pressure centres, all being reversed in the Southern Hemisphere (*Buys-Ballot law*). This effect is a direct consequence of the Earth's rotation, and the phenomenon is not appreciable locally. In practice, air is subjected to a force known as *Coriolis force*, the effects of which are as great as is the speed of air (Emeis, 2013) (Figure III.1).

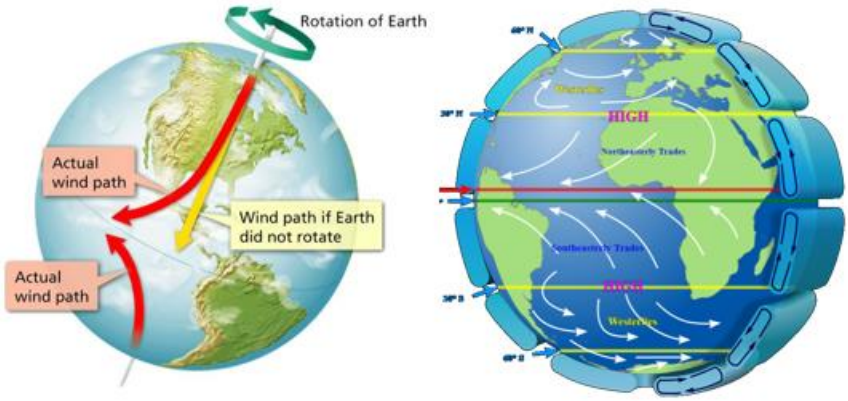

Figure III.1 *Coriolis force effects*

Wind intensity depends on the "baric gradient", i.e. the ratio between the pressure difference of two geographical points and the horizontal distance between the two points. In other words, wind will be as intense as the baric gradient will be. Pressure variation – and hence wind intensity – mainly depends on temperature variation. In fact, when temperature increases, pressure variation decreases, as hot air tends to expand, becoming less dense and lighter. The lower weight of the hot air mass reduces the air column pressure and thus the atmospheric pressure. Conversely, when air cools, its density increases, and the greater weight of the air mass increases the atmospheric pressure, which varies over 24 hours and changes between day and night. Hence, sudden changes in temperature are equal to substantial changes of weather conditions and, more in detail, of wind speed (Emeis, 2013).

Due to the solar radiation, areas of thermic discontinuity are created with the consequent formation of warm air masses and cold air masses, which, in their motions, move from high pressure to low pressure areas. When two air

masses at different temperatures come into contact with each other, a meteorological front, also called a weather front, is created. Weather fronts are active on a mesoscale and synoptic scale, from a few hundred to a few thousand kilometres. In detail, a weather front is a transition surface between two air masses with different temperature, pressure and humidity; the passage of a weather front determines changes in wind, both for wind speed and wind direction. The weather fronts that determine these changes are two: cold and warm fronts, to which the occluded front must be added, characterized by phenomena common to both fronts (Spellman, 2012). According to mesoscale theory, cold and warm weather fronts are characterized by two different speeds: cold fronts move faster than warm fronts, with a much faster variation, due to the higher vertical thermal gradient (Figure III.2a). Hence, when a cold front appears, the temperature drops sharply and the atmospheric pressure increases, thus producing a drastic change in the wind's direction (from southwest to northwest or from west to north in the Northern Hemisphere) and a sudden increase in wind speed (Figure III.3).

Conversely, a warm front appears when a mass of warm air advances, thus invading areas previously occupied by masses of cold air. As warm fronts feature less dense air, they tend to move over the cooler air gradually, thus moving more slowly than cold fronts (Figure III.2b). With the passage of the warm front, the temperature increases and the pressure decreases; therefore, the wind decreases in intensity and changes direction, thus rotating counterclockwise, when in the Northern Hemisphere, from south to south-west or west (Figure III.3) (Ackerman et al., 2007).

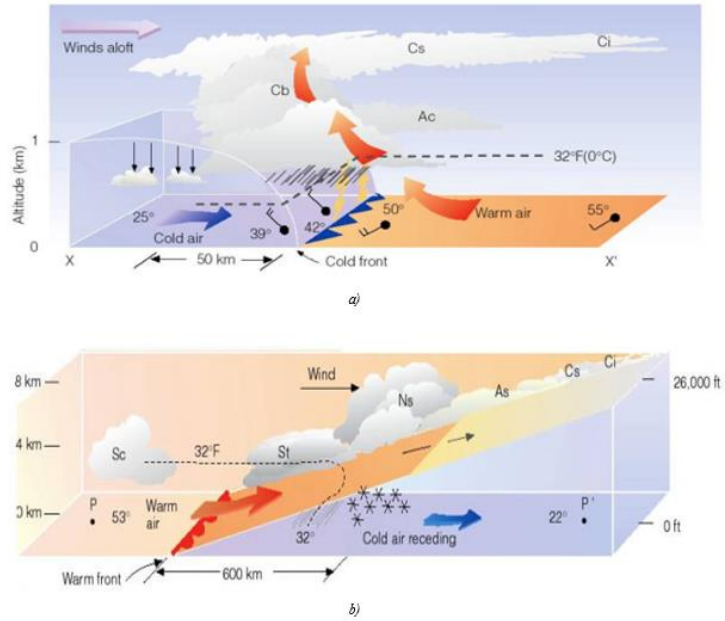

Figure III.2 *a) cold front formation b) warm front formation*

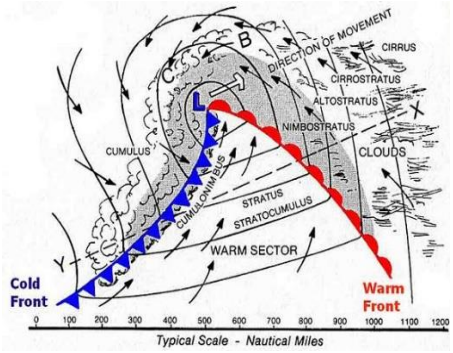

Figure III.3 *Cold and warm front effects*

The relationship between barometric pressure, temperature and wind speed and the influence of the weather phenomena from the surrounding regions on a chosen site are, as previously mentioned, the basis of the proposed model, which will be described in detail in the next paragraphs.

III.2 Problem formulation

According to eq. (II.2), the wind power of a given wind farm depends on wind speed *W*, which is the only quantity that is highly variable. Hence, the wind power on a chosen site S_0 at one day-ahead depends on wind speed at one day-ahead t^{+1}:

$$P(S_0, t^{+1}) = f(W(S_0, t^{+1})) \tag{III.1}$$

Therefore, in order to predict the wind power that a given wind farm can produce, it is necessary to forecast the wind speed of the chosen site.

As previously mentioned, according to the weather phenomena related to wind, wind speed depends on barometric pressure *P* (mb) and temperature *T* (°C).

The wind speed on a chosen wind farm located at S_0, at an instant t^{+1} depends on barometric pressure, *P*, temperature, *T* and wind speed data, *W* assumed in previous times t^{-k} in the same place S_0 and in more or less close points $S_{i,j}$ located around the point S_0 on the mesoscale distance $d(S_{i,j}, S_0)$.

The model can be formalized through the following equation:

$$W(S_0, t^{+1}) = f\begin{pmatrix} T(S_{i,j}, t_{i,j}^{-k}); P(S_{i,j}, t_{i,j}^{-k}); W(S_{i,j}, t_{i,j}^{-k}) \\ \vdots \\ T(S_{i,j}, t_{i,j}^{-2}); P(S_{i,j}, t_{i,j}^{-2}); W(S_{i,j}, t_{i,j}^{-2}) \\ T(S_{i,j}, t_{i,j}^{-1}); P(S_{i,j}, t_{i,j}^{-1}); W(S_{i,j}, t_{i,j}^{-1}) \\ T(S_0, t^0); P(S_0, t^0); W(S_0, t^0) \end{pmatrix} \tag{III.2}$$

In eq. (III.2), the space-time evolution of the weather front is represented by the variable $t^{k}_{i,j}$, where the subscripts i and j are, respectively, the distance and the direction of the point $S_{i,j}$ with respect to S_0, with $i \in \Delta$, where Δ is the set of distances and $j \in \Omega$, with Ω the set of directions, respectively. $k \in K = \{-k, \ldots, -1, 0, +1\}$ indicates the number of time steps taken by a weather front located at point S_i to reach point S_0 moving in the j direction, while the value *+1* indicates the future time with respect to which the forecast is made.

Even though in the model there are no constraints in positioning the points $S_{i,j}$, with respect to S_0, as will be seen in the next paragraph, in the proposed approach the points $S_{1,j}$ and $S_{2,j}$ lie on two concentric circles centred in S_0 and of radius $r_{1,j}$ and $r_{2,j}$ ($\Delta = \{r_{1,j}, r_{2,j}\}$) along the 8 main directions of the compass rose ($\Omega = \{N, NE, E, SE, S, SW, W, NW\}$).

In first approximation, the radii are chosen as follows:

$$r_{2,j} \cong 2r_{1,j} \tag{III.3}$$

Moreover, in the eq. (III.2), t^{+1} is the forecast time horizon, while $t^{-2}_{i,j}$ and $t^{-1}_{i,j}$ are the temporal instants preceding t^{+1} at the point $S_{i,j}$. These depend on t^0, the current time instant, and are defined as follows:

$$\begin{cases} t^{-1}_{r1,j} = t^0 - \tau \\ t^{-2}_{r2,j} = t^0 - 2\tau \end{cases} \tag{III.4}$$

where τ is the time-shift delay factor, used to carry into account the information relating to the temporal evolution of weather phenomena. The value of this factor will be defined in the next paragraphs.

III.3 Proposed forecasting model

In this thesis, starting from the problem model just introduced, a wind predictor based on MLP artificial neural network (ANN-MLP) to forecast the daily wind speed on an actual wind farm (Shanmuganathan et al., 2016) was built. The predictor is composed of three layers – input, output and one hidden layer – and the back propagation algorithm is used for the supervised learning phase.

The building of the neural predictor model is structured in accordance with the model described in paragraph III.2. In order to analyse the weather fronts phenomena, the model is built on the basis of the nesting theory (NT) (Coiffier, 2012) used for advancing global numerical weather, including the ECMWF[3] and in the COSMO LAM model (Bohme et al., 2011).

[3] https://www.ecmwf.int/en/research/modelling-and-prediction

The model's inputs are temperature *T*, pressure *P* and wind *W*, measured at different times and at different points around point S_0, where the forecast is to be made (which will also be called Point of Interest - POI), whereas the model's output is wind speed *W* at point S_0 time t^{+1}.

According to the NT, in order to obtain large-scale weather predictions, the identification of hundreds or even thousands sites located around the POI is necessary. In this thesis, a simplified version of the NT is proposed. Around the area of the POI, a grid based on the 8 main directions of the compass rose - defined in the set $\Omega = \{N, NE, E, SE, S, SW, W, NW\}$ - on two different distances was built, for a total of 16 points, over the POI. Starting from the site where wind speed has to be forecasted (POI), the model identifies eight sites $S_{2,j}$ at distance r_2 (500 km) from the POI S_0, and eight sites $S_{1,j}$ at a short distance, r_1, 250 km (Figure III.4a and III.4b). The data considered are the average weather data at three different times to describe, according to mesoscale model (Pielke, 2013), the daily evolution of weather fronts (Figure III.4c). According to the seasonality of meteorological fronts, the weather data related to each identified site are clustered.

In this way, the data set constructed for the proposed model contains meteorological information related to the sites near the point chosen for the prediction and to the point itself.

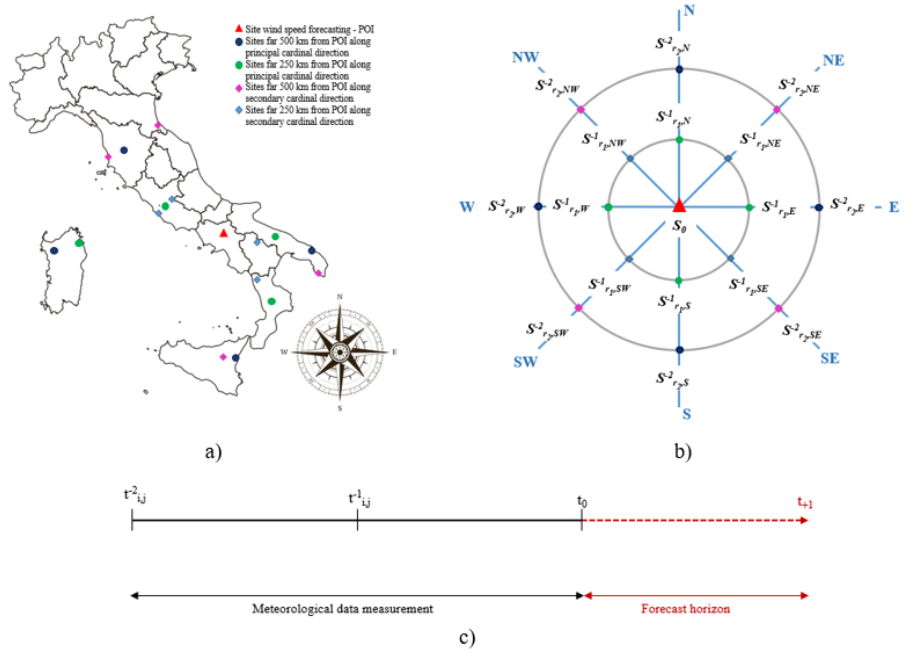

Figure III.4 *a) Geographical location of the sites and POI. b) Schematic illustration of the sites along the principal and secondary cardinal directions. c) Time forecast horizon*

III.3.1 Model's structure

The first phase of the forecasting model's building process, as described in Figure III.5, is data filtering. In this phase, according to a distance r_1 and r_2 from S_0, the two regions where the points $S_{i,j}$ are located are identified, with respect to which historical pressure, temperature and wind data (quarter-hourly, hourly or daily average) are acquired. Subsequently, starting from the data analysis, the value of the time-shift delay (*τ-factor*) is determined, which, as previously mentioned, depends on the choice of the points. From an operational point of view, the choice of the *τ-factor* is made by trial and error procedure, implementing a set of ANN-MLP for different τ values and evaluating the error. Once the τ-factor has been identified, three training sets are built, as per eq. (III.3) and eq. (III.4). In order to reduce the forecast error, the neural predictor was trained by the constructed training sets and, by comparing the neural network performances, the best training is identified. After that, the model proceeds with the wind speed forecasting. The forecast results are compared with the real-world wind speed registered by the weather station, and, in order to verify the effectiveness of the proposed approach, the model's performances are evaluated.

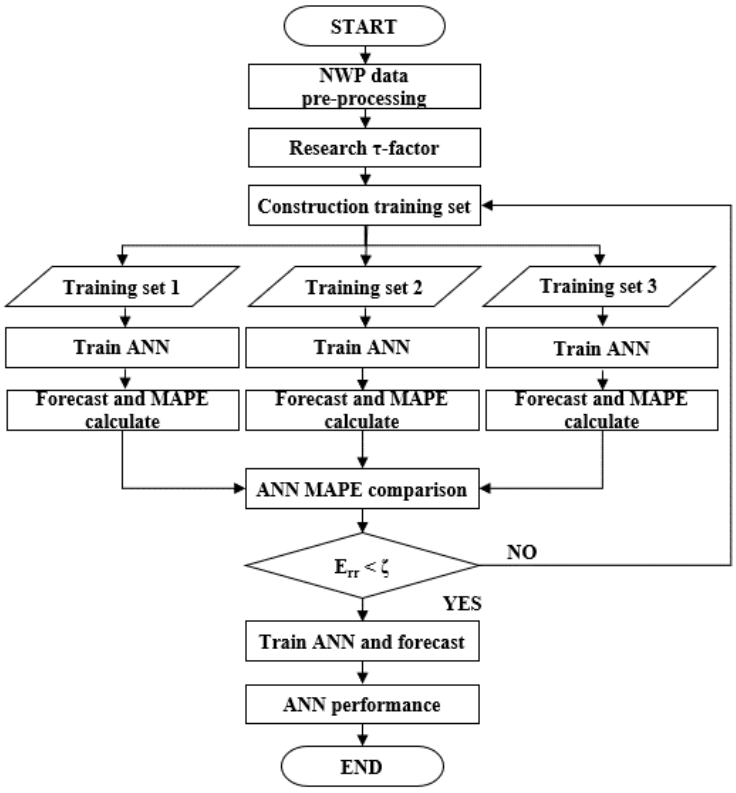

Figure III.5 *Flowchart of the proposed model*

Evaluation of time-shift delay

The use of the time-shift delay allows to describe, in the proposed neural predictor, the temporal evolution of the weather fronts taking into account the characteristics of the area covered by the forecast. More in detail, the input vectors of the proposed model are the collected meteorological data that are shifted in time according to the time relationship expressed in eq. (III.4), where the time-shift delay, *τ-factor*, belongs to {3 *h*; 6 *h*; 9 *h*; 12 *h*; 15 *h*, 18 *h*; 21 *h*; 24 *h*}.

Since the speed of the fronts is generally a seasonal function, in order to determine the *τ-factor*, the implemented ANN-MLP is trained with four clusters of three months, and it is used to forecast wind speed in the central month of each cluster.

The four clusters are:

- **cluster I**: December, January, February;
- **cluster II**: March, April, May;
- **cluster III**: June, July, August;
- **cluster IV**: September, October, November.

The clusters, and hence the training set, contain the historical weather information series that cover a period of a few years (four in the implemented case).

The criteria used for choosing the *τ-factor* are the model's performances in terms of MAPE: the case of lowest MAPE corresponds to the best *τ-factor* (Table III.1).

Table III.1 *MAPE for different τ-factor*

τ-factor	**Months**			
	JAN	**APR**	**JUL**	**OCT**
τ = 3 *h*	29.38%	42.29%	27.82 %	34.41%
τ = 6 *h*	16.96%	20.64%	12.35 %	24.67%
τ = 9 *h*	21.83%	19.69%	13.63%	21.75%
τ = 12 *h*	11.74%	12.24%	7.27%	11.87%
τ = 15 *h*	15.61%	14.35%	14.22%	17.39%
τ = 18 *h*	22.21%	19.09%	19.21%	23.04%
τ = 21 *h*	26.88%	32.22%	29.13%	32.49%
τ = 24 *h*	28.22%	36.09%	32.85%	34.58%

The evolution of MAPE, calculated for the various simulations with the different τ values, showed that MAPE, for the choice of the points $S_{i,j}$,

decreases for *τ-factor* equal to 12 *h* and 15 *h* (green area in the graph – Figure III.6).

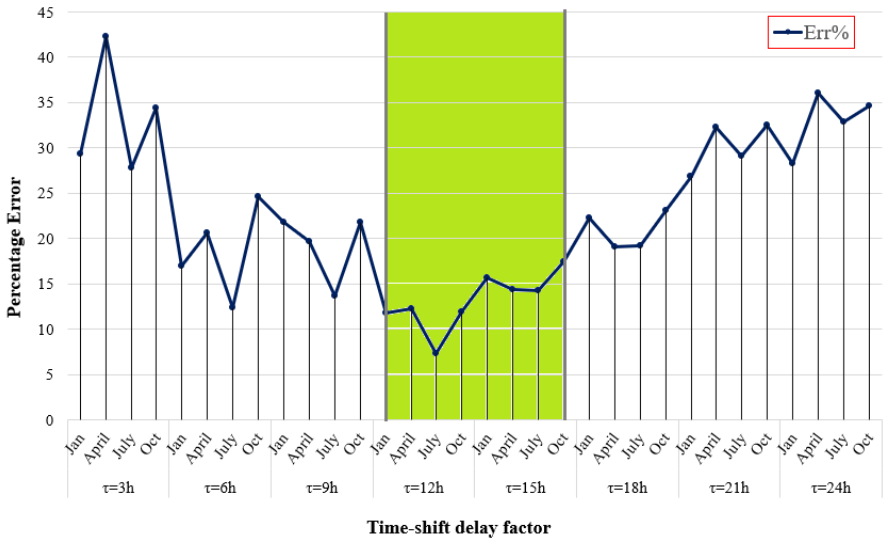

Figure III.6 *MAPE for all values of τ-factor*

Therefore, the *τ-factor* set is reduced, and it becomes {12 *h*, 13 *h*, 14*h*, 15 *h*}. As before, in order to determine the best *τ-factor*, the criteria are the model's performances in terms of MAPE: the wind speed values are forecasted, characterizing eq. (III.4) with the new *τ-factor* set. In the table below, the performances related to each wind speed prediction are reported.

Table III.2 *MAPE values in the new τ-factor set*

τ-factor	**Months**			
	JAN	**APR**	**JUL**	**OCT**
τ= 12 *h*	11.74%	12.24%	7.27%	11.87%
τ= 13 *h*	12.73%	14.92%	11.48%	14.42%
τ= 14 *h*	10.74%	13.79%	15.43%	17.42%
τ= 15 *h*	15.61%	14.35%	14.22%	17.39%

As depicted in Figure III.7, the evolution of the percentage error, related to the various simulations with the new range of *τ-factor*, shows that the percentage error is lower in the case of *τ-factor* equal to 12 *h* than in the other cases (selection area of the graph – Figure III.7).

Hence, in the analysed case, the best value of *τ-factor* is 12 *h*.

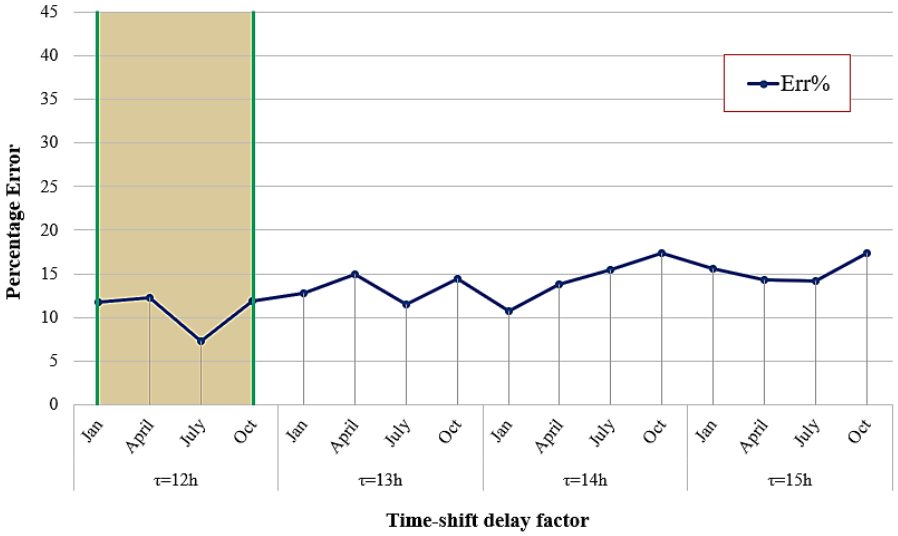

Figure III.7 *MAPE for the new τ-factor set and best τ-factor value area*

It is important to note that a single *τ-factor* will be used, even though the model allows to specify a different time-shift delay factor for each cluster and for each direction.

After the choice of the *τ-factor*, the model proceeds with the training of the neural network. More in detail, after determining eq. (III.4) with the best *τ-factor*, the best training procedure is investigated in the model.

Training procedure

The training phase is an important part of the neural model, as in it, the predictor learns the relationship between wind speed and meteorological phenomena. Hence, finding the best training set is important to obtain a good wind forecast. To this regard, the ANN-MLP is trained with three different training sets; subsequently, the predictor is used for wind speed forecasting and then, through a performance analysis in terms of MAPE, the best training set is found. The training procedure uses, in all cases, the back propagation learning algorithm, whose aim is to minimize the mean square error.

Of the three training sets constructed, two are seasonal and one is dynamic. Following the seasons, in the first case the year is divided into four clusters, whereas in the second case the year is divided into three clusters. The third set is a dynamic training set, which moves in a dynamic temporal window, according to the forecast horizon. In particular, the training set is built considering data referring to 45 days before the time of the forecast and 45 days after it.

Below, Table III.3 describes the three cases.

Table III.3 *The three training sets*

CASES	TRAINING SET	DESCRIPTION
1° CASE	Seasonal Set: 4 CLUSTER	1 CLUSTER: Dec, Jan, Feb; 2 CLUSTER: Mar, Apr, May; 3 CLUSTER: Jun, Jul, Aug; 4 CLUSTER: Sep, Oct, Nov
2° CASE	Seasonal Set: 3 CLUSTER	1 CLUSTER: Nov, Dec, Jan, Feb; 2 CLUSTER: Mar, Apr, May, Jun; 3 CLUSTER: Jul, Aug, Sep, Oct;
3° CASE	Dynamic Set	The training set covers a variable with a temporal window of 90-days

The implemented forecasting model is used for predicting wind speed in the most critical months of the year (January, April, July and October), in which the variations of the weather conditions are frequent due to the continuous weather fluctuations, typical of seasonal changes.

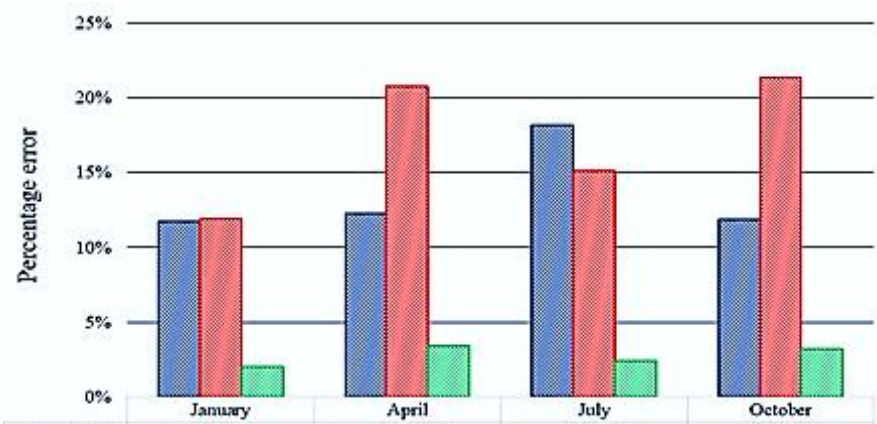

	January	April	July	October
1° trainMLP	11,74%	12,24%	18,20%	11,87%
2° trainMLP	11,90%	20,77%	15,14%	21,37%
3° trainMLP	2,04%	3,38%	2,41%	3,18%

Figure III.8 *Comparison of MAPE performance in all three cases*

The forecast's results – obtained in all cases – are compared with the real-world data registered by the weather stations in those particular months; then the model proceeds with the performance analysis. According to the MAPE performance, the best training set is the dynamic one (Figure III.8).

III.4 Case study

The implemented forecasting model is used for predicting the daily wind speed on a wind farm sited in Campania, Southern Italy. As previously mentioned, the implemented predictor is an ANN-MLP, with one hidden layer, and the activation function chosen is the logistic sigmoid function. The training set and the validation set cover respectively 80% and 20% of the data set, which covers a period of four years, and the forecasting period is refers to a whole year.

III.4.1 Input data

The implemented model is applied on a data set of daily average meteorological information. As explained in the previous section, the data set is dynamic and varies with the forecast's time; it contains three variables: wind speed W (m/s), air temperature T (°C) and barometric pressure P (mb). The weather data used refer to the mesoscale α model, which is able to describe the meteorological fronts' effects in a range of 200–2000 km (Pielke, 2013).

The data sampling frequency is 10 min/point, but in the case of daily prediction, the daily average value of each meteorological data is calculated using only one value for each day (see Appendix A). The meteorological data, for each of the sixteen chosen sites, are provided by the *Italian Air Force Meteorological Service* weather station sited in each of the points considered. The data of the point S_0 are also provided by IVPC, registered by an anemometer and a weather station installed in its own wind farm, chosen as a test site. The wind data of the considered weather stations are referred to 10 meters.

III.4.2 Results and discussion

The simulation's results refer to a period of one year and are compared to the measured values. The predicted values are the mean (not the best!) of 10-runs of network simulation; in this way, all the prediction values, not only the results with low prediction error, are considered, with the aim of demonstrating the robustness of the model. The effectiveness of the proposed model is proven by the comparison between the forecasted results and the real-world values in the months where the continuous variations of the meteorological phenomena are frequent. Moreover, the simulation's results – related to the same months – are compared with the results of the typical benchmark model, the persistence method.

In Figure III.9 and Figure III.10, the high forecasting accuracy of the proposed approach is shown: the simulation's results are better in the proposed approach than in the persistence model, especially in the months of January and in October.

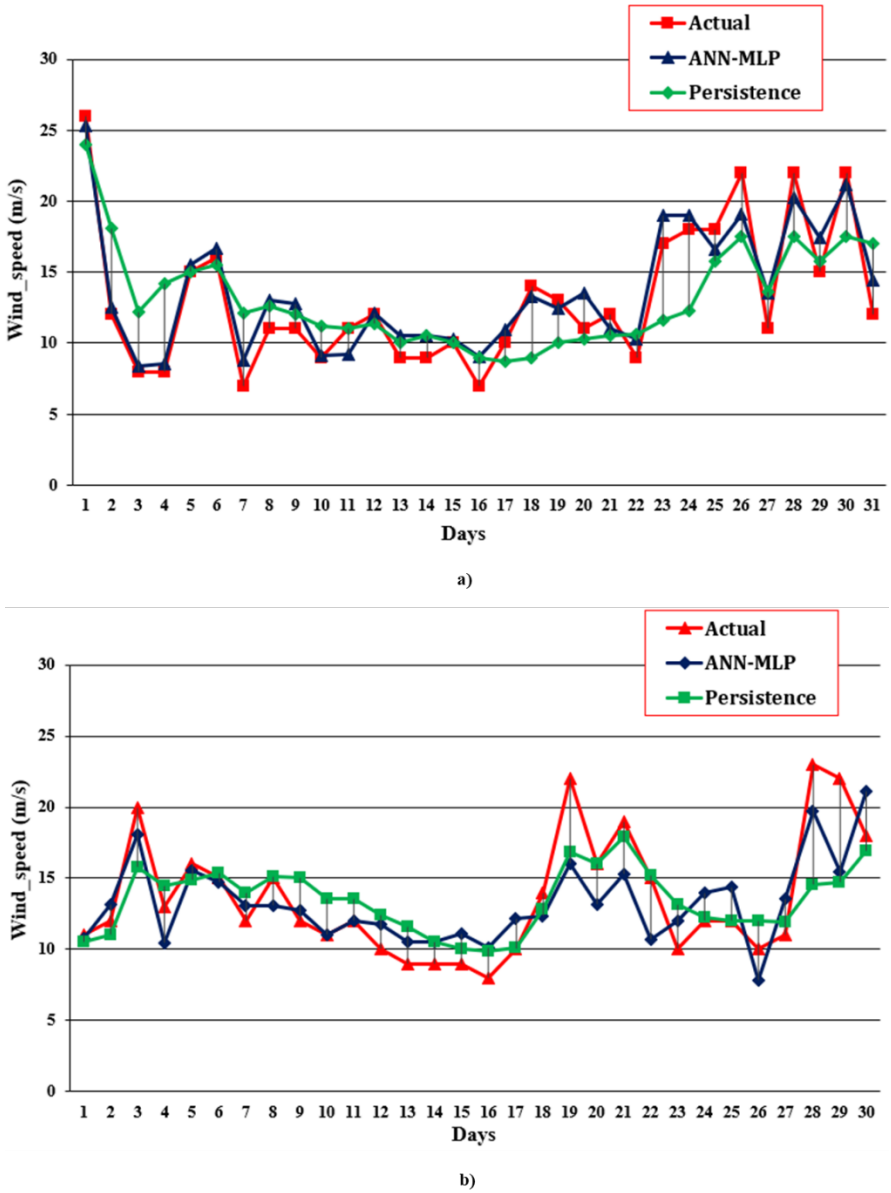

Figure III.9 *Wind speed prediction in the most critical months of 2015 - a) wind speed forecasting in January; b) wind speed forecasting in April*

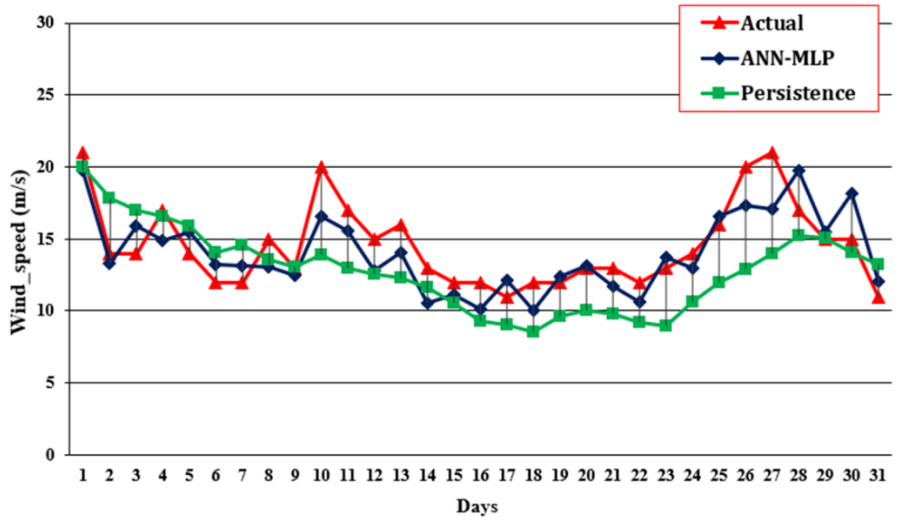

Figure III.10 *Wind speed prediction in the most critical months of 2015 - a) wind speed forecasting in July; b) wind speed forecasting in October*

The effectiveness of the proposed model is confirmed by the evaluation of the major figures of merit, described in the previous chapter.

The next paragraph proposes in detail the figures of merit analysis.

III.5 Evaluation metrics of the proposed model

In order to investigate the effectiveness of the proposed model, the major figure of merits - MAE, MAPE, MSE, RMSE – are calculated, first for the wind forecasts obtained in the most critical months (Table III.4) and then for the predictions of the whole year (Table III.5).

The figures of merit analysis, as shown in Table III.4, demonstrates that the proposed model forecasts wind speed better than the persistence model. In fact, considering the forecasts in the critical months, the values of MAE, MAPE, MSE and RMSE are lower when the ANN-MLP solution is considered.

Table III.4 *Forecasting performance of the proposed approach and the persistence model*

MONTH	MODEL							
	Persistence Model				ANN-MLP			
	MAE	MAPE	MSE	RMSE	MAE	MAPE	MSE	RMSE
JANUARY	2.65	22.26%	10.97	3.31	1.31	11.13%	2.36	1.54
APRIL	1.94	13.89%	7.79	2.79	2.14	15.53%	6.88	2.62
JULY	2.76	18.76%	10.55	3.25	1.58	10.61%	3.35	1.83
OCTOBER	4.00	24.96%	24.16	4.92	2.79	15.71%	10.55	3.25

The performance evaluation over the whole year confirms the effectiveness of the proposed models. Table III.5 reveals lower values of the figures of merit for the proposed model when compared to the persistence model: the ANN-MLP predicts wind speed with an improvement over the persistence model up to 35.75% for MAE and MAPE, and up to around 25% for the MSE and RMSE.

Table III.5 *Comparison between ANN-MLP model and persistence method and improvement for wind speed prediction*

MODEL	Evaluation metrics			
	MAE	MAPE	MSE	RMSE
Persistence Model	2.84	20,72%	8.014	2.83
ANN MLP	1.83	13,31%	5.11	2.21
Improvement [%]	35.40%	35,75%	36.24%	22.10%

Hence, as shown by the performance analysis, the proposed ANN-MLP model is able to accurately forecast wind speed: the information about the meteorological fronts and the dynamic training set give forecasts up to 35% better than the persistence model.

Chapter IV
Hour-ahead wind prediction

The fourth chapter describes the hourly wind speed forecast (HWSF) model. As for the previous section, the chapter starts with a description of the basic methodology and then moves on to analyse the flowchart and the achieved results. Mesoscale references and the COSMO model used in meteorology are the starting point of the model proposed, and their descriptions are also included in this chapter. Furthermore, the formulation of the problem, the optimization phases and data clustering are explained. As in the previous chapter, a number of analysed case studies, based on real-world data, were implemented to test the effectiveness of the model.

The chapter ends with a discussion of the obtained results and the performance of the implemented neural model, according to the main figures of merit used in the literature.

IV.1 Methodology

As mentioned before, an accurate wind prediction is important for the TSO to plan and to dispatch the wind power generation (WPG) into the existing network systems not only on a daily basis, as seen in the previous chapter, but also and above all on an hourly basis for power dispatching.

As in the case introduced and discussed in the preceding chapter, the basis of the proposed model is the phenomenology that describes the atmosphere's evolution. The atmosphere, regarded as a fluid, is governed by a set of the continuous equations, such as the *Navier-Stokes* equations of fluid mechanics, and by the laws of thermodynamics. Due to the complexity of these equations, in meteorology, NWP models are constructed in order to solve said equations and hence describe the evolution of weather systems on an hourly basis (Kalnay, 2003).

As mentioned in chapter II, the NWP models, according to the horizontal size of the phenomena, classify the atmosphere and its evolution into different weather scales (Kalnay, 2012): the global weather scale, which describes

phenomena that extend from one end of the globe to another; the synoptic weather scale, for phenomena that extend from a few hundred to several thousand kilometres; the mesoscale weather scale, for phenomena such as weather fronts or local wind, that extend from a few kilometres to several hundred kilometres; this scale can be classified into three categories: *meso-α* (2000-200 km), *meso-β* (200-20 km) and *meso-γ* (20-2 km) (Pielke, 2013). The last weather scale is the microscale that refers to particular and very fast events, such as turbulence, that are smaller than 1 kilometre in size and very short-lived.

In this chapter, in order to implement the model for an hourly basis, a mesoscale weather scale approach is considered. The proposed model can be regarded as a simple version of LAMs such as COSMO[4], in which, in order to describe the evolution of meteorological phenomena in the *meso-β* area, a nesting theory is applied. In this case also, the model's leading idea is to study how the weather in the surrounding area influences the weather in the POI and, hence, the wind generation in the POI. The characteristics of *meso-β* region are used to describe the phenomenon of weather fronts, which have effects on the hourly wind speed evolution in the *meso-β* region, with a spatial range from a few to hundreds of kilometres, and the relationship between wind and other meteorological factors (Trapp, 2013). Also, for the hourly forecasts, the basic parameters which condition wind formation, i.e. barometric pressure P (mb) and air temperature T (°C) gradients, were considered, as suggested in the literature (Warner, 2010).

Unlike the approaches followed in the literature, which consider a grid of hundreds, or even thousands of sites located around the POI (A. Mazur, 2018) (Bohme et al., 2011), the proposed model considers the relationship between the spatio-temporal evolution of weather fronts and the local wind speed with a weak mesh of points. This simplification does not invalidate the results, as will be seen below, and it is justified by the fact that the forecast only focuses on one point (the POI) and that it is only aimed at wind speed.

In the next paragraphs, the proposed model will be described in detail.

[4] http://www.cosmo-model.org/

IV.2 Structure and overview of the model

The proposed model is based, similarly to what seen in the previous chapter for the daily model, on the wind's dependence on barometric pressure *P* and temperature *T*, and its evolution in the *meso-β* region is expressed as follows:

$$W(S_0, t^{+1}) = f\begin{pmatrix} T(S_{i,j}, t_{i,j}^{-k}); P(S_{i,j}, t_{i,j}^{-k}); W(S_{i,j}, t_{i,j}^{-k}) \\ \vdots \\ T(S_{i,j}, t_{i,j}^{-2}); P(S_{i,j}, t_{i,j}^{-2}); W(S_{i,j}, t_{i,j}^{-2}) \\ T(S_{i,j}, t_{i,j}^{-1}); P(S_{i,j}, t_{i,j}^{-1}); W(S_{i,j}, t_{i,j}^{-1}) \\ T(S_0, t^0); P(S_0, t^0); W(S_0, t^0) \end{pmatrix} \quad \text{(IV.1)}$$

where W is wind speed, $S_{i,j}$ are the chosen sites around the POI, S_0, at maximum distance δ_{max} and minimum distance δ_{min} (Figure IV.1). The time instants $t^{-k}{}_{ij}$, $t^{-2}{}_{ij}$, $t^{-1}{}_{ij}$ and t^0 describe the temporal evolution of the weather phenomena. In this case also, a simplifying hypothesis is adopted, which makes the model particularly agile: the models have considered the measured data referring at past time $t^{-2}{}_{ij}$, $t^{-1}{}_{ij}$ in the points spaced r_2 and r_1 respectively from the POI, all referring to only two moments of time according to the following expression:

$$\begin{cases} t_{i,j}^{-1} = t^0 - \tau \\ t_{i,j}^{-2} = t^0 - 2\tau \end{cases} \quad \text{(IV.2)}$$

where t^0 is the current instant, the indices i and j describe the spatial evolution of weather phenomena and respectively belong to $\Delta = \{\delta_{max}, \delta_{min}\}$ and $\Omega = \{N, NE, E, SE, S, SW, W, NW\}$, while τ is the time-shift delay factor which time-shifts the weather data of each site $S_{i,j}$.

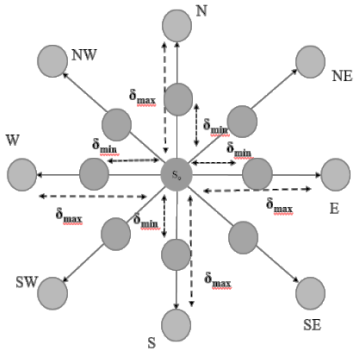

Figure IV.1 *S_0 and the chosen sites $S_{i,j}$ around it, along the cardinal directions*

Although the basic formulation of the proposed hourly prediction model is the same as that of the daily forecasting model described in the previous

chapter, a hybrid model for data clustering was proposed in this case. Moreover, the neural network used is still an MLP albeit assisted by a particle swarm optimization (PSO) algorithm. This is due to the need to obtain a more accurate wind forecast, since for hourly forecasts we start from a more rapidly variable database, as this is averaged over a few values.

In detail, the proposed HWSF model is composed of three main phases:

- the clustering phase, in which the dataset is divided, according to *k-means* algorithm, into four groups. After the construction of the four datasets obtained from clustering, each dataset is split into training, validation and test sets;
- the model construction phase, in which the forecasting hybrid model, PSO-ANN, is constructed. The proposed predictor is based on an MLP-ANN structure optimized by a PSO algorithm, whose coefficients are used as the initial weights and the thresholds of the MLP-ANN model;
- the forecasting phase, in which wind speed is predicted using the neural predictor developed in the previous stage with the manipulated data as input. After that, an analysis of the model's performance is carried out in terms of the main figures of merit and in terms of comparison with the persistence model, regarded as the benchmark for forecasting models.

These three main phases will be explained in detail in the next paragraph, focusing attention on the importance of data clustering in order to avoid false forecasting results.

IV.3 Wind speed forecasting model

In this thesis, the proposed HWSF model merges ANNs, clustering and optimization algorithms. In detail, the implemented neural predictor is an optimized ANN-MLP with three layers, where the Particle Swarm Optimization (PSO) algorithm optimizes the ANN parameters, as suggested in (Olsson, 2011).

As previously mentioned, in the proposed model, the dataset construction covers the first part of it: in order to consider the most useful data, the weather data are clustered into four groups, by using the *k-means* algorithm, and for each group a correlation analysis is conducted. After the dataset construction, as shown in the Figure IV.2, the approach proceeds with the implementation of the PSO-ANN, the model's core. Here, the ANN is built and trained, according to the search of the global extremum and the position of the optimal particle. The last part is dedicated to wind speed forecasting and performance analysis, in which the effectiveness of the proposed model is investigated, not only through the figures of merit evaluation, but also through the comparison of the model's results with the persistence model's forecasting values.

These phases of the model will be explained in detail in the following sections.

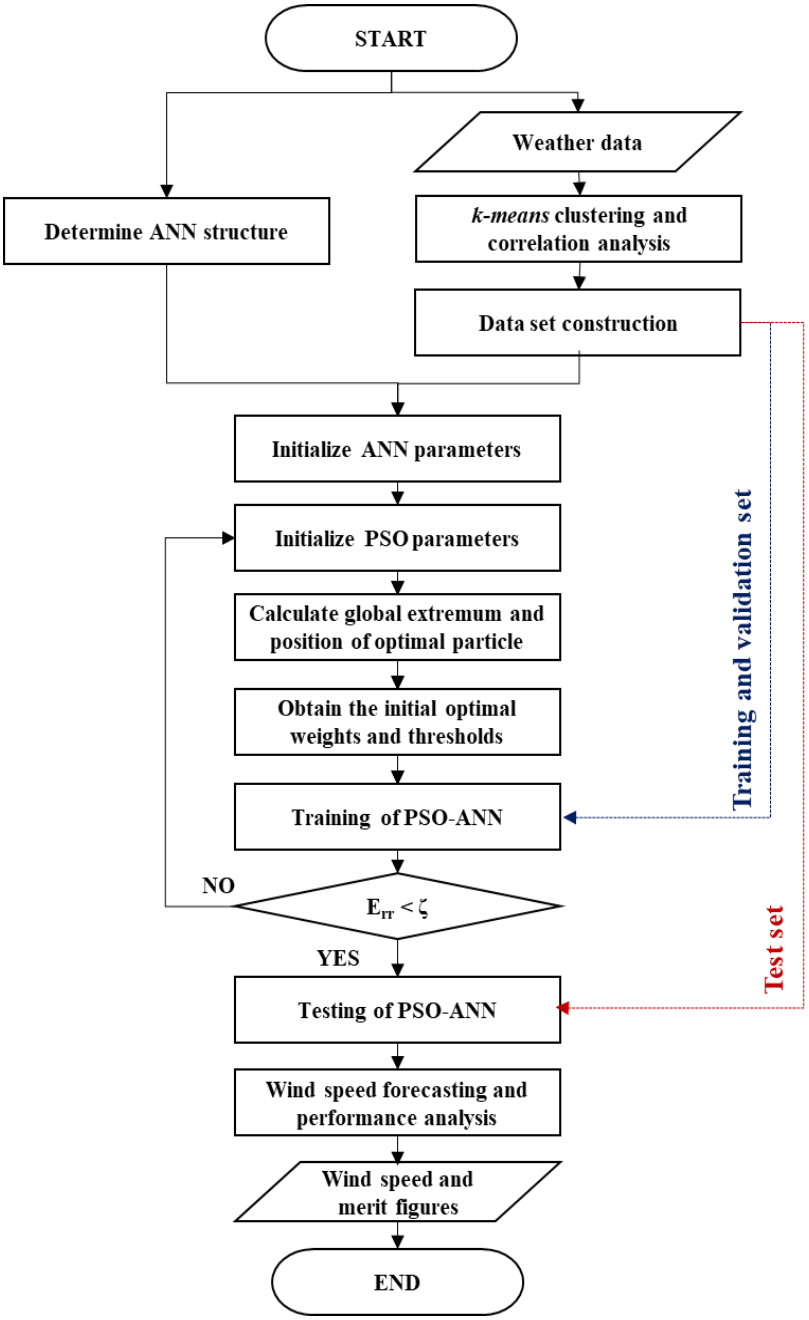

Figure IV.2 *Flowchart of the proposed PSO-ANN model*

IV.3.1 k-means clustering phase

In this phase, the dataset construction criteria are investigated. Due to the large amount of data, after data collecting, data clustering is necessary: according to an analysis of similar features, the dataset is clustered with a *k-means* algorithm, one of the most widespread clustering algorithms (Aggarwal et al., 2013) mostly used in the wind forecasting research field (Wang et al., 2018) (Wu et al., 2017) (Hao et al., 2019) (Dong et al., 2016) (Ghofrani et al., 2016). In detail, the *k-means* algorithm divides the dataset into several subgroups based on the similarity characteristic: the basic idea is to divide the whole dataset according to distance between the *k-centre* and the remaining data (Gan et al., 2007).

In the proposed model, the clustering phase can be described as consisting of three main phases. The first one involves the initialization of input algorithm parameters and the definition of *k* centroids (one for each cluster). After that, the clustering phase proceeds with the assignment of the data points to a cluster, while the last phase is dedicated to updating the *k* centroids' position. The initialization of the input parameters and the choice of *k* centre points is made on the basis of seasonal changes that have an impact on temperature and pressure variation and hence on wind generation (Emeis, 2018). After that, according to the value of Euclidean distance (calculated among all data), each data is assigned to its closest centre point C_k, which is expressed as follows:

$$C_k = \frac{1}{N_k} \sum_{i=1}^{N_k} x_i^k \tag{IV.3}$$

where x_i is the i_{th} data in the k_{th} cluster and N_k are all data points of each cluster. Each centre point C_k, is updated by calculating the average value of every cluster until the value stops changing. Therefore, the dataset is divided, according to the high similarity of data, into season clusters. In detail, the training set and the validation set are composed of hourly wind speed data and hourly meteorological data, expressed as $\boldsymbol{H} = h_1, h_2, \ldots, h_N$, and, as previously mentioned, all data are classified into different classes or clusters through a *k-means* algorithm. After that, in order to choose the most useful data of each cluster, the model proceeds with a correlation data analysis (Figure IV.3). In detail, the evaluation of Pearson correlation index, calculated for each cluster data, is used to investigate the data correlation degree: the sign and the value of this index confirms the correlation between data (Shevlyakov et al., 2016).

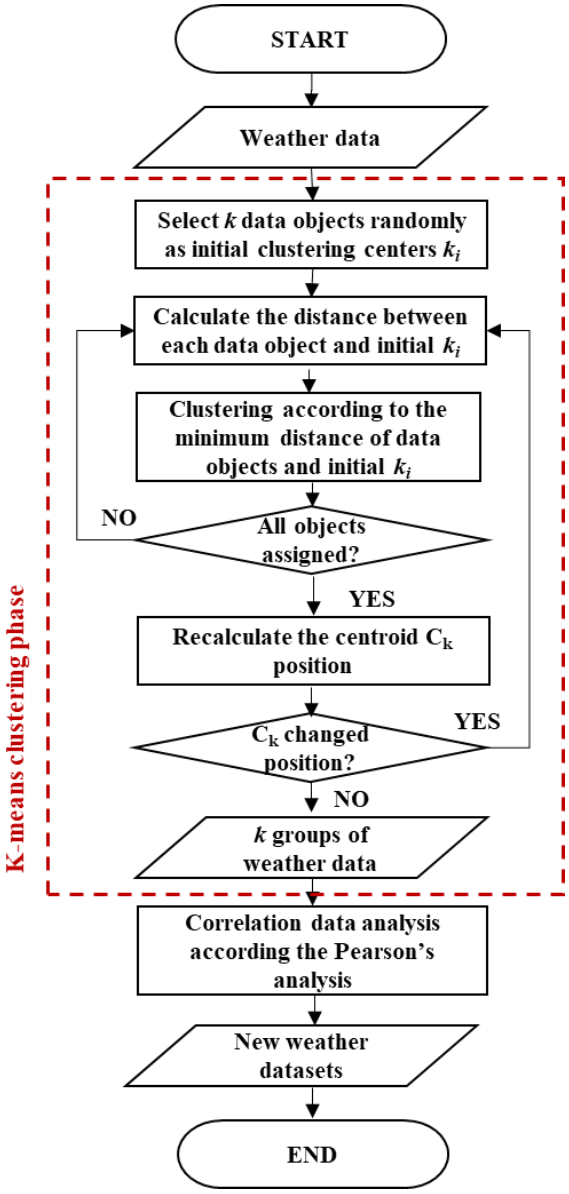

Figure IV.3 *Flowchart of the k-means clustering phase*

IV.3.2 PSO-ANN forecasting phase

This phase is dedicated to the construction of the hybrid prediction model and therefore, to wind speed forecasting. In the neural model proposed, in order to improve convergence and to minimize the prediction error, the PSO algorithm, which is able to solve the problem of local minimum of the simple backpropagation MLP, is utilized (Fausett, 1994).

The PSO is a computational global searching algorithm whose aim is to search the global optimum of a problem through an iterative process that stops when the stopping criterion, established by a chosen fitness function, is met. In the PSO, each particle is considered as a potential solution to the optimization problem and it is characterized by three parameters: position, velocity and fitness value, determined by the fitness function (Olsson, 2011).

In the literature, some hybrid approaches based on the PSO, both for wind power prediction and wind speed forecasting, are proposed (Kumar et al., 2019) (Fazelpour et al., 2016). For example, in (Ma et al., 2017), the authors propose a forecasting model that combines a Fuzzy-ANN and a PSO in order to predict wind speed. In detail, in the aforementioned work, a spectrum analysis optimized by the optimization algorithm is applied to pre-process the original wind speed data in order to obtain a smoother sequence, subsequently used for forecasting wind speed. Conversely, in (Yue et al., 2017), the PSO is combined with Least Squares Support Vector Machine (LSSVM): the kernel and the regularization parameters of the LSSVM are optimized by the PSO. Hence, the authors propose a wind speed prediction model using the optimized parameters, thus improving the model's forecasting accuracy. For initializing and training, the abovementioned models use the model data which refer to the weather phenomena occurring at the prediction point, while the proposed model uses the influence of weather phenomena that occur around the prediction point. Therefore, the proposed model, taking inspiration from the approaches in the literature, combines an ANN-MLP and a PSO, which is utilized to obtain the best set of weights, the position vector of particles with the best solution, taking into account the weather data of the prediction point and of the larger area around it.

After the data clustering phase, the design of the neural predictor begins with the randomised initialization of a three-layer ANN-MLP, weight and bias; then, these parameters are evaluated according to a fitness function for the PSO algorithm. The dimension of the search space is identified, according to the ANN-MLP structure, with the total number of weights and biases of the neural network, which are initialized at the beginning, once the number of neurons of the intermediate states and the number of inputs and outputs is chosen. Hence, the weight and the threshold value of the proposed neural model are expressed through the particle status in the PSO. The MSE produced by the ANN-MLP is the criterion to define the PSO fitness function: according to the fitness function value of each particle, the individual extreme values and the global ones are computed. Then, each current value of fitness function is compared with the previously calculated value and then it is updated. The PSO algorithm ends when the stopping criterion is met and hence, the set of global optimum solutions corresponding to the particle position becomes the network's weight and the threshold vectors that will be used in the training of the ANN-MLP. After that, the optimized neural network is trained and tested through the datasets which were constructed in the

clustering phase, and then the model is used to obtain the final wind speed prediction value.

IV.4 Case study

The implemented hybrid forecasting model is tested on an actual wind farm sited in Campania, Southern Italy, to predict the hourly wind speed one day in advance. As previously mentioned, the implemented predictor is an ANN-MLP combined with a PSO; the settings adopted for implementing the model are summarized in Table IV.1.

Table IV.1 *Optimized ANN-MLP parameters setting*

MODEL_PARAMETERS	VALUE_PARAMETERS
Number of input layers	One with 1224 neurons
Number of hidden layers	1
Hidden layer transfer function	'LinearSigmoid'
Output layer transfer function	'LinearSigmoid'
Training algorithm	Back propagation with momentum
Momentum	0.5
Error criterion figure	MSE
Maximum epochs	2000
PSO fitness function	MSE
Number of k-means clusters	4

IV.4.1 Input data

The input dataset is composed of the hourly average meteorological information. As explained in the previous section, the dataset, according to the similarity characteristic of the seasons, is divided into four clusters (see Appendix A). The input dataset covers a period of four years, while the training set and the validation set cover respectively 80% and 20% of the input set. The dataset contains three weather variables: wind speed W (m/s), air temperature T (°C) and barometric pressure P (mb). The weather data used refer to the *mesoscale* β model, which describes the meteorological phenomena that occur in a range of 200–20 km (Pielke, 2013). The data considered have a sampling frequency of 1 hour/point, and they are time-shifted according to eq. IV.2, in which the time shift delay factor τ is equal to 1 hour. The meteorological data refer to sixteen chosen sites at a minimum distance δ_{min}, 20 km, and at a maximum distance δ_{max}, 50 km. The real-world meteorological data were provided by the *Italian Air Force Meteorological Service* and by the IVPC, having been registered respectively on actual weather stations sited in each of the chosen sites, and on a particular test site. The wind data of the considered weather stations are referred to 10 meters.

IV.4.2 Prediction results

The simulation period refers to four specific days of the year, in which the weather undergoes critical changes: the summer solstice, the winter solstice, the spring equinox and the autumn equinox. In order to consider not just the model's best results but all forecasting values, the predicted values are averaged on a 10 run network simulation.

The effectiveness of the proposed model is demonstrated by the comparison between the forecasted results of the hybrid PSO-ANN-MLP predictor and the real-world values registered by an actual weather station in the period considered. Moreover, in order to confirm the validity of the proposed approach, the simulation's results are also compared with the wind speed forecasts obtained with the typical benchmark model, i.e. the persistence model.

The high forecasting accuracy of the proposed hybrid model is demonstrated by the following figures, in which the proposed approach proves to be better at obtaining good predictions than the persistence model.

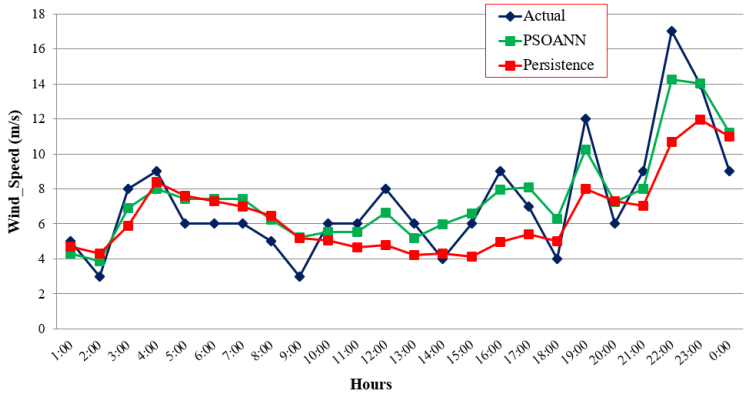

Figure IV.4 *Wind speed forecasting - spring equinox (PSOANN model and persistence model)*

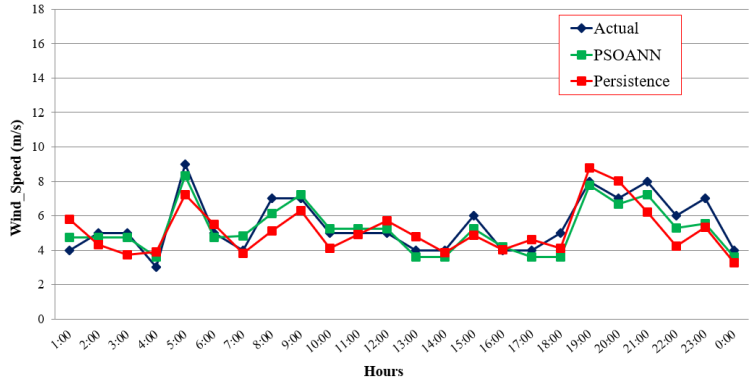

Figure IV.5 *Wind speed forecasting - fall equinox (PSOANN model and persistence model)*

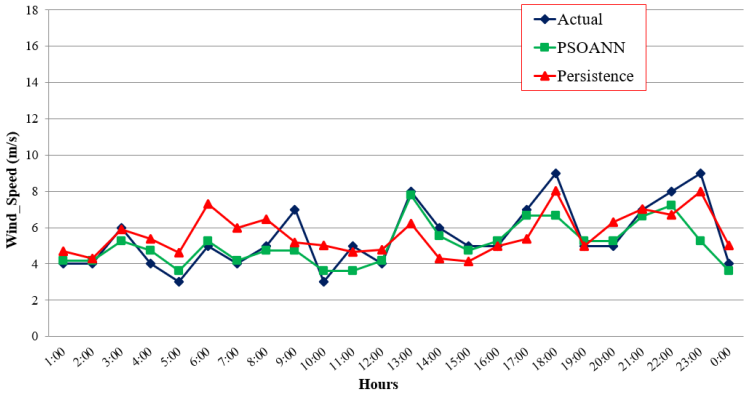

Figure IV.6 *Wind speed forecasting – summer solstice (PSOANN model and persistence model)*

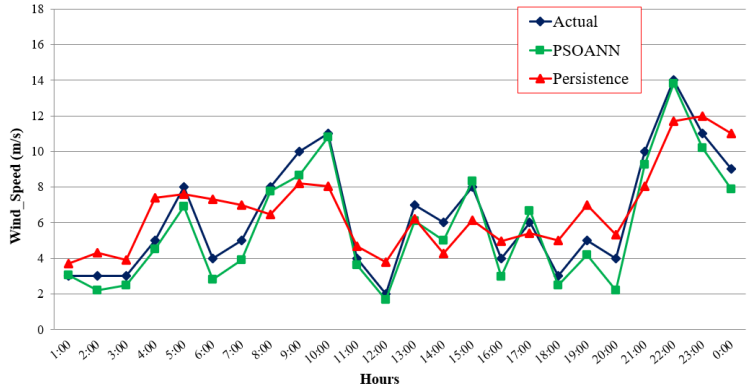

Figure IV.7 *Wind speed forecasting – winter solstice (PSOANN model and persistence model)*

IV.5 Wind speed forecasting error analysis

In order to investigate the effectiveness of the proposed model, the main figures of merits – MAE, MAPE, MSE, and RMSE – are evaluated for the wind speed forecasts obtained in the simulation period defined above (Table IV.2).

The analysis of the model's performance and the comparison with the persistence model demonstrate, as shown in Table IV.2, that the proposed hybrid model forecasts hourly wind speed with a lower forecasting error than the persistence model – the classical benchmark proposed in the literature – especially in the cases related to autumn and winter.

Table IV.2 *Forecasting performance of the proposed hybrid approach and the persistence model*

DAY	MODEL							
	Persistence Model				PSO-ANN-MLP			
	MAE	MAPE	MSE	RMSE	MAE	MAPE	MSE	RMSE
SPRING	1.90	17.84%	5.34	2.31	1.27	16.98%	2.04	1.43
AUTUMN	0.95	24.97%	1.4	1.18	0.56	14.54%	1.17	1.08
SUMMER	1.10	15.16%	1.69	1.30	0.72	14.14%	1.26	1.12
WINTER	1.60	20.41%	3.09	1.76	0.73	12.78%	0.71	0.84

According to Table IV.2, the values of the error metrics of the persistence model and the hybrid model change, respectively, from 25% of MAPE and 2.31 of RMSE to 17% and 0.84 (considering the maximum and minimum values of error metrics calculated for the four cases).

Hence, the proposed hybrid model is able to accurately forecast wind speed: the information about the evolution of meteorological fronts and the clustering and the optimization phases provide better forecasts than the persistence model, which predicts wind speed with a forecasting error of around 25%.

Chapter V
From wind speed to wind power: an Italian case study

In this chapter, the wind speed forecasting model described in the previous chapters is used to obtain the amount of wind power available on an Italian wind farm. The chapter starts with the description of the theoretical method based on the Betz theory and of the proposed model, which are used for calculating the wind power of a chosen wind farm, given the characteristic power curve and the technical characteristics of the wind farm and the wind turbine. Subsequently, the case study is presented. In detail, the structure and the technical features of the chosen wind farm are described, focusing the attention on the wind turbines installed in the wind farm, and its characteristic power curves.

This chapter ends with the obtained results analysis and hence, with the model performance evaluation.

V.1 The Betz theory

The Betz theory indicates the maximum possible energy obtainable from a wind turbine. The theory was firstly developed by Albert Betz in 1920. He applied the linear momentum theory to a simple one-dimension model to evaluate the ideal and frictionless efficiency of a wind turbine, modelling the rotor as a uniform "actuator disk", which is confined in the assumed control volume (Figure V.1) (Cengel et al., 2017) (Manwell et al., 2010).

The surface and the cross section of a stream tube, in which the fluid passes through the rotor, define the control volume. The rotor makes the pressure of the fluid that flows through it discontinuous (Figure V.2).

The actuator disk model is based on a few assumptions: the fluid's flow is steady, homogenous, inviscid, incompressible and irrotational; the rotor blades are infinite, and the fluid's flow and thrust are uniform across the

actuator disk area. In addition, the speed of the air beyond the rotor is regarded as axial (Schmitz, July 2019) (Zhao et al., August 2019).

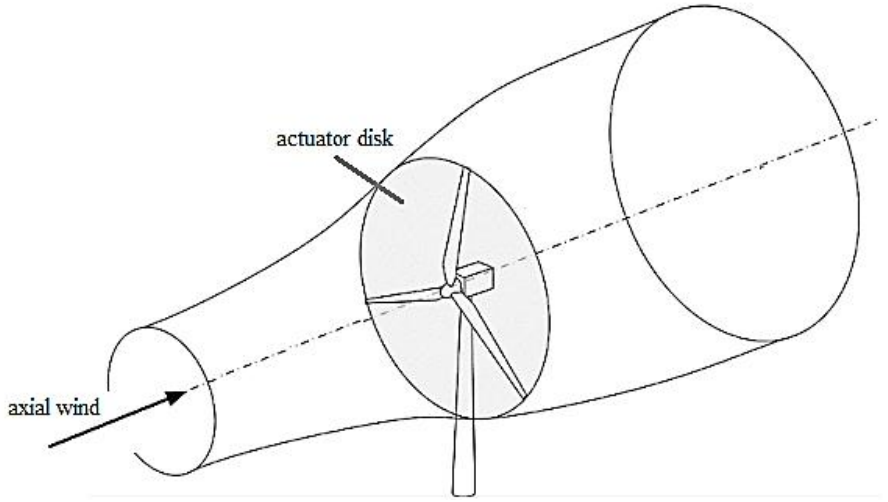

Figure V.1 *Wind rotor actuator disk model*

In the ideal rotor model shown in the Figure V.2, according to said assumptions, the wind speed passing through the turbine rotor is uniform as V; its values V_1 and V_2 are respectively the upwind speed and downwind speed, and they refer to the upwind air cross-section S_1 and the downwind air cross-section S_2. As the extraction of mechanical energy by the rotor occurs by reducing the kinetic energy of the air stream from upwind to downwind, the speed V_2 is lower than V_1 and hence, the air stream cross actuator disk increases from the upwind surface S_1 to downwind surface S_2 (Carriveau, 2011). If wind speed is regarded as an incompressible flow, the mass flow rate is constant, and the continuity equation can be written as follows:

$$\dot{m} = \rho S_1 V_1 = \rho S V = \rho S_2 V_2 = \text{constant} \tag{V.1}$$

where ρ is the air density.

As is known, the power of free unobstructed air moving at a constant speed V depends on the variation of kinetic energy, which, in the case of wind stream, is proportional to the force exerted by the wind on the rotor:

$$P = \frac{dE}{dt} = F \cdot \frac{dx}{dt} = F \cdot V \tag{V.2}$$

where, according to Euler's Theorem, the force F depends on the mass and the time variation of the speed V:

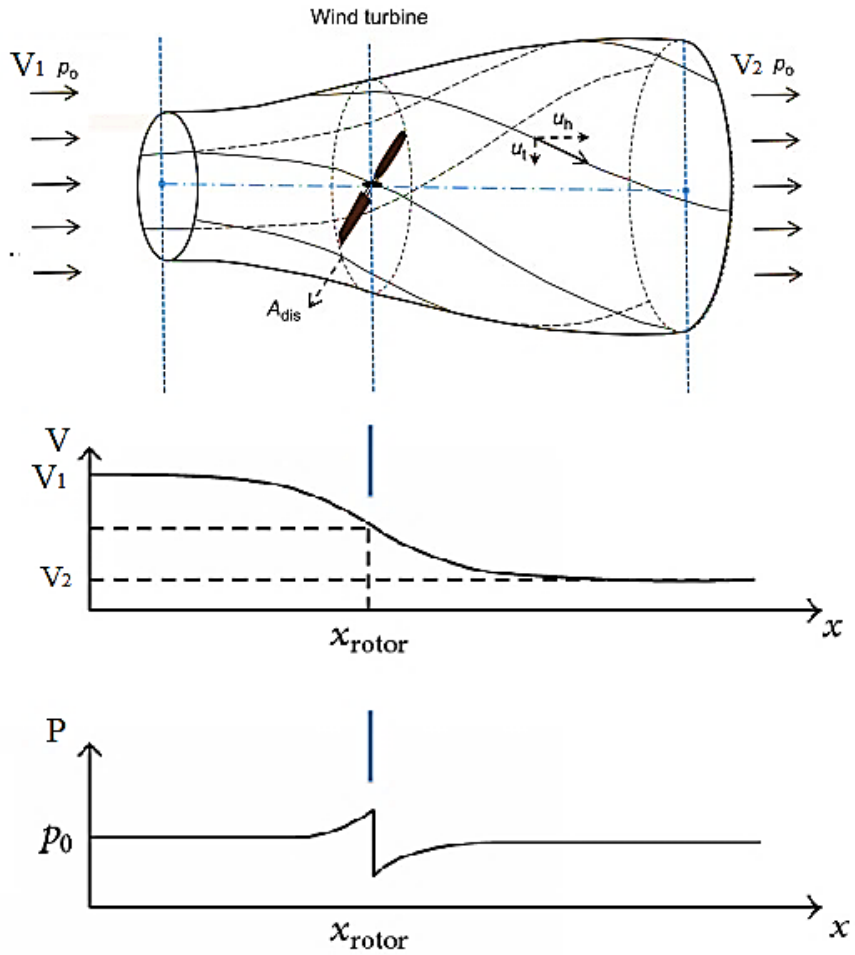

Figure V.2 *Speed variation and pressure in the ideal wind turbine model*

$$F = m \cdot a = m \cdot \frac{dV}{dt} = \dot{m}\Delta V = \rho S V (V_1 - V_2) \qquad \text{(V.3)}$$

Hence, substituting the force F in eq. V.2, the extractable power from wind is:

$$P = \rho S V^2 (V_1 - V_2) \qquad \text{(V.4)}$$

The power from the upwind surface to the downwind surface is calculated by applying the law of energy conservation:

$$P \cong \frac{\Delta E}{\Delta t} = \frac{\frac{1}{2} m V_1^2 - \frac{1}{2} m V_2^2}{\Delta t} = \\ = \frac{1}{2} \dot{m} (V_1^2 - V_2^2) = \frac{1}{2} \rho S V (V_1^2 - V_2^2) \quad \text{(V.5)}$$

Combining the two conservation equations (mass and energy) and equating the two expressions of power, the general wind speed *V* can be related to the upstream wind speed and the downstream wind speed:

$$V = \frac{1}{2}(V_1 + V_2) \quad \text{(V.6)}$$

This means that the wind speed at the rotor may be considered as the average of the upstream wind speed and the downstream wind speed, and hence, eq. V.5 can be rewritten as follows:

$$P = \frac{1}{2} \rho S (V_1^2 - V_2^2)(V_1 + V_2) \quad \text{(V.7)}$$

In order to measure the efficiency of a wind turbine at extracting the energy of a wind stream, Betz introduces the performance coefficient C_p, which is expressed as:

$$C_p = \frac{P}{W} \quad \text{(V.8)}$$

where *W* is the available power in the undisturbed upstream over a cross sectional area *S*, when the wind speed *V* is equal to V_1. The available power, *W*, is defined as:

$$W = \frac{1}{2} \rho S V_1^2 \quad \text{(V.9)}$$

while, introducing the interference parameter *a*, which is the ratio of the upstream wind speed and the downstream wind speed:

$$a = \frac{V_2}{V_1} \quad \text{(V.10)}$$

The wind power *P* becomes:

$$P = \frac{1}{4}\rho S V_1^3 (1-a^2)(1+a) \qquad \text{(V.11)}$$

Substituting eq. V.9 and V.11 in eq. V.8, the relationship between the performance coefficient and the interference parameter is obtained:

$$C_p = \frac{P}{W} = \frac{1}{2}(1-a^2)(1+a) \qquad \text{(V.12)}$$

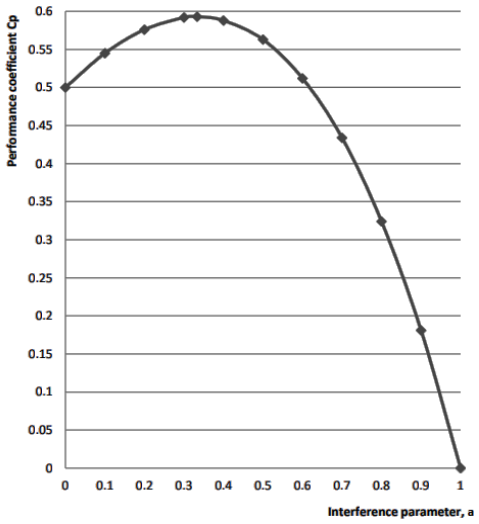

Figure V.3 *Graph of the performance coefficient C_p*

According to the graph of C_p shown in Figure V.3, the performance coefficient decreases with the increase of the interference parameter; in fact, when the interference parameter reaches the maximum value (*a=1*), the upstream wind speed is equal to the downstream wind speed and the performance coefficient is zero. Conversely, when the interference parameter is zero the performance coefficient is 0.5. From the graph, it can be seen that C_p reaches the maximum value when the interference parameter is around 0.3.

The maximum value of C_p represents Betz's limit and it is the maximum extractable power fraction from an ideal wind turbine.

Betz's limit is obtained by deriving eq. V.12 and equating the derivate to zero and then substituting the calculated value of *a*. The maximum value of C_p is referred to *a=1/3* and it becomes, from eq. V.12:

$$C_{\max,p} = \frac{1}{2}(1-a^2)(1+a) = \frac{16}{27} = 0.5926 = 59.26\% \qquad \text{(V.13)}$$

Betz's limit represents the theoretical value of the power fraction that can be extracted from a wind turbine. In general, the actual extractable wind power from a turbine depends on the building characteristics of the rotor and the actual operating conditions of the wind farm which influence the wind farm's production capacity. Hence, the actual wind turbines operate at a lower, non-ideal performance coefficient, which varies between 35% and 50% (Ricerca sul Sistema Energetico – RSE SpA, 2012).

V.2 Proposed forecasting approach

The problem of wind energy forecasting can be tackled in two different ways: either by predicting wind energy, considering both the meteorological and production information of the wind farm, or by developing a two-stage forecasting model which forecasts the wind speed first and then the wind power. In this thesis, unlike other works from the literature, the proposed approach follows the second way. More in detail, a number of researchers in the literature propose power prediction models that use both weather and power information (Giebel et al., 2017) (Chen et al., 2018) (Santhosh et al., 2020). For example, Demolli et al. propose a wind power forecasting approach that uses wind speed data and old wind power data as inputs of five machine learning algorithms in order to model wind power on the long-term (Demolli et al., 2019). Other researchers propose models based on a two-stage approach and only on old wind power data. For example, in the latter models, the first stage is used for a composite prediction of a decomposed power sequence and optimized BP neural networks predict the general wind power trend and the correlation of various factors respectively. Then, in the second stage, another BP neural network, with the results of the first stage as input, is used to predict wind power (Zhang et al., 2015). On the other hand, Hao et al. propose, for wind power prediction, a two-stage forecasting architecture based on error factor, composed of two main stages: in the first one, in order to forecast the power components broken down by variational mode decomposition and forecast errors, an optimized extreme learning machine is used. Then, a nonlinear ensemble method based on the optimized extreme learning machine is utilized to integrate all the components and forecast error values and hence, to forecast multi-step wind power (Hao et al., 2019). Conversely, a few models use the modelling of power curves for predicting wind power, as in (Vahidzadeh et al., 2019), in which the authors propose a model based on the evolution of wind power, considering the Betz theory and the information about wind speed and the production capacity of WFs. In the proposed approach, the Betz theory is also used, but unlike the aforementioned models, in order to reduce the prediction error, the weather information and the historical series of wind power data are represented, respectively, by the input from the first and second stage (Figure V.4).

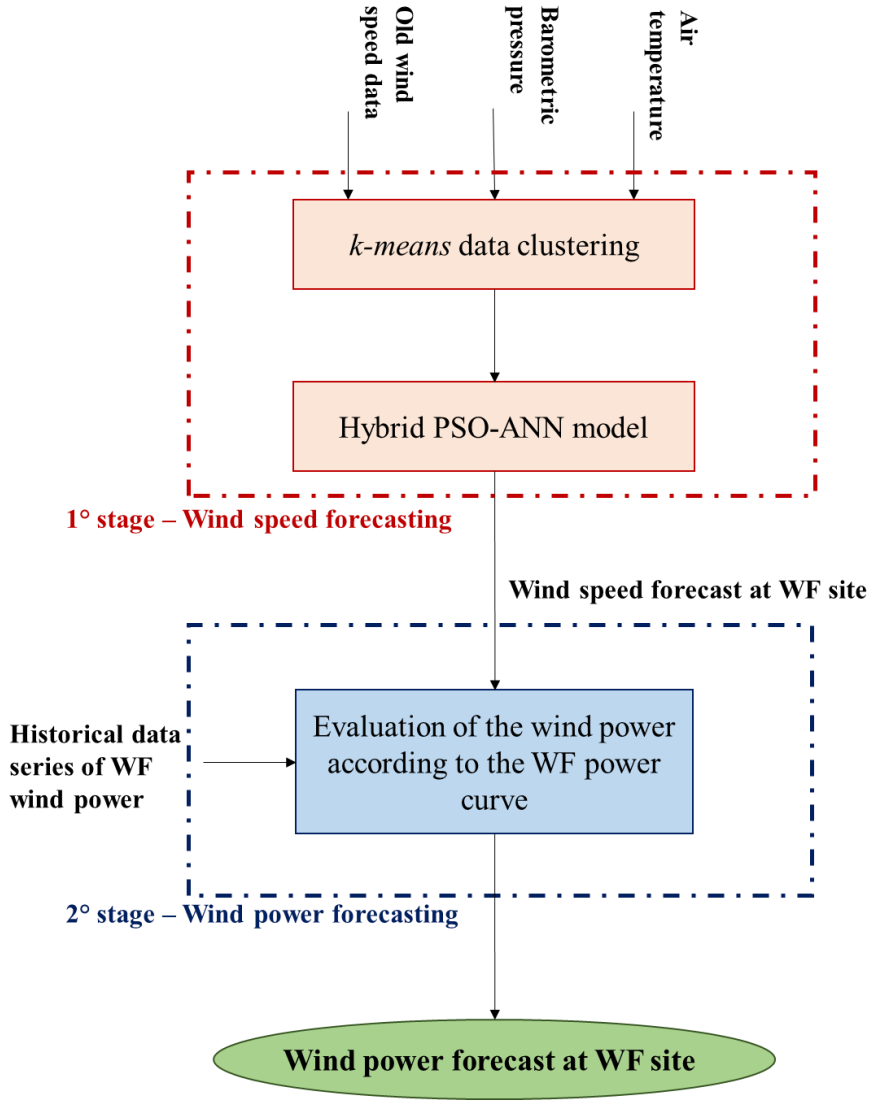

Figure V.4 *Structure of wind power forecasting model*

In the proposed approach, in order to forecast wind speed, a hybrid PSO-ANN model, which was described in the previous chapter, was implemented. As previously mentioned, the input data of the first stage are only meteorological information: barometric pressure (mb), air temperature (°C) and a historical series of wind speed data. According to the PSO-ANN model developed, the input data refer not only to the WF site, but also to sixteen chosen points around the WF site. In the second stage, according to the Betz theory and using the historical wind power data and the wind power curves of the WF, the wind power at the WF site is predicted. More in detail, the wind

power at the WF site is obtained, considering the wind speed forecasts in the first stage and the actual values of C_p referring to the wind power curves of the WF.

Hence, the hourly wind power is the sum of the wind power of all wind turbines that compose the WF, and it is obtained as follows:

$$P(t_{+1}) = \sum_{i=1}^{N} P_i(t_{+1}) = \sum_{i=1}^{N} \left[\frac{1}{2} \rho A C_p \right]_i v^3(t_{+1}) \qquad \text{(V.14)}$$

where the index *i*, referring to the wind turbine, is considered among the N wind turbines that compose the WF, and A_i is the technical characteristic of the wind turbine considered, while $v^3(t_{+1})$ indicates the wind speed values forecasted in the first stage. The real values of C_p are evaluated considering the relationship between the wind power data and the wind speed data, both referring to the WF test site and provided by IVPC.

V.3 Case study

The proposed approach is used for predicting hourly wind power on a WF sited in Southern Italy. The input dataset for the first stage is composed of hourly average weather data – barometric pressure (mb), air temperature (°C) and historical wind speed series – and it covers a period of four years.

Following the hybrid PSO-ANN wind speed forecasting model described in the previous chapter, the dataset is divided into four clusters, and the meteorological data refer to the WF site and to the sixteen points sited around the WF site. The weather data have a sampling frequency of 1 hour/point.

The real-world meteorological data have been provided by the *Italian Air Force Meteorological Service* – COMet - and by the IVPC, having been registered, respectively, on actual weather stations sited in each chosen site, and on a WF located in Southern Italy. The wind data of the considered weather stations are referred to 10 meters. Instead, the historical wind power data, i.e. the input from the second stage, refer to the WF and cover a period of one year (see Appendix A).

In the next section, the characteristic of the WF are described.

V.3.1 Italian wind farm

The WF test site is located in Southern Italy, one of the areas with the highest concentration of wind energy. It is composed of two different typologies of wind turbines: the first one has a nominal power of 1.8 MW, and the second has a nominal power of 2 MW. In the figure below, the theoretical power curves of these two types of wind turbine are reported.

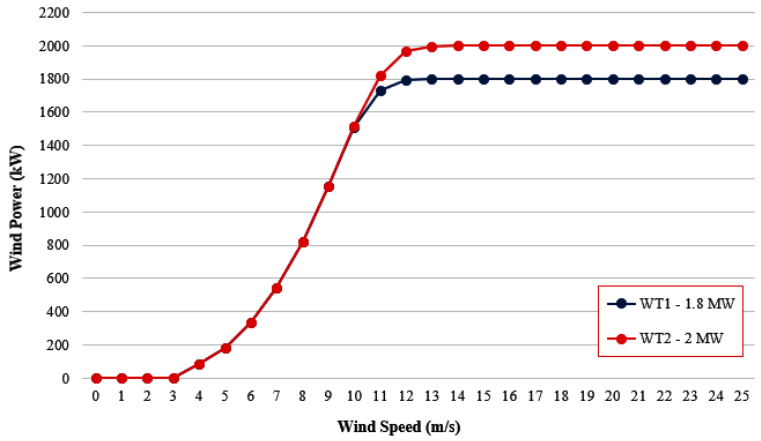

Figure V.5 *Wind power curves of the two wind turbines*

The WF wind power production data are provided by IVPC and they have a sampling frequency of 10 min/point, but in the analysed case, in order to predict the hourly wind power, the hourly average value of each production data was calculated. The dataset covers a period of one year.

V.3.2 Wind power forecasting results

The test period refers to two particular times of the year. The first period covers four days and the second refers to the first week of spring. In these two times of the year, the weather undergoes significant changes and, as wind speed suffers strongly from meteorological changes, wind power becomes even more variable compared to other periods of the year. The model's results refer to the time of day and each forecast begins at 1a.m. and ends 24 hours later.

The effectiveness of the proposed approach is tested by comparing the obtained results with real-world wind power production data registered by IVPC in the simulation period considered. Moreover, the effectiveness of the model is also tested by the comparison between the forecasting results and the wind power forecasts obtained with the persistence method.

The following figures report the obtained results and the comparison with both the real-world data and the persistence forecast values.

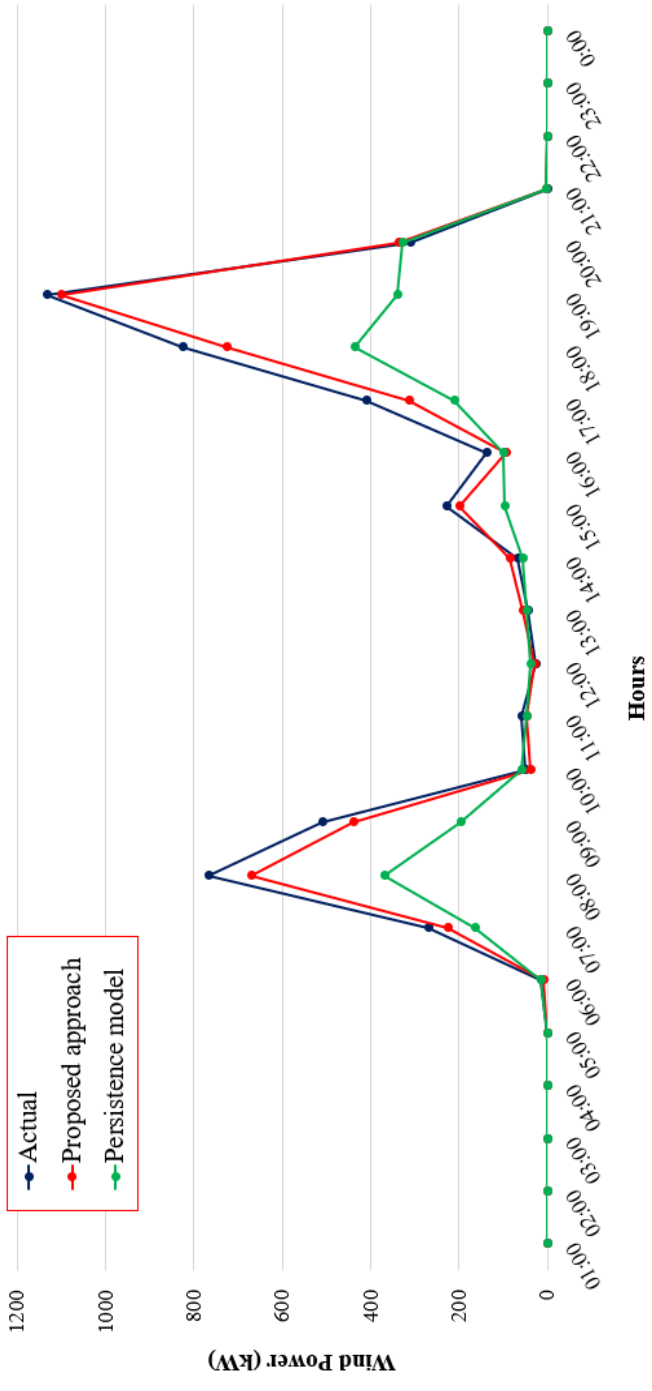

Figure V.6 *Hourly wind power forecasting at WF - spring equinox*

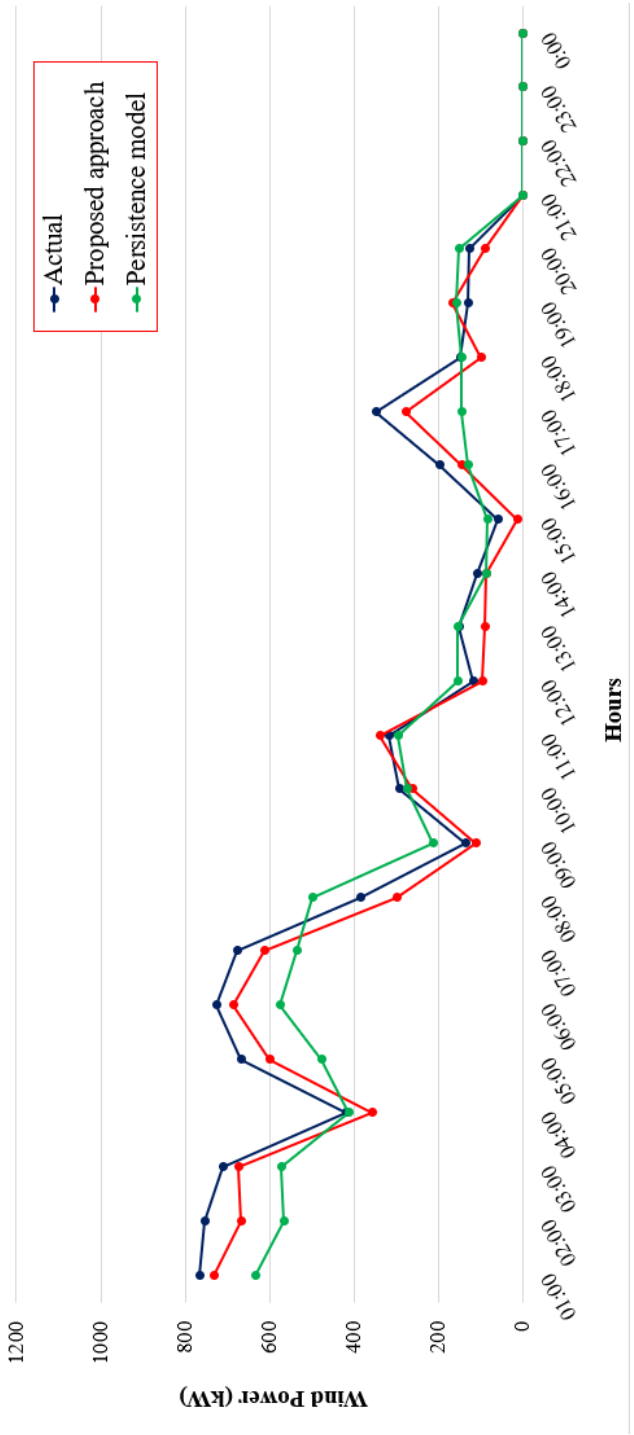

Figure V.7 *Hourly wind power forecasting at WF - fall equinox*

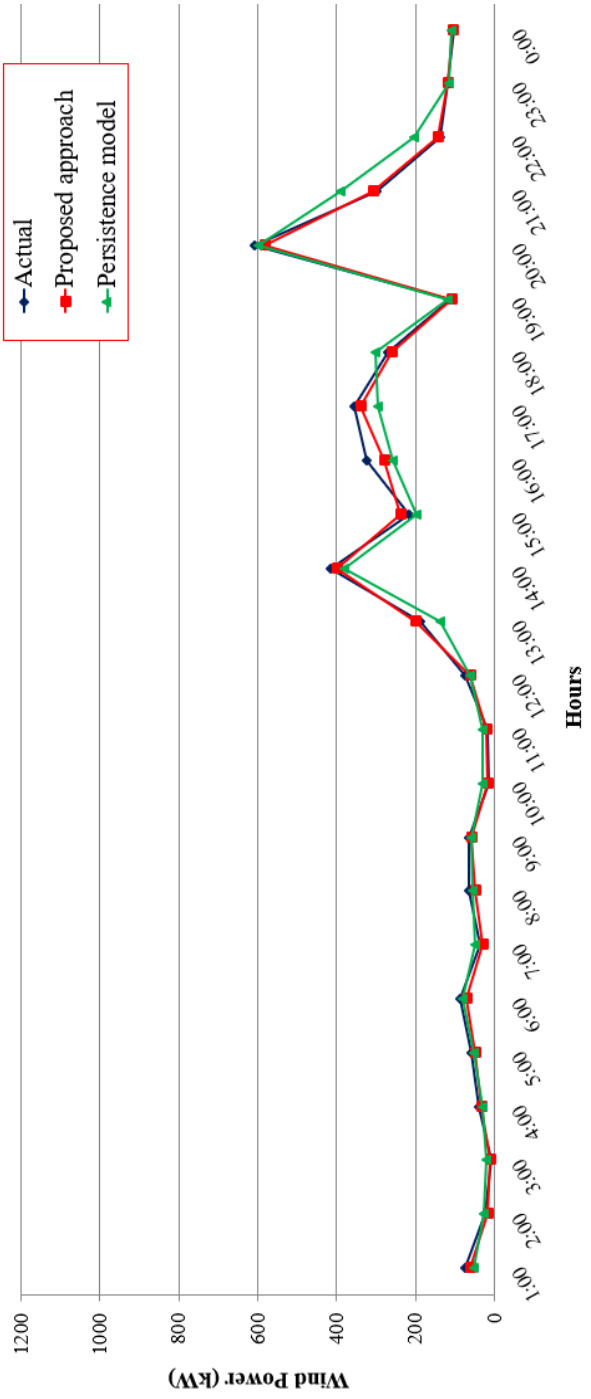

Figure V.8 *Hourly wind power forecasting at WF - summer solstice*

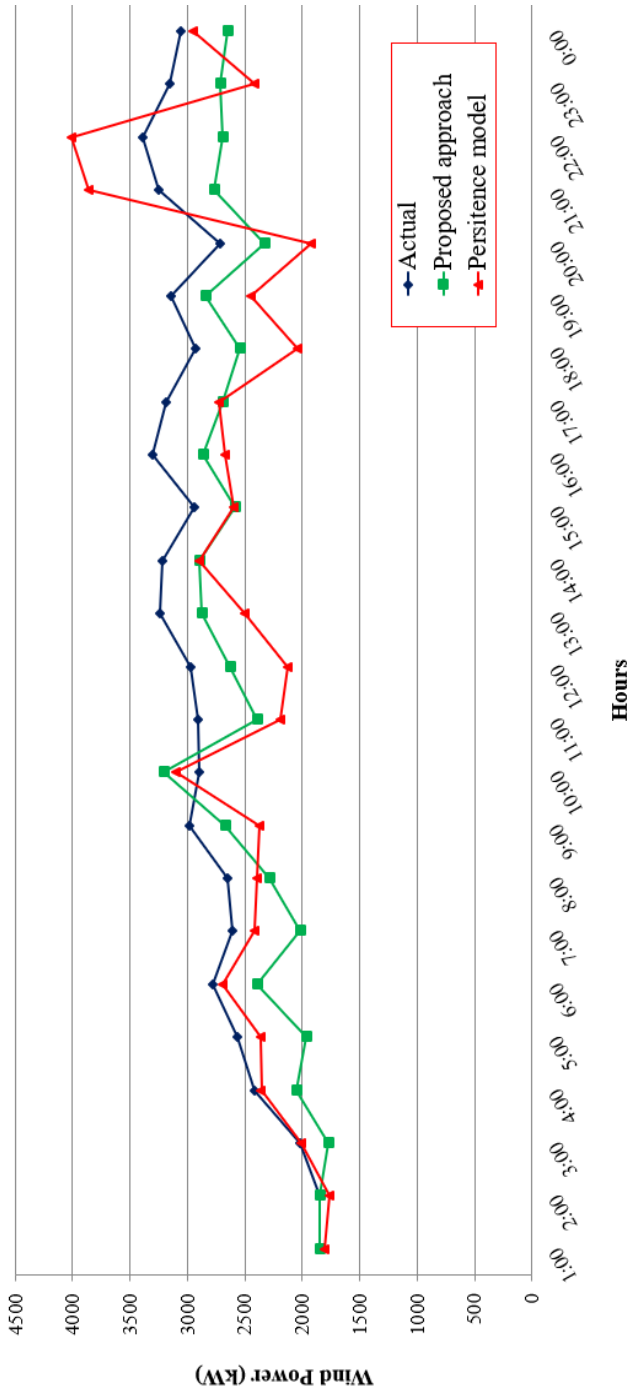

Figure V.9 *Hourly wind power forecasting at WF - winter solstice*

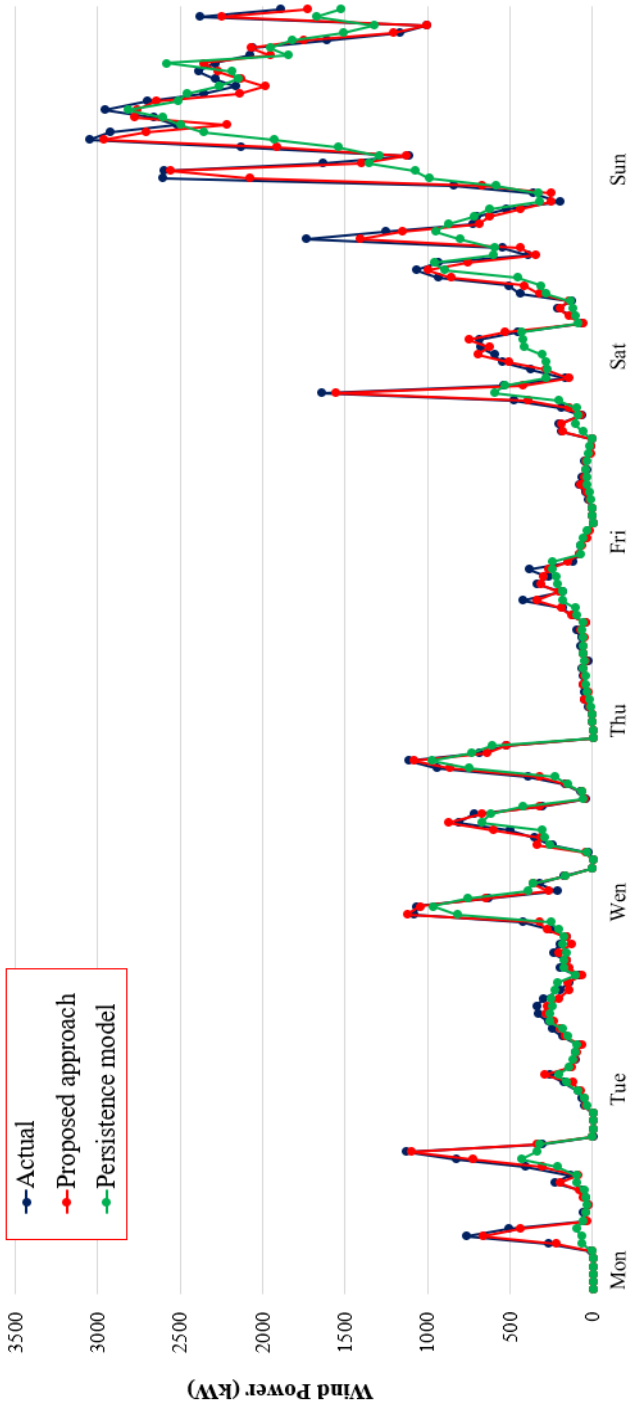

Figure V.10 *Hourly wind power forecasting at WF - first spring week*

In both test periods, as shown in the figures above, the implemented model is able to predict wind power better than the persistence model. The high forecasting accuracy of the proposed approach is demonstrated especially in the first three cases, in which the proposed model follows the sudden changes of wind power better than the persistence model. The high forecasting capacity of the proposed model is also found in the case in which the wind power forecasting of the first week of spring is considered (Figure V.10).

V.4 Model performance analysis

The model's effectiveness is demonstrated by the evaluation of MAE and MAPE in both test periods, first for the wind power forecasts obtained in the most critical days (Table V.1) and then for the predictions in the first week of spring (Table V.2). In fact, as shown in Table V.1, the proposed approach forecasts wind power better than the persistence model: in the most critical days, the values of MAE and MAPE are lower when the proposed approach is considered.

Table V.1 *Evaluation metrics of the proposed approach and the persistence model*

DAY	MODEL			
	Persistence Model		Proposed approach	
	MAE	MAPE	MAE	MAPE
SPRING	101.31	23.95%	25.25	13.97%
FALL	66.22	19.36%	39.99	17.30%
SUMMER	23.76	26.84%	11.38	12.22%
WINTER	427.49	17.42%	377.93	13.00%

The model's performance analysis reveals that the proposed approach presents lower values for the figures of merit than the persistence model: in all four days, the maximum forecasting error changes from 26.84%, when the persistent model is applied, to 12.22 % in the proposed approach.

The evaluation of MAE and MAPE, calculated in the second test period, also confirms the effectiveness of the proposed approach. According to the analysis of the evaluation metrics, the proposed approach predicts the wind power that the WF produces in the first week of spring, with a mean MAPE - calculated on the whole week - which is much lower than the persistence model. In fact, this changes from about 27% in the case of the persistence model to 14% in the proposed approach, with an improvement of about 40% (Table V.2).

Table V.2 *Proposed approach and persistence model forecasting performance and wind power prediction improvement*

MODEL	Evaluation metrics	
	MAE	**MAPE**
Persistence Model	135.97	51.82%
Proposed approach	26.94	14.11%
Improvement [%]	61.89%	47.65%

In conclusion, according to performance analysis, the proposed approach, based on tackling the WPF problem into two sub-problems, is more able to accurately forecast wind power than the persistence model. As weather information and wind power production data are used in two different phases of the model separately, as in a few models in the literature, wind power forecasting uncertainty is reduced. In detail, in the proposed approach the main uncertainty of wind power is investigated in the first phase, in which, in order to predict wind speed, only weather information is used as the input of the PSO-ANN model. After this phase, considering the WPG historical data and hence the WF power curve, the wind speed forecast values are used for obtaining wind power with a mean MAPE around 14%, which is considerably lower than the persistence model.

Conclusions

Environmental issues and the depletion of raw materials have led to an increasing interest in sustainable energy sources. Due to the volatility of RESs, especially wind energy, an accurate integration of the latter into the power system has become necessary. In order to solve the wind integration problem, an optimal wind power forecasting model is crucial.

In the literature, researchers have proposed wind power forecasting models based on local information referring to a single forecasting point, without considering the information regarding the surrounding areas. However, by observing the meteorological phenomena that contribute to wind formation and that affect its speed and by understanding how such phenomena evolve over time and across space, it is easy to see that an accurate wind power forecast has to take into consideration the dependence of wind power, at any given point, on the phenomena occurring in the surrounding areas.

In this PhD dissertation, new wind speed forecasting models which consider the temporal and spatial evolution of the meteorological phenomena, and a new wind power prediction model, based on the structural and production characteristics of a WF, have been proposed. The models here developed and presented show how the dependence on the surrounding areas on a mesoscale basis strongly influences the performance of the forecasting models. In fact, the prediction errors typically found in the models from the literature, based on local forecasting systems, are greater than those of models that consider the evolution of wind under the influence of meteorological phenomena over time and across space such as those here proposed.

In addition, a two-stage model has been shown to predict the power produced by a wind farm. In the first stage, the wind speed prediction is determined and then, starting from the wind prediction, the wind power forecasting from the wind farm power plant is obtained. This approach further improves the forecasting performance.

In addition to the formalization of the models, their implementation was presented. In particular, two forecasting models for two time-horizons, daily and hourly, were developed and implemented. The implementations of both models have shown that taking into account the spatio-temporal evolution of wind strongly improves the forecasting quality of the wind prediction models.

In order to test the model's performance, weather data from meteorological stations of the *National Air Force Meteorological Service* - C.O.Met. (Centro Operativo per la Meteorologia), and by IVPC (*Italian Vento Power Corporation*), one of Europe's most important wind energy companies, were used. Moreover, the wind production data, the wind power curves and the structural characteristics of a WF were provided by IVPC.

The core of the work was divided into two parts, the first dedicated to the implementation of the daily wind speed forecasting model for estimating the availability of energy from wind sources, and the second focusing on the hourly wind speed forecasting model for estimating the quarter-hour power available from wind sources to organize the dispatching service.

The daily prediction model is based on weather information and on one of the most widespread machine learning methods, the ANN. In order to consider the spatio-temporal evolution of weather fronts, a nesting grid was built. Unlike the advanced global numerical weather prediction models, where large-scale weather predictions are obtained through the identification of hundreds or even thousands of sites located around the prediction point, in the implemented model, considering the eight main directions of the compass rose and two different distances from the prediction site, a simplified grid version was used. According to the mesoscale model, in order to describe the daily evolution of the weather fronts, the data used for the model's training are shifted in time of a *τ-factor*, identified through an optimization process. In order to obtain a good performance in terms of a low prediction error, the implemented model was trained with three datasets, two seasonal and one dynamic, the last one moving as a dynamic temporal window according to the forecast horizon. After a comparative analysis, the dynamic set was chosen.

The effectiveness of the implemented model was demonstrated by the evaluation of the main figures of merit and by the comparison with the results obtained from the persistence model, the typical benchmark for prediction models. The implemented ANN-MLP model represents an improvement over the persistence model of about 35% in terms of MAPE.

To forecast the hourly wind speed, instead, a hybrid model, based on ANNs, clustering and optimization algorithms, was implemented. The implemented neural predictor is an optimized ANN-MLP, in which the ANN parameters are optimized by the PSO algorithm. The basic idea for the model developed, much like the one for daily forecasting, was to construct a nesting grid to consider the evolution of weather phenomena. However, in the hourly model the two distances are different, and hence the data used refer to a different type of mesoscale. In order to optimize the dataset, the weather data were clustered into four groups according to the k-means algorithm, and for each group a correlation analysis was considered. The effectiveness of the proposed model was confirmed by the model's performance, in terms of the main figures of merit and by the comparison with the persistence model, which showed that the maximum value of MAPE was reduced by about 16%.

The last part of the work is dedicated to the hourly wind power forecasting – the most interesting type of forecast for both wind producers and TSOs – at a WF located in Southern Italy. The forecasting methods proposed in the literature were discussed, then the implemented two-stage forecasting approach was described.

Unlike the approaches proposed in the literature, the implemented model forecasts wind power using the meteorological data and the wind power data separately. The first stage of the proposed approach is dedicated to wind speed forecasting and it is based on the optimized ANN model previously described; the second stage, on the other hand, is dedicated to the evaluation of the wind power. The Betz theory was analysed to explain the wind power expression considered and, using the historical production data of the WF, the WF's structural characteristics and the wind speed predicted at the first stage, the wind power was obtained.

The implemented approach was tested in several test cases: four representative days of the year and the first week of spring. The performance and the comparative analysis have confirmed the effectiveness of the implemented forecasting approach: the proposed model performs better than the persistence model for all the four days, with a MAPE reduction of about 14% and an improvement, in terms of average MAPE over a week period, of about 40% in the second test case.

The good performance of the proposed approach may open up new development scenarios for the scientific community and for applications to electrical systems aimed at a better integration of non-programmable renewable sources such as wind power, which can lead to further improving or extending the methodology presented in this thesis. In the proposed approach, it was assumed that at a given time-step a single prevailing wind direction was sufficient to describe the weather evolution over the whole area considered. However, if large areas with various and sudden local wind changes are chosen, it could be beneficial to take into account several dominant wind directions instead of only one. In this case, varying correlation models or clustering techniques could be employed.

Another possible development could be constructing a denser nesting grid to include other meteorological phenomena such as rain events, humidity, convection clouds etc., which indirectly influence wind formation. These data could be provided by radar or satellite images and become new inputs of the model which, although more complex, could better follow and predict wind fluctuations and hence power fluctuations: the evaluation of the expected error of wind power fluctuations could be investigated in respect to wind speed fluctuations.

Moreover, in order to improve the model, the optimization phase, which in the proposed model only concerns the ANN parameters, could be extended to the data used for training the model. A possibility could be implementing a new hybrid model based on GAs and the PSO algorithm to optimize both the

dataset and the model's parameters. In this way, false or inaccurate data could be removed, and the training phase could get faster. Moreover, if a larger WF made up of different types of wind turbines is considered, the new optimization phase could be included in the second stage of the proposed methodology to identify the best production power curves and hence the most useful data for evaluating wind power.

References

A. Mazur, 2018. *Artificial Neural Network in EPS calibration – an alternative for linear regression and for simple EPS mean.* Bologna, EUMETNET.

Abe et al., 2010. *Support Vector Machines for Pattern Classification.* 2nd Edition a cura di s.l.:Springer, Advances in Computer Vision and Pattern Recognition.

Ackerman et al., 2007. *Meteorology: Understanding the Atmosphere.* 2Nd Edition a cura di s.l.:Thomson Brooks/Cole.

Ackerman, 2012. *Wind Power in Power Systems.* 2nd Edition a cura di s.l.:John Wiley & Sons Inc.

Aggarwal et al., 2013. *Data Clustering: Algorithms and Applications.* 1st Edition a cura di s.l.:Chapman and Hall/CRC Press.

Akcay et al., 2017. Short-term wind speed forecasting by spectral analysis from long-term observations with missing values. *Elsevier, Applied Energy,* Volume 191, pp. 653-662.

Aldana et al., 2019. *Global Energy Outlook (GEO) 2019: The next generation of energy.*

[Online]Available at: https://www.rff.org/publications/reports/global-energy-outlook-2019/

Alencar et al., 2017. Different Models for Forecasting Wind Power Generation: Case Study. *Energies,* Volume 10, pp. 1-27.

Alessandrini et al., 2013. A comparison between the ECMWF and COSMO Ensemble Prediction Systems applied to short-term wind power forecasting on real data. *Elsevier, Applied Energy,* Volume 107, pp. 271-280.

Anderson et al., 2007. *Optimal Control: Linear Quadratic Methods.* USA: Dover Publications.

ARERA, 2016. *Ulteriori interventi per la valorizzazione degli sbilanciamenti effettivi, per l'anno 2017, nell'ambito del regime transitorio introdotto dalla deliberazione dell'autorità 444/2016/r/eel.* s.l.:delibera 444/2016/R/EEL.

Autorità per l'energia elettrica e il gas., 20 Dicembre 2007. *Condizioni per la gestione della priorità di dispacciamento relativa ad impianti di produzione da fonti rinnavabili in situazioni di criticità del sistema elettrico nazionale.* s.l.:Delibera n. 330/07.

Autorità per l'energia elettrica e il gas, 25 Luglio 2008. *Verifica del codice di trasmissione e di dispacciamento in materia di condizioni per la gestione della produzione da fonte eolica.* s.l.:Delibera ARG/elt98/08.

Autorità per l'energia elettrica e il gas, 7 Luglio 2005. *Avvio di procedimento per la formazione di provvedimenti aventi ad oggetto condizioni per la gestione della priorità di dispacciamento relativa ad impianti di produzione da fonti rinnovabili in situazioni di criticità del sistema elettrico nazionale.* s.l.:Delibera n. 138/05.

Autorità per l'energia e il gas, 5 Luglio 2012. *Revisionedel dispacciamento dell'energia elettrica per le unità di produzione di energia elettrica alimentate da fonti rinnovabili non programmabili.* s.l.:Delibera 281/12.

Barry et al., 2009. *Atmosphere Weather and Climate.* 9th Edition a cura di s.l.:Rutledge India.

Bispo R. & al., 2019. *Wind Energy and Wildlife Impacts - Balancing energy sustainability with wildlife conservation.* 1st edition a cura di s.l.:Springer.

BNEF, 2019. *New Energy Outlook Report.* [Online] Available at: https://about.bnef.com/new-energy-outlook/

Bohme et al., 2011. Long-term evaluation of COSMO forecasting using combined observational data of the GOP period. *Meteorologische Zeitschrift,* Volume 1, pp. 119-132.

Bonavita et al., 2005. Assimilation of ATOVS retrievals and AMSU-A radiances at the Italian Weather Service: Current status and perspectives. *Meteorology and Atmospheric Physics,* Volume 88, pp. 39-52.

Bonavita et al., 2008. The ensemble Kalman filter in an operational regional NWP system: preliminary results with real observations. *Quarterly Journal of the Royal Meteorological Society - Wiley InterScience,* Volume 134, pp. 1733-1744.

Bonavita et al., 2010. Ensemble data assimilation with the CNMCA regional forecasting system. *Quarterly Journal of the Royal Meteorological Society,* Volume 136, pp. 132-145.

Bonfil et al., 2016. Wind speed forecasting for wind farms: A method based on support vector regression. *Elsevier, Renewable Energy,* Volume 85, pp. 790-809.

BP, 2019a. *Energy outlook report 2019 Edition.* [Online] Available at: https://www.bp.com/content/dam/bp/business-site/en/global/corporate/pdfs/energy-economics/energy-outlook/bp-energy-outlook-2019.pdf

BP, 2019b. *Energy outlook, Statistical review of world energy, 68th Edition.* [Online]
Available at: https://www.bp.com/content/dam/business-sites/en/global/corporate/pdfs/energy-economics/statistical-review/bp-stats-review-2019-full-report.pdf

Carriveau, 2011. *Fundamental and Advanced Topics in Wind Powe.* 1st Edition a cura di s.l.:InTechOpen.

Cengel et al., 2017. *Fluid Mechanics Fundamentals and Applications.* 4th Edition a cura di New York: McGraw Hill Education.

Chandra, 2017. *Wind Integration Studies in Power Systems: Forecasting, Stability and Load Management Issues.* s.l.:LAP LAMBERT Academic Publishing.

Chang et al., 2016. *Ahybrid model for forecasting wind speed and wind power generation.* Boston, IEEE Power and energy society general meeting.

Chang et al., 2017. An improved neural network-based approach for short-term wind speed and power forecast. *Elsevier, Renewable Energy,* Volume 105, pp. 301-311.

Chatfield, 2000. *Time-Series Forecasting.* Boca Raton, FL, United States: Taylor & Francis Ltd.

Chen et al., 2018. Wind Power Forecasting. *Elsevier, IFAC,* 51(28), pp. 414-419.

Chen et al., 2018. Wind speed forecasting using nonlinear learning ensemble of deep learning time series prediction and extremal optmization. *Elsevier, Energy Conversion and Managmement,* Volume 165, pp. 681-695.

Coiffier, 2012. *Fundamentals of Numerical Weather Prediction.* s.l.:Cambridge University Press.

Colak et al., 2015. *Multi-time series and time scale modelling for wind speed and wind power frecasting part I: statistical methods, very short-term and short-term applications.* Palermo, International Conference on Renewable Energy Research and Applications (ICRERA).

Colins, 2017. *Machine Learning: An Introduction to Supervised and Unsupervised Learning Algorithms.* s.l.:Micheal Colins.

COP21, 2016. *United Nations framework convention on climate change (UNFCC) - Paris Agreement.* Paris: s.n.

Cortes et al., 1995. Machine Learning – Support Vector Networks. *Springer,* 20(3), pp. 273-297.

Demolli et al., 2019. Wind power forecasting based on daily wind speed data using machine learning approaches. *Elsevier, Energy Conversion and Management,* 198(111823), pp. 1-12.

Dong et al., 2016. Wind power day-ahead prediction with cluster analysis of NWP. *Elsevier, Renewable and Sustainable Energy Reviews,* Volume 60, pp. 1206-1212.

Dowell et al., 2016. Very-Short-Term probabilistic wind power forecasts by sparse vector autoregression. *IEEE Transaction on Smart Grid,* 7(2), pp. 763-770.

Eldali, 2016. *Employing ARIMA models to improve wind power forecasts: A case study in ERCOT.* Denver, USA, North American Power Symposium (NAPS).

El-Sharkawi, 2015. *Wind Energy: An Introduction.* 1st Edition a cura di s.l.:CRC Press.

Emeis, 2013. *Wind Energy Meteorology - Atmospheric Physics for wind power generation.* s.l.:Springer.

Emeis, 2018. *Wind Energy Meteorology - Atmospheric Physics for Wind Power Generation.* 2nd Edition a cura di s.l.:[46] Stefan Emeis, "Wind Energy Meteorology - AtmoSpringer, Green Energy and Technology.

Eseye et al., 2017. *Short-term wind power forecasting using a double-stage hierarchical hybrid GA-ANFIS approach.* Chengdu, China, IEEE 2nd International Conference on Cloud Computing and Big Data Analysis (ICCCBDA).

Eurostat, 2019. *Renewable energy statistics.* [Online] Available at:

https://ec.europa.eu/eurostat/statistics-explained/index.php/Renewable_energy_statistics

Farret et al., 2017. *Integration of Renewable Sources of Energy.* 2nd Edition a cura di s.l.:Wiley.

Fausett, 1994. *Fundamentals of neural networks: architectures, algorithms, and applications.* 1st Edition a cura di s.l.:Prentice-Hall.

Fazelpour et al., 2016. Short-term wind speed forecasting using artificial neural networks for Tehran, Iran. *Springer, International Journal of Energy and Environmental Engineering,* Volume 7, pp. 377-390.

Focken et al., 2001. *Previento – A Wind Power Prediction System With an Innovative Upscaling Algorithm.* Copenhagen, Denmark, European Wind Energy Conference.

Gan et al., 2007. *Data Clustering: Theory, Algorithms, and Applications.* 1st Edition a cura di Virginia: G. Gan, C. Ma and J. Wu, "DaASA-SIAM Series on Statistics and Applied Mathematics, SIAM Editor.

Gazzetta Ufficiale della Repubblica Italiana, 2012. *Attuazione dell'art. 25 del decreto legislativo 3 marzo 2011, n.28, recante incentivazione della produzione di energia elettrica da impianti solari fotovoltaici (c.d. Quinto Conto Energia).* s.l.:D. M. 5 Luglio 2012 n. 143.

Gazzetta Ufficiale della Repubblica Italiana, 29 Dicembre 2003. *Attuazione della direttiva 2001/77/CE relativa alla promozione dell'energia elettrica prodotta da fonti energetiche rinnovabili nel mercato interno del'elettricità.* s.l.:D. Lgs. n. 387/03.

Gazzetta Ufficiale della Repubblica Italiana, Settembre 2001. *Sulla promozione dell'energia elettrica prodotta da fonti energetiche rinnovabili nel mercato interno dell'elettricità.* s.l.:Direttiva 2001/77/CE n. 283/33.

Ghofrani et al., 2016. *K-means clustering with a new initialization approach for wind power forecasting.* Dallas, TX, USA, 2016 IEEE/PES Transmission and Distribution Conference and Exposition (T&D).

Giebel et al., 2017. Wind power forecasting - a review of the state of the art. In: *Renewable Energy Forecasting - From Models to Applications.* s.l.:Woodhead Publishing Series in Energy, pp. 59-109.

Giebiel et al., 2002. *The Zephyr Project – The Next Generation Prediction System.* Paris, Global Windpower Conference and Exhibition.

Giebiel, 2003. *Report - The State of the art in Short-Term Prediction of Wind Power - A Literature Overview.* Roskilde : Risø National Laboratory.

GSE, 2019. *Statistical report on electricity production in Italy.* [Online] Available at: https://www.gse.it/documenti_site/Documenti%20GSE/Rapporti%20statistici/GSE%20-%20Rapporto%20Statistico%20FER%202018.pdf

GWEC, 2018. *Global wind report.* [Online] Available at: https://gwec.net/global_wind_report_2018

Haiqiang et al., 2017. Ultra-short term wind speed forecasting method based on spatial and temporal correlation models. *IET, the Journal of Engineering,* 2017(13), pp. 1071-1075.

Hansen, L. M. O., 2015. *Aerodynamics of wind turbines.* 3rd edition a cura di s.l.:Routledge Taylor&Francis Group.

Hao et al., 2019. A novel clustering algorithm based on mathematical morphology for wind power generation prediction. *Elsevier, Renewable Energy,* Volume 136, pp. 572-585.

Hao et al., 2019. A novel two-stage forecasting model based on error factor and ensemble method for multi-step wind power forecasting. *Elsevier, Applied Energy,* Volume 283, pp. 368-383.

Hau, 2013. *Wind Turbines - Fundamentals, Technologies, Application, Economics.* 3rd Edition a cura di s.l.:Springer.

Horst, 2008. *The Weibull Distribution: A Handbook.* 1st Edition a cura di s.l.:Chapman and Hall/CRC.

Hua et al. , 2017. *Wind speed optimisation method of numerical prediction for wind farm based on Kalman filter method.* Wuhan, China, 6th Internaitonal Conference on Renewable Power Generation (RPG).

IEA, 2018a. *Status of Power System Transformation.* [Online] Available at: https://www.21stcenturypower.org/assets/pdfs/main-report.pdf

IEA, 2018b. *World Energy Outlook 2018.* [Online] Available at: https://www.worldenergyoutlook.org/weo2018/

IEA, 2018c. *Global Energy&CO_2 status report - The latest trends in energy and emissions in 2018.* [Online] Available at: https://www.iea.org/reports/global-energy-co2-status-report-2019

IEA, 2019. *International Energy Outlook 2019 - with projection to 2050.* [Online]
Available at: https://www.eia.gov/outlooks/ieo/pdf/ieo2019.pdf

IRENA, 2017. *Renewable Energy Statistics.* [Online] Available at:
https://www.irena.org/-/media/Files/IRENA/Agency/Publiction/2017/Jul/IRENA_Renewable_Energy_Statistics_2017.pdf

IRENA, 2019. *Global Energy Transformation - A Road Map to 2050.* [Online] Available at: https://www.irena.org/DigitalArticles/2019/Apr/-/media/652AE07BBAAC407ABD1D45F6BBA8494B.ashx

Jain, 2016. *Wind Energy Engineering.* 2nd Edition a cura di s.l.:McGraw-Hill Education.

Jenkins et al., 2008. *Time Series Analysis: Forecasting and Control.* 4th Edition a cura di New York, NY, USA: Wiley.

Jiang et al., 2017. Short-term wind speed forecasting using a hybrid model. *Elsevier, Energy,* Volume 119, pp. 561-577.

Jiauzhou et al., 2016. Analysis and application of forecasting models in wind power integration: a review of multi-step-ahead wind speed forecasting models. *Elsevier, Renewable and Sustainable Energy Reviews*, Volume 60, pp. 960-981.

Jones, 2014. *Renewable Energy Integration - Practical Management of Variability, Uncertainty, and Flexibility in Power Grids.* 1st Edition a cura di s.l.:Academic Press.

Kadhem et al., 2017. Advanced Wind Speed Prediction Model Based on a Combination of Weibull Distribution and an Artificial Neural Network. *Energies,* 10(1174).

Kalnay, 2003. *Atmospheric modeling, data assimilation and predictability.* 2nd Edition a cura di s.l.:Cambridge University Press.

Kalnay, 2012. *Atmospheric Modeling, Data Assimilation and Predictability.* s.l.:Cambridge University Press.

Karakuş et al., 2017. One-day ahead wind speed/power prediction based on polynomial autoregressive model. *IET Renewable Power Generation,* 11(11), pp. 1430-1439.

Kariniotakis, 2017. *Renewable Energy Forecasting - From Models to Applications.* 1st Edition a cura di s.l.: Woodhead Publishing.

Kassa et al., 2016. *A GA-BP hybrid algorithm based ANN model for wind power prediction.* s.l., IEEE Smart Energy Grid Engineerin (SEGE).

Kaur et al., 2016. *Application of artificial neural network for short term wind speed forecasting.* Bangalore, India, Biennial International Conference on Power and Energy Systems: Towards Sustainable Energy (PESTSE).

Kavousi et al., 2016. A new Fuzzy –Based Combined Prediction Interval for Wind Power Forecasting. *IEEE Transaction on Power System,* 31(1), pp. 18-26.

Kiplangat et al., 2016. Improved week-ahead predictions of wind speed using simple linear models with wavelet decomposition. *Elsevier, Renewable Energy,* Volume 93, pp. 38-44.

Kong et al., 2015. Wind speed prediction using reduced support vector machines with feature selection. *Elsevier, Neurocomputing,* Volume 169, pp. 449-456.

Kumar et al., 2019. Investigation on short-term wind power forecasting using ANN and ANN-PSO. *Springer, Applications of Computing, Automation and Wireless Systems in Electrical Engineering,* Volume 553, pp. 1103-1116.

Kurdikeri et al., 2018. *Comparative Study of Short-Term Wind Speed Forecasting Techniques Using Artificial Neural Networks.* Coimbatore, India, IEEE International Conference on Current Trends towards Converging Technologies (ICCTCT).

Landberg, 2015. *Meteorology for Wind Energy: an introduction.* s.l.:Wiley.

Li et al., 2015. Modeling dynamic spatial correlations of geographiccaly distributed wind farms and constructing ellipsoidal uncertainty sets for optmization-based generation scheduling. *IEEE Transaction on Sustainable Energy,* 6(4), pp. 1283-1291.

Li et al., 2017. *A double-stage hierarchical hybrid PSO-ANFIS model for short-term wind power forecasting.* Denver, CO, USA, 9th Annual IEEE Green Technologies Conference (GreenTech).

Liu et al., 2014. Short-term wind speed forecasting using wavelet transform and support vector machines optimized by genetic algorithm. *Elsevier, Renewable Energy,* Volume 62, pp. 592-597.

Liu et al., 2017. A Hybrid Forecasting Method for Wind Power Ramp Based on Orthogonal Test and Support Vector Machine (OT-SVM). *IEEE Transaction on sustainable energy,* 8(2), pp. 451-457.

Lydia et al., 2016. Linear and non-linear autoregressive models for short-term wind speed forecasting. *Elsevier, Energy Conversion and Management ,* Volume 112, pp. 115-124.

Ma et al., 2017. A generalized dynamic fuzzy neural network based on singular spectrum analysis optimized by brain storm optimization for short-term wind speed forecasting. *Elsevier, Applied Soft Computing,* Volume 54, pp. 296-312.

Makhloufi et al., 2017. *Wind speed and wind power forecasting using wavelet denoising - GMDH neural network.* Malang, 5th IEEE International Conference on Electrical Engineering.

Manwell et al., 2010. *Wind Energy Explained: theory, design and application.* 2nd Edition a cura di s.l.:Wiley.

Marsigli et al., 2005. The COSMO-LEPS mesoscale ensemble system: validation of the methodology and verification. *Nonlinear Processes in Geophysics,* Volume 12, pp. 527-536.

Marugàn et al., 2018. A survey of artificial neural network in wind energy systems. *Elsevier, Applied Energy,* Volume 228, pp. 1822-1836.

Meng et al., 2011. Limited-area ensemble-based data assimilation. *Monthly Weather Review,* 139(7), pp. 2025-2045.

Meng et al., 2016. Wind speed forecasting based on wavelet packet decomposition and artificial neural networks trained by crisscross optmization algorithm. *Elsevier, Energy Conversion and Management,* Volume 114, pp. 75-88.

Ministero dello Sviluppo Economico, 2016. *Incentivazione dell'energia elettrica prodotta da fonti rinnovabili diverse dal fotovoltaico.* s.l.:D. M. 23 Giugno 2016 n. 150 - Gazzetta Ufficiale della Repubblica Italiana.

Mitchell, 1996. *An Introduction to Genetic Algorithms.* s.l.:MIT Press Ltd.

Mohssen , 2016. *Machine Learning: Algorithms and Applications.* 1st Edition a cura di s.l.:CRC Press.

Montgomery et al., 2008. *Introduction to Time Series - Analysis and Forecasting.* Hoboken, New Jersey: John Wiley & Sons.

Moustris et al., 2016. *24-h Ahead Wind Speed Prediction for the Optimum Operation of Hybrid Power Stations with the Use of Artificial Neural Networks.* s.l., Springer, Perspectives on Atmospheric Sciences.

NREL, 2009. *Hourly Wind Power Variation in Texas.* s.l.:USA.

Olsson, 2011. *Particle Swarm Optimization: Theory, Techniques and Applications.* UK Edition a cura di s.l.:Engineering Tools, Techniques and Tables, Nova Science Pub Inc.

Paolella, 2018. *Linear Models and Time-Series Analysis: Regression, ANOVA, ARMA and GARCH.* s.l.:Wiley.

Parlamento Europeo , 2002. *Ratifica ed esecuzione del Protocollo di Kyoto alla Convenzione quadro delle Nazioni Unite sui cambiamenti climatici, fatto a Kyoto l'11 dicembre 1997.* Roma: Law n. 120.

Parlamento europeo, 5 giugno 2009. *Promozione dell'uso dell'energia da fonti rinnovabili, recante modifica e successiva abrogazione delle direttive 2001/77/CE e 2003/30/CE.* s.l.:Direttiva 2009/28/CE.

Parlamento Italiano, 1999. *Disposizioni in materia di perequazione, razionalizzazione e federalismo fiscale.* s.l.:L. 133/99.

Parlamento Italiano, 23 Agosto 2004. *Riordino del settore energetico, nonchè delega al Governo per il riassetto delle disposizioni vigenti in materia di energia.* s.l.:Law 239/04.

Parlamento Italiano, 31 Marzo 1999. *Attuazione della direttiva 96/92/CE recante norme comuni per il mercato interno dell'energia.* s.l.:D. Lgs. 79/99 n. 75 - Gazzetta Ufficiale.

Pielke, 2013. *Mesoscale Meteorological Modeling.* 3rd Edition a cura di University of Colorado, Boulder, CO, USA: Academic Press.

Pielke, 2013. *Mesoscale Meteorological Modeling.* 3rd Edition a cura di s.l.:International Geophysics - Academic Press.

REN21, 2019. *Renewables Global Status Report (GSR) - Full Report.* [Online]
Available at:
https://www.ren21.net/wp-content/uploads/2019/05/gsr_2019_full_report_en.pdf

Ricerca sul Sistema Energetico – RSE SpA, 2012. *L'energia elettrica dal vento.*
[Online] Available at:
http://www.rse-web.it/applications/webwork/site_rse/local/doc-rse/RSE%20Monografia%20Eolico/RSE_Monografia_Eolico.pdf

Ross, 2016. *Fuzzy Logic with Engineering Applications.* 4th Edition a cura di USA: John Wiley and Sons Ltd.

Sánchez et al., 2002. *Sipreólico - A wind power prediction system based on flexible combination of dynamic models. Application to the Spanish power system.* Norrköping, Sweden, First IEA Joint Action Symposium on Wind Forecasting Techniques, FOI - Swedish Defence.

Santhosh et al., 2020. Current advances and approaches in wind speed and wind power forecasting for improved renewable energy integration: A review. *Wiley, Engineering reports,* 2(6), pp. 1-20.

Sanz et al., 2008. *Short-term wind speed prediction by hybridizing global and mesoscale forecasting models with artificial neura networks.* Barcelona, Spain, 8th IEEE International conference on hybrid intelligent system.

Schmitz, July 2019. *Aereodynamics of wind turbines: a physical basis fro analysis and design.* 1st Edition a cura di s.l.:Wiley.

Shakir et al., 2020. Grid Integration Challenges of Wind Energy: A Review. *IEEE Access*, 8(19313361), pp. 10857 - 10878.

Shanmuganathan et al., 2016. *Artificial Neural Network Modelling.* 1st Edition a cura di s.l.:Springer.

Shevlyakov et al., 2016. *Robust Correlation: Theory and Applications.* 1st Edition a cura di s.l.:Wiley Series in Probability and Statistics, Wiley.

Shiarifian et al., 2018. A new method based on Type-2 fuzzy neural network for accurate wind power forecasting under uncertain data. *Elsevier, Renewable Energy,* Volume 120, pp. 220-230.

Singh et al., 2018. *Analysis of Fuzzy Logic, ANN and ANFIS based models for forecasting of wind power.* New Delhi, India, 2nd IEEE International Conference on Power Electronics, Intelligent Control and Energy System (ICPEICES).

Skittides et al., 2014. Wind forecasting using Principal Component Analysis. *Elsevier, Renewable Energy,* Volume 69, pp. 365-374.

Skittides, 2015. *Statistical modelling of wind energy using Principal Component Analysis.* Heriot-Watt University: PhD Thesis.

Spellman, 2012. *The Handbook of Meteorology.* Norfolk, Virginia USA: Rowman & Littlefield.

Ssekulima et al., 2016. Wind speed and solar irradiance forecasting techniques for enhanced renewable energy integration with the grid: a review. *IET Renewable Power Generation Journal,* Volume 10, pp. 885-898.

Stathopoulos et al., 2013. Wind power prediction based on numerical and statistical models. *Elsevier, Journal of Wind Engineering and Industrial Aerodynamics,* Volume 112, pp. 25-38.

Stensurd, 2009. *Parameterization Schemes: Keys to Understanding Numerical Weather Prediction Models.* Cambridge, UK: Cambridge University Press.

Terna, 2018. *Statistical report on electricity production in Italy.* [Online] Available at:

https://www.terna.it/it/sistema-elettrico/statistiche/pubblicazioni-statistiche

Terna, 2019. *Contesto ed evoluzione del sistema elettrico - Statistical Report 2019.*

[Online] Available at:

https://download.terna.it/terna/Contesto%20ed%20evoluzione%20del%20Sistema%20Elettrico_8d75639fa148d01.pdf

Tian, 2018. *Wind Power Forecasting Based on ARIMA-LGARCH Model.* Guangzhou, China, International Conference on Power System Technology (POWERCON).

Towler, 2014. *The future of energy.* 1st Edition a cura di s.l.:Elsevier.

Trapp, 2013. *Mesoscale-Convective Processes in the Atmosphere.* Indania: Cambridge University Press.

Vahidzadeh et al., 2019. Modified Power Curves for Prediction of Power Output ofWind Farms. *MDPI, Energies,* 12(1805), pp. 1-19.

Vasquez, 2002. *Weather Forecasting Handbook.* 5th Edition a cura di s.l.:Weather Graphics Tecnologies.

Vasquez, 2015. *Weather Analysis & Forecasting.* s.l.:Weather Graphics Technologies.

Wang et al., 2016. Analysis and application of forecasting models in wind power integration: A review of multi-step-ahead wind speed forecasting models. *Elsevier, Renewable and Sustainable Energy Reviews,* Volume 60, pp. 960-981.

Wang et al., 2016a. Wind speed forecasting based on the hybrid ensemble empirical mode decomposition and GA-BP neural network method. *Elsevier, Renewable Energy,* Volume 94, pp. 629-636.

Wang et al., 2016b. Hybrid forecasting model-based data mining and genetic algorithm-adaptive particle swarm optimization: a case study of wind speed time series. *IET Renewable Power Generation,* 10(3), pp. 287-298.

Wang et al., 2018. Deep belief network based k-means cluster approach for short-term wind power forecasting. *Elsevier, Energy ,* 165(Part A), pp. 840-852.

Warner, 2010. *Numerical Weather and Climate Prediction.* National Center for Atmospheric Research, Colorado: Cambridge University Press.

Wu et al., 2017. A Data Mining Approach Combining K -Means Clustering With Bagging Neural Network for Short-Term Wind Power Forecasting. *IEEE Internet of Things,* 4(4), pp. 979-986.

Xie et al., 2019. A nonparametric bayesian framework for short-term wind power probabilistic forecast. *IEEE Transactions on Power System,* 34(1), pp. 371-379.

Xu et al., 2015. A short-term wind power forecasting approach with adjustment of numerical weather prediction input by data mining. *IEEE Transaction on Sustainable Energy,* 6(4), pp. 1283-1291.

Yatiyana et al., 2017. *Wind speed and direction forecasting for wind power generation using ARIMA model.* Melbourne, Australasian Universities Power Engineering Conference (AUPEC).

Yin et al., 2017. An effective secondary decomposition approach for wind power forecasting using extreme learning machine trained by crisscross optimization. *Elsevier, Energy Conversion and Management,* Volume 150, pp. 108-121.

Yu et al., 2017. *The short-term forecasting of wind speed based on EMD and ARMA.* Cambodia, 12th IEEE Conference on Industrial Electronics and Applications (ICIEA).

Yuan et al., 2015. Short-term wind power prediction based on LSSVM–GSA model. *Elsevier, Energy Conversion and Management,* Volume 101, pp. 393-401.

Yue et al., 2017. *Short-term wind speed combined prediction for wind farms.* Takamatsu, Japan, IEEE International Conference on Mechatronics and Automation (ICMA).

Zajaczkowski et al., 2011. A preliminar study of assimilating numerical weather prediction data into computational fluid dynamics models for wind prediction. *Journal of Wind Engineering and Industrial Aerodynamics,* Volume 99, pp. 320-329.

Zhang et al., 2012. A Fuzzy Group Forecasting Model Based on Least Squares Support Vector Machine (LS-SVM) for Short-Term Wind Power. *Energies,* 5(9), pp. 3329-3346.

Zhang et al., 2015. A Two-Stage Combination Model for Wind Power Forecasting. *Applied Mechanics and Materials,* pp. 9-13.

Zhang et al., 2015. *Ahybrid EMD-SVM based short-term wind power forecasting model.* Palmer, IEEE PES Asia-Pacific Power and Energy Engineering Conference (APPEEC).

Zhang et al., 2016. A gaussian process regression based on hybrid approach for short-term wind speed prediction. *Elsevier, Energy Conversion and Management,* Volume 126, pp. 1084-1092.

Zhao et al., August 2019. *Wind Turbines and Aerodynamics Energy Harvesters.* 1st Edition a cura di s.l.:Academic Press.

Zheng et al., 2017. Day-Ahead Wind Power Forecasting Using a Two-Stage Hybrid Modeling Approach Based on SCADA and Meteorological Information, and Evaluating the Impact of Input-Data Dependency on Forecasting Accuracy. *Energies,* 10(1988), pp. 1-24.

Zuluaga et al., 2015. Short-term wind speed prediction based on robust Kalman filtering: an experimental comparison. *Elsevier, Applied Energy,* Volume 156, pp. 321-330.

List of Acronyms

AEEG	Authority for Electricity and Gas
ALADIN	Aire Limitée Adaptation dynamique Développement InterNational
ANN	Artificial Neural Network
AR	Autoregressive model
ARERA	Authority for Energy, Grids, and Environment
ARIMA	Autoregressive Integrated Moving Average
ARMA	Autoregressive with Moving Average
ARMAX	Autoregressive Moving Average with Exogenous inputs
BNEF	Bloomberg New Energy Finance
BP	Back-Propagation
BUFR	Binary Universal Form for the Representation of meteorological data
CFD	Computational Fluid Dynamics
COSMO	Consortium for Small-scale Modelling
DA	Directional Accuracy
ECMWF	European Centre for Medium-Term Forecast
EMD	Empirical Mode Decomposition
EO	Extremal Optimization
ERCOT	Electric Reliability Council of Texas
EUMETCAST	European Organisation for the Exploitation of meteorological satellites
FL	Fuzzy Logic

GA	Genetic Algorithm
GC	Green Certificate
GFS	Global Forecasting System
GSE	Gestore dei Servizi Energetici
GTS	Global Telecommunication System
GWEC	Global Wind Energy Council
HIRLAM	High Resolution Limited Area Model
HWSF	Hourly wind speed forecast
IEA	International Energy Agency
IMF	Intrinsic Model Function
IPP	Independent Power Producer
IRENA	International Renewable Energy Agency
ISO	Independent System Operator
LAM	Local Area Model
LATAM	Latin American Market
LETKF	Local Ensemble Transform Kalman Filter
LGARCH	Logarithmic Generalized Autoregressive Conditional Heteroskedasticity
LQE	Linear Quadratic Estimation
LSSVM	Least Squares Support Vector Machine
LSTM	Long Short-Term Memory artificial neural network
MAE	Mean Absolute Error
MAPE	Mean Absolute Percentage Error
MASE	Mean Absolute Scaled Error
MBE	Mean Bias Error
MLP	Multi-Layer Perceptron
MRE	Mean Relative Error
MSE	Mean Square Error
NCEP	National Centers for Environmental Prediction

NOAA	National Oceanic and Atmospheric Administration
NP-RES	Non-programmable renewable energy source
NREL	National Renewable Energy Laboratory
NT	Nesting Theory
NWP	Numerical Weather Prediction
OECD	Organization for Cooperation and Economic Development
OT	Orthogonal Test
POI	Point Of Interest
PSO	Particle Swarm Optimization
REN	Renewable Energy policy Network
RES	Renewable Energy Source
RMSE	Root Mean Square Error
SAPP	Scalable Acquisition and Pre-Processing
SVM	Support Vector Machine
TSO	Transmission System Operator
WF	Wind Farm
WMO	World Meteorological Organisation
WPG	Wind Power Generation
WPPT	Wind Power Prediction Tool
WRF	Weather Research and Forecast

List of Symbols

A_w	Weibull distribution scale factor
k_w	Weibull distribution shape factor
P_n	Nominal wind power
ρ	Air density
A	Area of wind turbine rotor
v	General wind speed
$\hat{y}^n$	Average value of the last n measure in the persistence model
η	Wind turbine efficiency ratio
C_p	Wind turbine performance coefficient
$c_{i,j}$	AR coefficients
ε_t	Prediction error for AR model
p	Order of the AR process
q	Order of the MA process
d	Order of non-seasonal differences in the ARIMA process
P, Q	Order of integrated parts in the ARIMA process
ϑ_j	MA coefficients
$w_{i,j}$	ANN synaptic weights
$x = [x_1,\ldots,x_n]$	Input vector of general ANN
$w = [w_1,\ldots,w_n]$	Weight vector of general ANN
$\varphi(\cdot)$	Transfer function of general ANN
k	Angular coefficient of the transfer function of general ANN

y_{rj}	Output y_i relative to example r
d_{rj}	Desired output relative to example r
w_{kj}	Synoptic weights between hidden and input layer
w_{jk}	Synoptic weights between output and hidden layer
e_i	Relative error between desired and forecasted value
n	Predictions vector of general ANN
S_0	Test wind farm site
P	Pressure historical data set
T	Temperature historical data set
W	Wind speed historical data set
t^{+1}	Prediction instant
K	Set of the temporal indexes
$t^{-k}{}_{i,j}$; $t^{-2}{}_{i,j}$; $t^{-1}{}_{i,j}$	Temporal instants before the prediction horizon, t^{+1}
t^0	Current time instant
Δ	Distances set for the daily/hourly prediction model
Ω	Directions set for the daily/hourly prediction model
$r_{1,j} - r_{2,j}$	Distances from test site, S_0
τ	Time-shift delay factor
$S_{i,j}$	Sites around test site, S_0
a	interference parameter
F	Force extracted by wind on the rotor
δ_{max} - δ_{min}	Minimum and maximum distances from the test site, S_0, when the hourly prediction is considered
k_i	k-means centroids
N_k	All data points of each cluster
C_k	Centre cluster points
H	Hourly meteorological data series
V	Wind speed passing through the turbine rotor
V_1	Upwind speed (Betz's law)

V_2	Downwind speed (Betz's law)
S_1	Upwind air cross-section (Betz's law)
S_2	Downwind air cross-section (Betz's law)
$\dot{m}$	Mass flow rate
W	Available power in the undisturbed upstream over a cross-section area (Betz's law)
P	Power from upwind surface to downwind surface
P_i	Power relative to the i^{th} wind turbine
P_0	Total wind power of the wind farm at the test site, S_0

Appendix A.
Datasets description

In the thesis, two different predictors are proposed: one for the forecast of the wind in the site where the wind farm is located – here called *wind predictor*; and a second one – here called *wind farm power predictor* – which, starting from the wind forecasted by the first predictor, provides information related to the power produced by the whole wind farm.

As for the *wind predictor,* two types have been developed and described: one operating on a daily scale, and the other operating on an hourly basis, both using the same inputs. The difference between the two *wind predictors* is related to the way in which the datasets are constructed.

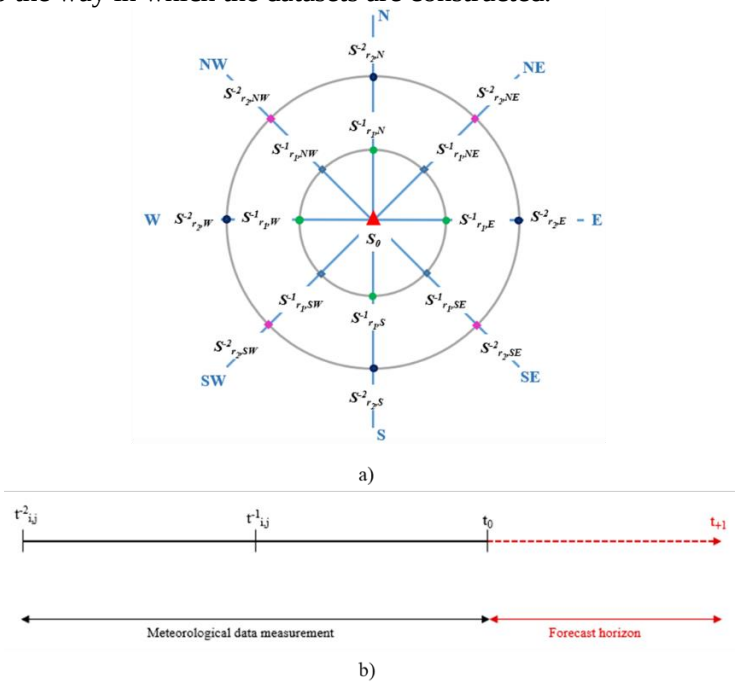

Figure A.1 *a) Schematic illustration of the sites along the principal and secondary cardinal directions. b) Time forecast horizon*

The following describes the datasets of the *wind predictor* in detail, starting with the description of the common parts first, and then analyzing the differences between them.

The datasets used as input to the proposed forecasting models include weather information obtained from measured data. The measured meteorological data refer to sixteen sites individuated at two distances, r_1 and r_2 respectively, distributed in two circles around the point S_0, where the wind is to be predicted (Figure A.1a), and the point S_0.

In order to consider the spatio-temporal evolution of the weather fronts, the weather data used for training the model are time-shifted by a proper delay, called *τ-factor*, according to the following relationships:

$$\begin{cases} t_{r1,j}^{-1} = t^0 - \tau \\ t_{r2,j}^{-2} = t^0 - 2\tau \end{cases} \quad \text{(A.1)}$$

where $t^{-1}{}_{r1,j}$ and $t^{-2}{}_{r2,j}$ are the temporal instants preceding t^{+1}, the forecast time horizon, t^0 is the current instant (Figure A.1b). The time delay factor, τ, changes according to the type of forecasting: it is equal to 1 day, if the daily forecast is considered, and to 1 *h* if the forecast is hourly. Likewise, the two different distances, r_1 and r_2, change according to the forecasting type: they are respectively 500 km and 250 km if the forecast is daily, and to 50 km and 20 km if the forecast is hourly.

The total number of points considered is, therefore, 16 + 1. The dataset for the 17 points contains the following data:

- date and time group;
- wind speed measured 10 meters above the ground;
- air temperature;
- barometric pressure.

All the data used for the setting-up of the dataset are obtained from real data provided by *National Air Force Meteorological Service* – C.O.Met. (Centro Operativo per la Meteorologia), as regards the meteorological data of the 16+1 points around S_0. IVPC *(Italian Vento Power Corporation)*, one of Europe's most important wind energy companies, also provided wind speed data at point S_0 and wind farm power production. The wind speed data from IVPC were verified by comparing them with those provided by C.O.Met., with which it coincided.

It should be noted that the data provided by C.O.Met. and IVPC had a higher resolution than those used by neural networks. Indeed, the measured meteorological data are the average values over 10 minutes and are thus provided 6 times in one hour; likewise, both the wind speed and the power production data, provided by IVPC every 15 minutes, represent the average of the respective data measured continuously in the fifteen minutes preceding the instant to which they refer (Figure A.2).

Hence, the new dataset is composed by 51 = 3 x (16 + 1) input, where 3 is the kind of data (wind speed, air temperature, barometric pressure), and 16+1 is the points considered.

DTG	Type	Wnd D	Wnd F	Wnd G	T	P
01/01/2011 23:50	Metar	SW	6		5	1014
02/01/2011 00:00	Metar	W	6		4	1014
02/01/2011 00:10	Metar	W	6		4	1014
02/01/2011 00:20	Metar	SW	6		4	1014
02/01/2011 00:30	Metar	NW	6		3	1014
02/01/2011 00:40	Metar	W	6		3	1014
02/01/2011 00:50	Metar	WSW	5		3	1014
02/01/2011 02:00	Metar	SW	7		3	1013
02/01/2011 02:10	Metar	SW	5		3	1013

a)

	L1 (kWh)	L2 (kWh)	Tot
01/01/2017 00:15	93,20	192,20	285,4
01/01/2017 00:30	19,20	28,40	47,6
01/01/2017 00:45	12,80	7,80	20,6
01/01/2017 01:00	33,00	3,40	36,4
01/01/2017 01:15	36,00	20,00	56
01/01/2017 01:30	56,00	49,40	105,4
01/01/2017 01:45	60,20	49,20	109,4

b)

Figure A.2 *a) Extract from the original weather dataset; b) Extract from the original wind production dataset*

With reference to the hourly forecast, the ANN input dataset for it is built on an hourly basis: for each hour *h*, the elements of the input vector are obtained as the average values from the measured data in the interval [*h*-30 min; *h*+30 min]. The two-thirds of the data were gathered to form the ANN-training procedure, whereas one-third was used to test the proposed procedure. Furthermore, the dataset for the ANN-training procedure was also divided into two different sub-sets: 70% for the training and 30% for the validation phase.

As for the dataset of the *wind farm power predictor*, the data provided by the IVPC were used. Specifically, the data, which refer to one year (2017), were divided into three sub-sets with the same criterion as above: 42.7% for the training phase, 20% for the validation phase, and the remaining 33% for the test.